Arctic Report Card 2021

Rapid and pronounced warming continues to drive the evolution of the Arctic environment

DOI: 10.25923/5S0F-5163

T.A. Moon, M.L. Druckenmiller
and R.L. Thoman; Eds.

December 2021

Twila A. Moon, Matthew L. Druckenmiller, Richard L. Thoman; Editors
Benjamin J. DeAngelo; NOAA Federal Advisor
Kelley A. Uhlig; NOAA Coordinating Editor

www.arctic.noaa.gov/Report-Card

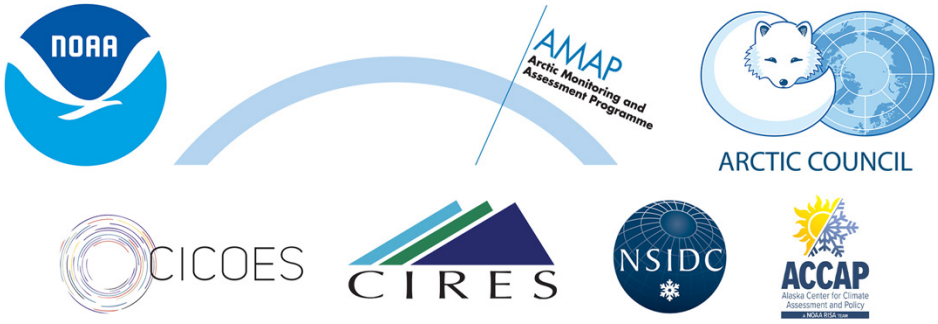

Citing the complete report or Executive Summary:

Moon, T. A., M. L. Druckenmiller, and R. L. Thoman, Eds., 2021: *Arctic Report Card 2021*, https://doi.org/10.25923/5s0f-5163.

Citing an essay (example):

Mudryk, L., A. Elias Chereque, C. Derksen, K. Luojus, and B. Decharme, 2021: Terrestrial snow cover. *Arctic Report Card 2021*, T. A. Moon, M. L. Druckenmiller, and R. L. Thoman, Eds., https://doi.org/10.25923/16xy-9h55.

(Note: Each essay has a unique DOI assigned)

Front cover photo credits

Center: Beaver lodge (center), dam (bottom center), and pond on the Seward Peninsula in western Alaska, 2021 – Kenneth D. Tape, Geophysical Institute, University of Alaska Fairbanks, Fairbanks, Alaska, USA

Bottom Left: Unalakleet, Alaska along the Norton Sound coast in the middle of winter. Shown here with mostly open water where there should be sea ice, 2019—Zachariah Hughes, Alaska Public Media and KNOM, Nome, Alaska, USA

Bottom Right: Donna Erickson cuts fish near Unalakleet, Alaska. The smokehouse is part of her family's harvesting infrastructure, 2015—Jeff Erickson, Unalakleet, Alaska, USA

Table of Contents

2021 Headlines 2

Executive Summary 4

Surface Air Temperature 8

Terrestrial Snow Cover 15

Greenland Ice Sheet 23

Sea Ice 32

Sea Surface Temperature 41

Arctic Ocean Primary Productivity: The Response of Marine Algae to Climate Warming and Sea Ice Decline 46

Tundra Greenness 58

Beaver Engineering: Tracking a New Disturbance in the Arctic 66

Ocean Acidification 72

River Discharge 78

2020 Foreign Marine Debris Event—Bering Strait 85

Glacier and Permafrost Hazards 93

The Changing Arctic Marine Soundscape 102

The Impact of COVID-19 on Food Access for Alaska Natives in 2020 109

Authors and Affiliations 119

2021 Headlines

Rapid and pronounced warming continues to drive the evolution of the Arctic environment

Cascading disruptions, extreme events, and increasing variability throughout the Arctic impact the safety and well-being of communities within and far away from the Arctic.

Highlights

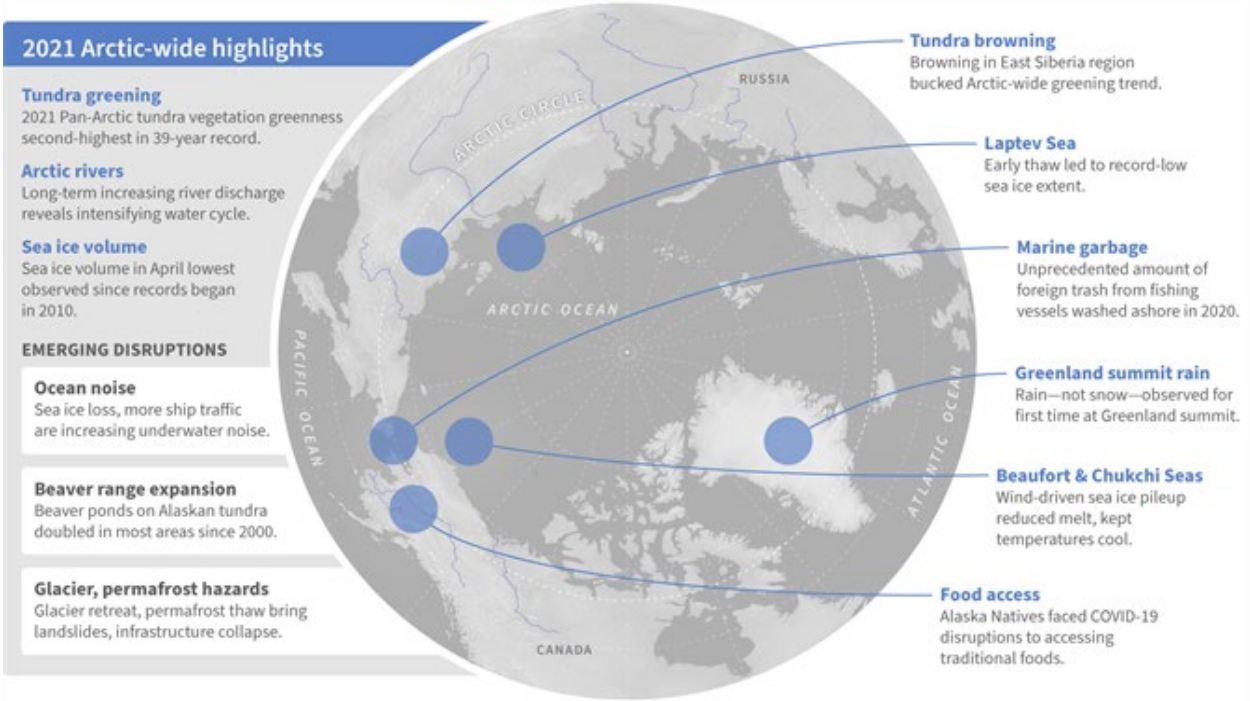

A sample of notable events and emerging disruptions from across the Arctic. Image by Climate.gov.

- The average **surface air temperatur**e over the Arctic for this past year (October 2020-September 2021) was the 7th warmest on record. This is the 8th consecutive year since 2014 that surface air temperatures were at least 1°C above the long-term average.
- The Arctic continues to warm more than twice as fast as the rest of the globe.

In the oceans

- The substantial decline in Arctic **sea ice** extent since 1979 is one of the most iconic indicators of climate change. Summer 2021 saw the second-lowest amount of older, multi-year ice since 1985, and the post-winter sea ice volume in April 2021 was the lowest since records began in 2010.
- Although there is considerable interannual variability in spatial **sea surface temperature** patterns, August mean SSTs show statistically significant warming trends for 1982-2021 in most regions of the Arctic Ocean that are ice-free in August.

- Seven of the nine Arctic regions observed showed higher **ocean primary productivity** in 2021 than the long-term average (2003-20). All regions continue to exhibit positive trends over the 2003-21 period, with the strongest trends in the Eurasian Arctic and the Barents Sea.
- Recent work on **ocean acidification** has shown that the Arctic Ocean is acidifying faster than the global ocean, but with high spatial variability. A growing body of research indicates that acidification in the Arctic Ocean could have implications for the Arctic ecosystem, including influences on algae, zooplankton, and fish.

On the land

- **Terrestrial snow cover** in the Eurasian Arctic in June 2021 was the 3rd lowest since records began in 1967. In the North American Arctic, snow cover has been below average for 15 consecutive years.
- The **Greenland Ice Sheet** experienced three extreme melt episodes in late July and August. On August 14, 2021, rainfall was directly observed at the 10,500-foot Summit Station for the first time ever.
- Exceptionally high midsummer productivity was observed in 2021 across the tundra. Satellites provide unequivocal evidence of widespread **tundra greening**, but extreme events and other drivers of local-scale "browning" have also become more frequent, highlighting regional disruption as an increasing component of Arctic change.
- **Beavers are colonizing the Arctic tundra** of western Alaska, transforming lowland tundra ecosystems and degrading permafrost by increasing the amount of unfrozen surface water on the landscape in winter.
- The long-term observations for Eurasian and North American Arctic **river discharges** demonstrate an upward trend, providing evidence for the intensification of the Arctic hydrologic cycle. In 2020, the combined discharge of the eight largest Arctic rivers was ~12% greater than the average over the 1981-2010 reference period.
- **Retreating glaciers and thawing permafrost are causing local to regional-scale hazards** that threaten lives and livelihoods, infrastructure, sustainable development, and national security. There is an urgent need for broad-scale hazard identification and assessment across the Arctic.

Marine shipping impacts

- During 2020, the Bering Strait region of Alaska experienced a **marine debris** event that brought garbage ashore that was different from the types and amounts typically observed, most associated with foreign ship traffic through the region.
- Arctic shipping traffic between the Pacific and Atlantic Oceans continues to increase and with it, ambient **marine noise** levels are increasing in the frequency bands used by marine mammals.

COVID-19 impacts on food access of Alaska Natives

- The COVID-19 pandemic has exacerbated existing challenges for Alaska Natives in accessing traditional foods. The strength of Indigenous cultural and economic practices such as food sharing networks helped mitigate these challenges.
- Policies and programs that support access to traditional foods and Indigenous sovereignty strengthen the ability of individuals and communities to respond to significant events that break down supply chains and restrict mobility.

Executive Summary

DOI: 10.25923/5s0f-5163

T. A. Moon[1,2], M. L. Druckenmiller[1,2], and R. L. Thoman[3,4]

[1]Cooperative Institute for Research in Environmental Sciences, University of Colorado Boulder, Boulder, CO, USA
[2]National Snow and Ice Data Center, Boulder, CO, USA
[3]Alaska Center for Climate Assessment and Policy, University of Alaska Fairbanks, Fairbanks, AK, USA
[4]International Arctic Research Center, University of Alaska Fairbanks, Fairbanks, AK, USA

As the influences of human-caused global warming continue to intensify, with the Arctic warming significantly faster than the globe overall, the 2021 Arctic Report Card (ARC2021) brings a broad view of the state of the Arctic climate and environment. The ARC2021 provides an update on seven Arctic *Vital Signs*, from sea ice to snow and air temperatures to tundra greenness, and checks in on three *Indicator* topics for updates on river discharge, ocean acidification, and observations of substantial Arctic beaver expansion. The noteworthy emerging topics in the four ARC2021 *Frostbites*—marine debris, marine noise, food access during the COVID-19 pandemic, and glacier and permafrost hazards—share a common link as they look at the impacts of more people and human activity in the Arctic as well as the challenges and hazards people face with the rapidly changing cryosphere. The scientific and observational story of the Arctic is a human story—of climate change, of increased shipping and industrial activity, and of communities responding to local and regional disruptions.

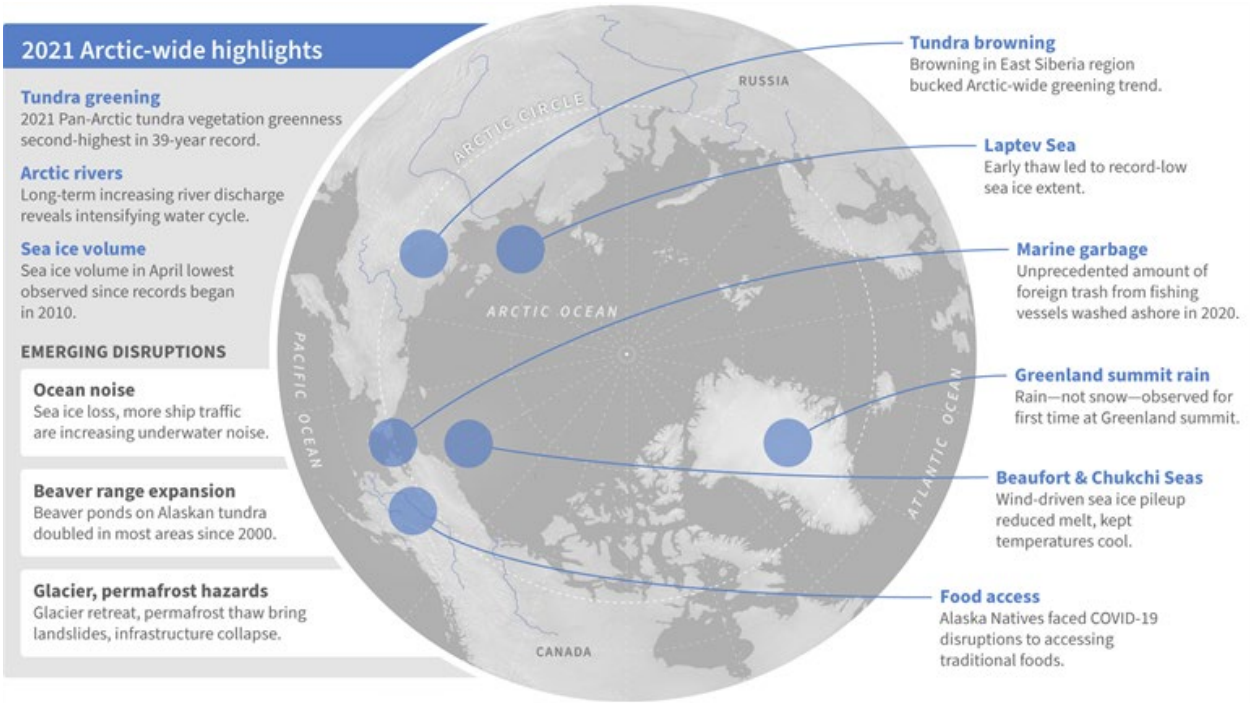

A sample of notable events and emerging disruptions from across the Arctic. Image by Climate.gov.

Rapid and pronounced warming continues to drive the evolution of the Arctic environment. As a connected system, links are visible across the many metrics and observations reported within the

ARC2021. The past year (October 2020-September 2021) was the seventh warmest over Arctic land since the record began in 1900. Pan-Arctic and Asian Arctic surface air temperatures set new record highs during Autumn 2020 (October-December), and especially warm surface air temperatures returned over northern Eurasia in spring 2021. This spring warming was notable for the Laptev Sea, which experienced early onset of sea ice melt and retreat that supported record low sea ice extent for the area during May and June. Eurasian Arctic snow cover extent was also particularly low in May and June 2021, representing the 5th and 3rd lowest values on record since 1967.

While frozen landscapes—sea ice, land ice, permafrost, and snow—may be hallmarks of the Arctic system, the transition of ice to water and intensification of hydrologic cycles are increasingly important issues. Arctic river discharge, a landscape-level integrator of precipitation, melt, and thaw, maintains a long-term increasing trend. Signs of seasonal change are also abundant, and dates that would historically have had precipitation fall as snow are experiencing precipitation as rain. The summer 2020 snow-free period across Eurasia was the longest since records began in 1998. During summer 2021, the Greenland ice sheet experienced three extreme melt events. The last heatwave, during August 2021, was the latest date of an extreme melt event within the 43-year satellite record. This event also brought the first observations of substantial rainfall to the highest Greenland ice sheet elevations at Summit Station, the long-term observatory and research station established in 1989. Unusual events are also evident across seasons. April 2021 saw the lowest post-winter sea ice volume since records began in 2010, likely influenced by an atypical lull in sea ice expansion during March-April, historically a time of continued ice growth. In September the amount of multi-year ice remaining was the second lowest on record (since 1985).

Environmental observations throughout the Arctic highlight important connections across seasons. Early spring 2021 sea ice loss in the Laptev Sea may have contributed to the high sea surface temperatures observed there during August, in parallel with warm sea surface temperatures in the Kara Sea and east of Greenland. In contrast, sea ice was advected into the Beaufort and Chukchi Seas during winter and spring, creating a late and limited sea ice retreat in the region. August sea surface temperatures in the Chukchi Sea were lower than normal, as well as in the northern Barents Sea and Baffin Bay.

Extreme events and amplified local processes indicate an Arctic of increasing regional and temporal variability. For example, while 2021 was yet another year of exceptionally high tundra greenness, extreme events and other local influences (e.g., permafrost thaw, pest outbreaks, or wildfires) are also creating more frequent local browning events. In another example, annual ocean primary productivity in 2021 was high (compared to the 2003-20 mean) for seven of nine Arctic study regions. Yet May 2021 data revealed a ~1700 km long swath of low chlorophyll-*a* concentrations stretching from the Greenland to Barents Seas.

Geography of the Arctic with major water bodies, rivers, and countries noted. Map by Climate.gov.

As the Arctic transforms, science in some cases is running to keep up. The added carbon in the atmosphere is warming the air and waters, and likely acidifying the Arctic Ocean faster than the global ocean. Facing difficulties to measure acidification in situ, researchers are striving not only to make more robust autonomous field instruments but also to enhance the theoretical and computer modeling infrastructure that assists in addressing this important change across such a vast and challenging ocean.

With research revealing new complex changes, collaborative groups are pushing for more coordination to communicate observations, impacts, and understanding across researchers, Arctic communities, agencies, and a range of stakeholders. The connections between physical environmental change and human impact are immutable, and rapid change demands new structures for people to work together across scales and institutions. As local observers and remote sensing scientists found a doubling of North

American beaver ponds in Alaska since 2000, they came together to establish an Arctic Beaver Observation Network that can aid collaboration, research, and information sharing. Natural hazard events that threaten lives and infrastructure are also increasing as glaciers melt and permafrost thaws. Researchers are in the early stages of understanding and projecting these events and are seeking routes to better inform stakeholders and affected communities.

The COVID-19 pandemic also brought disruption, for example, amplifying Alaska Natives' challenges in accessing traditional and store-bought foods. Indigenous cultural strengths, such as food sharing, were able to reduce stresses on food security. Yet when subsistence harvests are closed due to animal population concerns, Alaska Native communities are not only impacted financially, but also culturally, socially, and spiritually. Within an essay contributed by members of the Indigenous Foods Knowledges Network (IFKN) and across other ARC2021 essays, there's a clear need to reduce future harm in part by expanding the decision-making table, increasing Indigenous and local-Arctic research, management, and input.

Declining sea ice extent and shifting marine habitats are also bringing increased ship traffic to the Arctic. The uptick in human activity along with environmental change is altering the marine soundscape. The full scope of impacts is not yet known, though research indicates that marine mammal communication may drop and stress levels increase as the sound wavelengths animals use for communication are overlaid with human-produced sounds. Arctic marine traffic is also implicated in a widespread marine debris event that brought extensive garbage ashore within the Bering Strait region in 2020. Alaska residents in the Bering Strait region found excessive trash with foreign language labeling—a reminder that Arctic issues are international issues. Local Arctic residents are often required to carry the heaviest burden of dealing with the impacts for which they bear little to no responsibility. Responding to environmental changes, managing increasing human activities, and improving future outcomes will require attention and efforts at multiple levels of government, across communities and organizations, and amongst Arctic and non-Arctic countries.

The challenges of a changing Arctic are formidable. Yet the collaborative efforts apparent across ARC2021 essays give us hope that people from across communities are increasingly forging new relationships and connections that can help to understand, adapt to, and mitigate the challenges ahead. The Arctic story is a human story, and we all have a role to play in creating the best possible outcomes for the region, its residents, and all the citizens of the globe who depend on the Arctic as a critical component of our Earth system.

December 6, 2021

Surface Air Temperature

DOI: 10.25923/53xd-9k68

T. J. Ballinger[1], J. E. Overland[2], M. Wang[2,3], U. S. Bhatt[4], B. Brettschneider[5], E. Hanna[6], I. Hanssen-Bauer[7], S. -J. Kim[8], R. L. Thoman[1,9], and J. E. Walsh[1]

[1]International Arctic Research Center, University of Alaska Fairbanks, Fairbanks, AK, USA
[2]Pacific Marine Environmental Laboratory, NOAA, Seattle, WA, USA
[3]Cooperative Institute for Climate, Ocean, and Ecosystem Studies, University of Washington, Seattle, WA, USA
[4]Geophysical Institute, University of Alaska Fairbanks, Fairbanks, AK, USA
[5]National Weather Service Alaska Region, NOAA, Anchorage, AK, USA
[6]School of Geography and Lincoln Centre for Water and Planetary Health, University of Lincoln, Lincoln, UK
[7]Norwegian Meteorological Institute, Blindern, Oslo, Norway
[8]Korea Polar Research Institute, Incheon, Republic of Korea
[9]Alaska Center for Climate Assessment and Policy, University of Alaska Fairbanks, Fairbanks, AK, USA

Highlights

- This past year (October 2020-September 2021) was the seventh warmest on record over Arctic lands (beginning in 1900 with surface air temperature anomalies 1.1°C above the 1981-2010 mean).
- The *warmest* Pan-Arctic and Asian Arctic autumn (October-December) terrestrial air temperatures were observed in 2020.
- For the second consecutive year, much higher-than-normal air temperatures were observed over northern Eurasia, and especially the Laptev Sea, during autumn of 2020 and spring of 2021.
- Temperature extremes yielded some unprecedented impacts on the Arctic environment, including the *first* rainfall observed at Summit at the top of Greenland.

Introduction

Surface air temperatures (SAT), typically measured at a height of 1.5 to 2 meters above land, ocean, or ice cover, are one of the most telling observational indicators and drivers of Arctic climate change (Box et al. 2019). Averaged SAT across Arctic lands (north of 60 °N), which have a higher density of weather observations relative to the Arctic Ocean and glaciated environments, have shown a pronounced, positive warming trend of nearly 3°C since the mid-1960s (Fig. 1). These increased air temperatures have been associated with changes in the frequency, intensity, and duration of Arctic atmospheric and hydrological extremes (Walsh et al. 2020) with impacts on permafrost thaw, glacier melt, and sea ice decline amongst other components of the Arctic and broader Earth system (Moon et al. 2019; see essays on the *Greenland Ice Sheet* and *Sea Ice*). In this essay, we recap the annual and seasonal Arctic SAT conditions of the last year (October 2020-September 2021) and place them in context compared to recent decades.

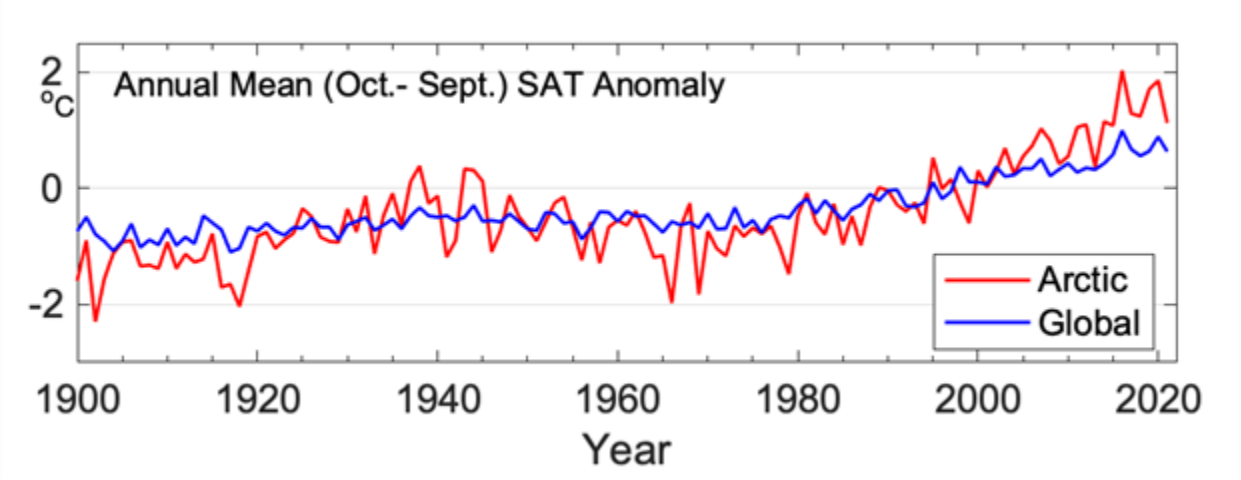

Fig. 1. Mean annual SAT anomalies (in °C) for weather stations located on Arctic lands, 60-90° N (red line), and globally (blue line) for the 1900-2021 period (n=122 years). Each temperature time series is shown with respect to their 1981-2010 mean. Source: CRUTEM5 SAT data are obtained from the Climate Research Unit (University of East Anglia) and Met Office.

Overview of the past year's terrestrial Arctic surface air temperatures

Averaged over the period from October 2020 to September 2021, the Arctic SAT anomaly for land areas north of 60° N was 1.1°C above the 1981-2010 mean (Fig. 1). This annual SAT anomaly marked the eighth consecutive year since 2014 that land temperature anomalies have reached at least 1°C. Considering the 1900 to 2021 historical period, 2021 was the seventh warmest year on record. The warmest autumn (October-December) and fourth warmest spring (April-June) in the Arctic strongly contributed to the annual temperature anomaly (Table 1). Autumn 2020 was also much warmer than average at the regional scale with record warming over the Asian Arctic, while the European Arctic saw its second highest SAT since 1900. The Greenland-Iceland region also had its third warmest summer (July-September) on record in 2021.

Table 1. Pan-Arctic and regional SAT rankings for different seasons during October 2020 through September 2021. The rankings are based on seasonal temperature data since 1900. Longitudinal bounds for each of the four regions are shown in parentheses, and the corresponding southern extent for all areas is 60° N. The warmest season since 1900 is shown in **bold**, while seasons of at least 90th percentile warming are shown in *italics*. Source: CRUTEM5 SAT data are obtained from the Climate Research Unit (University of East Anglia) and Met Office.

Season	Pan-Arctic	European Arctic (0-90° E)	Asian Arctic (90-180° E)	North American Arctic (180° E-60° W)	Greenland-Iceland Region (60° W-0° E)
OND 2020	**Warmest**	*2nd warmest*	**Warmest**	*7th warmest*	*6th warmest*
JFM 2021	53rd warmest	95th warmest	65th warmest	24th warmest	*5th warmest*
AMJ 2021	*4th warmest*	*5th warmest*	*7th warmest*	21st warmest	19th warmest
JAS 2021	*11th warmest*	*13th warmest*	*12th warmest*	28th warmest	*3rd warmest*

It is notable that since 2000, on average, annual Arctic SAT anomalies have exceeded their global mean SAT counterpart by more than a factor of two (Fig. 1). This enhanced boreal warming pattern, often termed "Arctic Amplification," results from a complex interplay of localized feedbacks and energy transport into the region (Previdi et al. 2021). These mechanisms vary in the Arctic across space and time, and their interactions can have compounding effects on Arctic change. For example, declines in the late spring and summer Arctic sea ice and Eurasian Arctic terrestrial snow cover decrease the albedo (solar reflectivity) of these respective areas, which enables more solar radiation absorption and accelerates surface warming (see essays on *Sea Ice*, *Sea Surface Temperature*, and *Snow Cover*). Meanwhile, oceanic and atmospheric heat transport can affect the Arctic cryosphere and interconnected ocean-ice-atmosphere interactions throughout the year (Cohen et al. 2020).

Seasonal recap of Arctic air temperatures

Arctic air temperature anomalies and extremes are further discussed by season: autumn 2020 (October-December [OND]), winter (January-March [JFM]), spring (April-June [AMJ]), and summer (July-September [JAS]) 2021 (Fig. 2). To emphasize large-scale air temperature patterns versus local variability, near-surface air temperatures at 925 hPa (~750 meters above the surface) are described. The seasons are defined to span the water year (October-September) and coincide with annual cycles of variables discussed in the Arctic Report Card. For example, melt of Arctic sea-ice tends to begin in spring and reach its seasonal minimum in late summer, i.e., September.

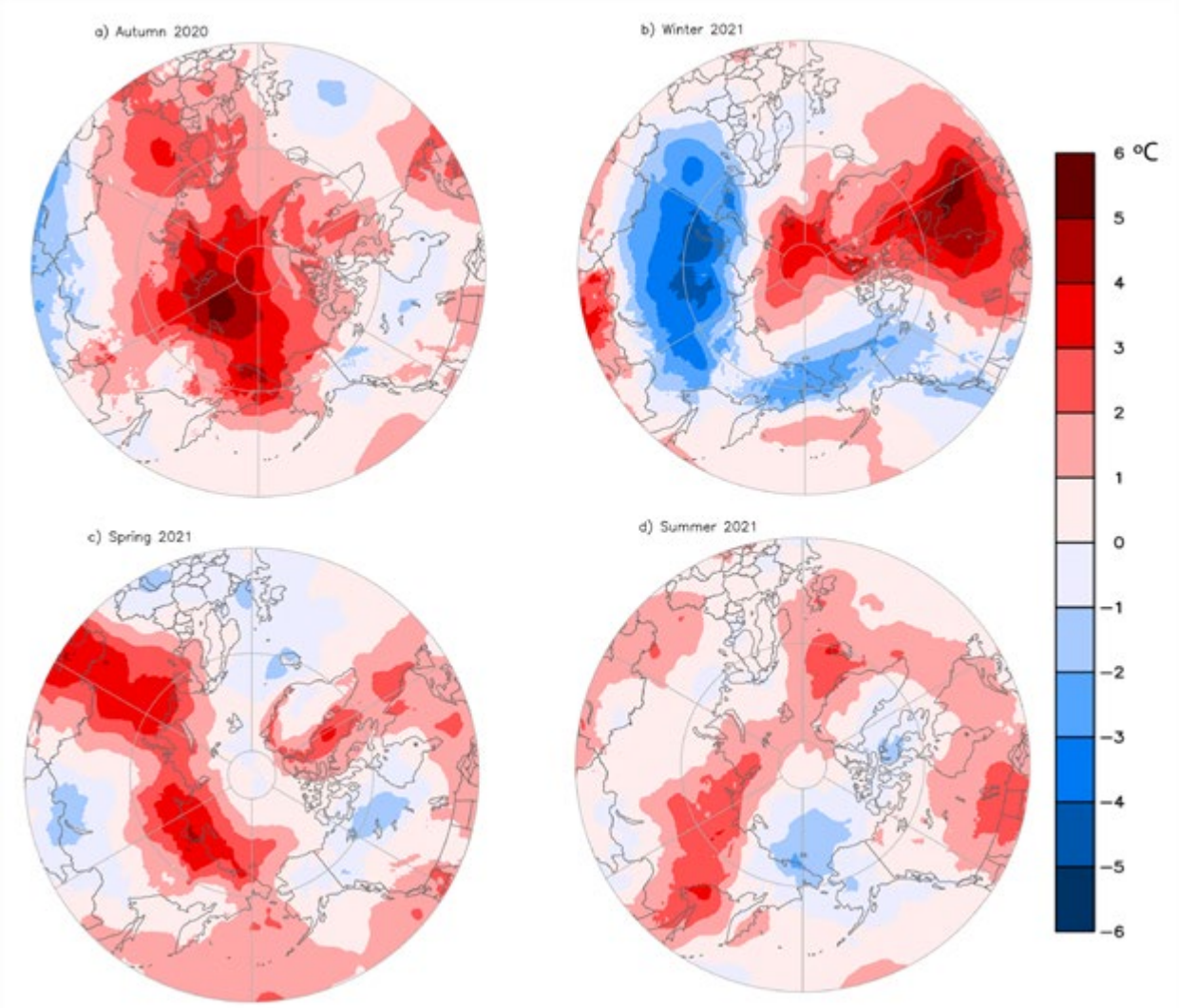

Fig. 2. Near-surface (925 hPa) seasonal air temperature anomalies (in °C) for (a) autumn 2020, (b) winter 2021, (c) spring 2021, and (d) summer 2021. Anomalies are shown relative to their 1981-2010 means. Source: ERA5 reanalysis air temperature data are obtained from the Copernicus Climate Change Service.

Autumn 2020. Widespread air temperature anomalies of at least 1-2°C above normal were observed across the Arctic Ocean and adjacent lands during autumn (Fig. 2a). Temperature anomalies were warmest atop the Laptev Sea (5-7°C) and over Chukotka extending into the Chukchi Sea (4-6°C). A trough in the jet stream over eastern Eurasia (Fig. 3a) supported relatively warm, southerly airflow across the Chukchi (see essay on *Sea Ice*). This wind pattern, coupled with heat exchange from the warm, upper ocean to the overlying atmosphere, likely contributed to the Chukchi region's positive air temperature anomaly. Terrestrial high-latitude temperatures were also above average within autumn. November was characterized by record warmth both in Norway (tying the record set in 2011 in a series starting in 1900; Grinde et al. 2020) and in Sweden (0.1°C above the previous record from 2000 in a series dating from 1860; SMHI 2020).

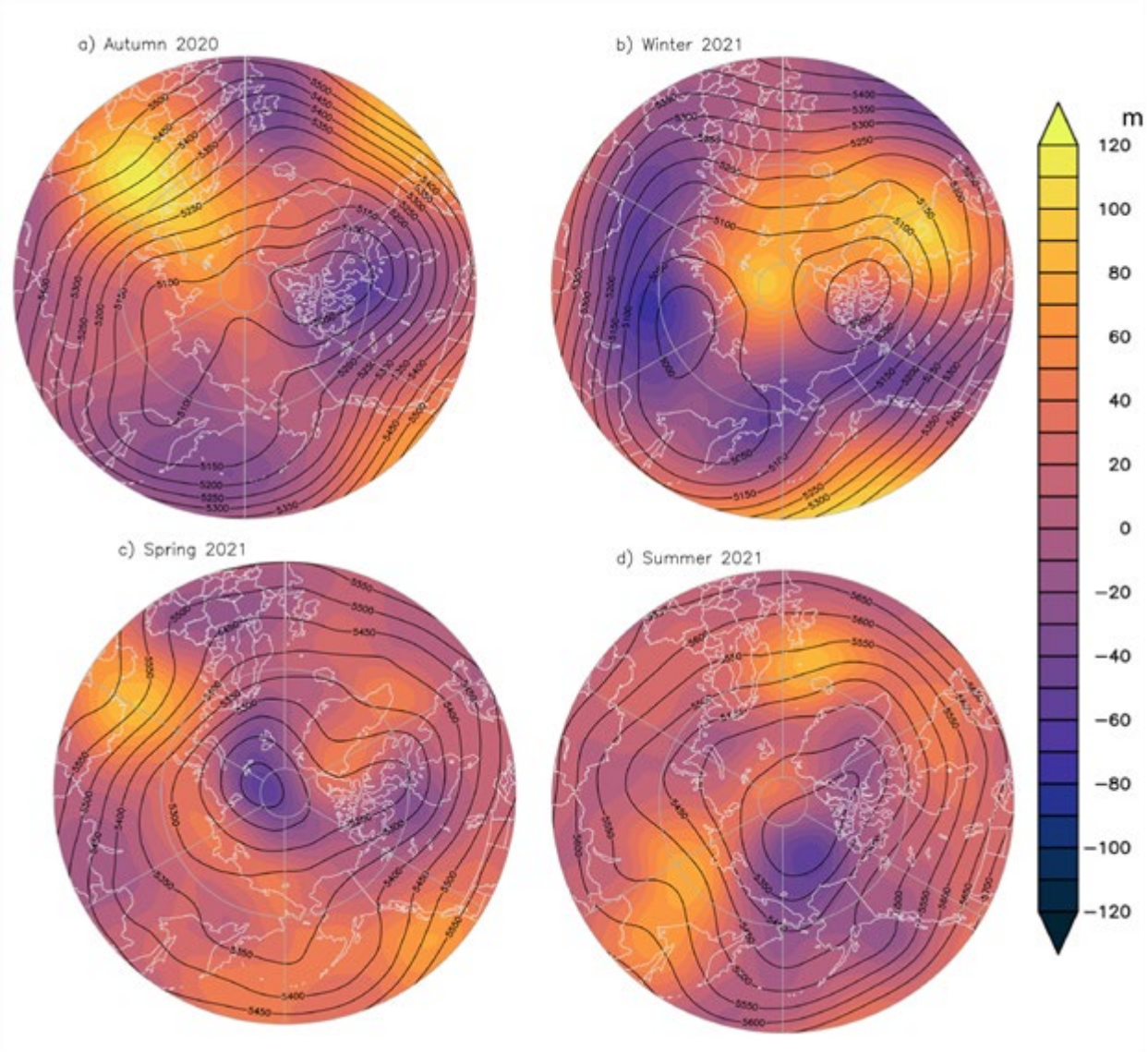

Fig. 3. Mid-tropospheric circulation patterns described by 500 hPa geopotential heights (contours) for (a) autumn 2020, (b) winter 2021, (c) spring 2021, and (d) summer 2021. The geopotential height values are listed in meters (m) from the surface. Anomaly values in the 500 hPa seasonal fields are overlaid for reference (shading). Corresponding winds tend to circulate clockwise around higher height values. Source: ERA5 reanalysis geopotential height data are obtained from the Copernicus Climate Change Service.

Winter 2021. During winter, a sharp temperature contrast between the Arctic Ocean and lands was present over much of the region. The central Arctic Ocean SAT remained 2-4°C warmer than normal, while cold anomalies predominantly extended from coastal zones southward into northern Eurasia and northwestern North America, including north-central Alaska and the Yukon and Northwest Territories (Fig. 2b). Much of western Greenland, Baffin Bay, Labrador Sea, and adjacent northeastern Canadian lands experienced near-surface air temperatures 3-5°C above average. Two lobes developed in the winter jet stream with one lobe steering polar air southward into north-central Eurasia and the other lobe transporting cold air into the North American lower latitudes (Fig. 3b).

Spring 2021. Springtime coincided with warmer-than-average conditions over the Arctic Ocean and adjacent lands (Fig. 2c). Air temperatures in northern Eurasia coastal areas and adjacent Arctic waters were 2-4°C warmer than the 1981-2010 average. Air temperatures over Baffin Bay and the Labrador Sea were also above normal. The swath of higher-than-normal Eurasian spring air temperatures was associated with low snow cover and anomalously early melt of the Laptev Sea's ice cover (see essays on *Terrestrial Snow Cover* and *Sea Ice*). Several air temperature records were set at Arctic weather stations, including 39.9°C (103.8°F) observed at Fort Smith, Northwest Territories, Canada, on 30 June 2021, which broke the provincial maximum surface temperature record (Henson and Masters 2021).

Summer 2021. The highest summer air temperature anomalies were found over northern Iceland and the Greenland Sea (2-3°C) and across the Sea of Okhotsk (3-4°C), extending into Eurasia (Fig. 2d). Another active wildfire season in eastern Siberia was associated with warmer-than-normal air temperatures (Dixon 2021). Air temperatures of 1-2°C below normal were found in the Pacific Arctic over portions of the Beaufort, Chukchi, and East Siberian Seas. Positive temperature anomalies were present over the North Atlantic Arctic during which anomalous air temperature events occurred in late July and mid-August, producing melt extremes on the Greenland Ice Sheet. Of note, the National Science Foundation's Summit Station, situated at the highest point on the ice sheet, experienced a rare melt event, and rain was reported for the first time since the station's inception in 1989 (see essay on *Greenland Ice Sheet*).

Data overview

CRUTEM5 SAT data (Osborn et al. 2021) are used to place pan-Arctic and regional land temperatures in an annual and seasonal context. ERA5 reanalysis (Hersbach et al. 2020) is implemented to show large-scale seasonal air temperature and geopotential height fields. Previous iterations of the ARC have used NCEP/NCAR reanalysis (Kalnay et al. 1996) to highlight similar climate variables, though in the 2021 essay we transition to the newer, higher spatiotemporal resolution ERA5 reanalysis that has generally been shown to perform well in Arctic terrestrial and marine environments (Graham et al. 2019; Avila-Diaz et al. 2021).

References

Avila-Diaz, A., D. H. Bromwich, A. B. Wilson, F. Justino, and S. -H. Wang, 2021: Climate extremes across the North American Arctic in modern reanalyses. *J. Climate*, **34**, 2385-2410, https://doi.org/10.1175/JCLI-D-20-0093.1.

Box, J. E., and Coauthors, 2019: Key indicators of Arctic climate change: 1971-2017. *Environ. Res. Lett.*, **14**, 045010, https://doi.org/10.1088/1748-9326/aafc1b.

Cohen, J., and Coauthors, 2020: Divergent consensuses on Arctic Amplification influence on mid-latitude severe winter weather. *Nat. Climate Change*, **10**, 20-29, https://doi.org/10.1038/s41558-019-0662-y.

Dixon, R., 2021: Siberia's wildfires are bigger than all the world's other blazes combined. The Washington Post, https://www.washingtonpost.com/world/2021/08/11/siberia-fires-russia-climate/ (11 August 2021).

Graham, R. M., and Coauthors, 2019: Evaluation of six atmospheric reanalyses over Arctic sea ice from winter to early summer. *J. Climate*, **32**, 4121-4143, https://doi.org/10.1175/JCLI-D-18-0643.1.

Grinde, L., J. Mamen, K. Tunheim, and O. E. Tveito, 2020: Klimatologisk oversikt. November 2020, MET info 11/2020 (in Norwegian), ISSN 1894-759X.

Henson, B., and J. Masters, 2021: Western Canada burns and deaths mount after world's most extreme heat wave in modern history. Yale Climate Connections, https://yaleclimateconnections.org/2021/07/western-canada-burns-and-deaths-mount-after-worlds-most-extreme-heat-wave-in-modern-history/ (1 July 2021).

Hersbach, H., and Coauthors, 2020: The ERA5 global reanalysis. *Q. J. Roy. Meteor. Soc.*, **146**, 1999-2049, https://doi.org/10.1002/qj.3803.

Kalnay, E., and Coauthors, 1996: The NCEP/NCAR 40-year reanalysis project. *Bull. Amer. Meteor. Soc.*, **77**, 437-472, https://doi.org/10.1175/1520-0477(1996)077<0437:TNYRP>2.0.CO;2.

Moon, T. A., and Coauthors, 2019: The expanding footprint of rapid Arctic change. *Earths Future*, **7**, 212-218, https://doi.org/10.1029/2018EF001088.

Osborn, T. J., P. D. Jones, D. H. Lister, C. P. Morice, I. R. Simpson, J. P. Winn, E. Hogan, and I. C. Harris, 2021: Land surface air temperature variations across the globe updated to 2019: the CRUTEM5 dataset. *J. Geophys. Res.-Atmos.*, **126**, e2019JD032352, https://doi.org/10.1029/2019JD032352.

Previdi, M., K. L. Smith, and L. M. Polvani, 2021: Arctic amplification of climate change: A review of underlying mechanisms. *Environ. Res. Lett.*, **16**, 093003, https://doi.org/10.1088/1748-9326/ac1c29.

SMHI, 2020: November 2020–Värmerekord efter värmerekord. Månadens väder, November 2020 (in Swedish) Published 30 Nov 2020, Updated 17 Feb 2021.

Walsh, J. E., T. J. Ballinger, E. S. Euskirchen, E. Hanna, J. Mård, J. E. Overland, H. Tangen, and T. Vihma, 2020: Extreme weather and climate events in northern areas: A review. *Earth-Sci. Rev.*, **209**, 103324, https://doi.org/10.1016/j.earscirev.2020.103324.

November 17, 2021

Terrestrial Snow Cover

DOI: 10.25923/16xy-9h55

L. Mudryk[1], A. Elias Chereque[2], C. Derksen[1], K. Luojus[3], and B. Decharme[4]

[1]Climate Research Division, Environment and Climate Change Canada, Toronto, ON, Canada
[2]Department of Physics, University of Toronto, Toronto, ON, Canada
[3]Arctic Research Centre, Finnish Meteorological Institute, Helsinki, Finland
[4]Météo-France/CNRS, Centre National de Recherches Météorologiques, Toulouse, France

Highlights

- Eurasian Arctic snow cover extent (SCE) anomalies were strongly negative in both May (5th lowest in the record since 1967) and June (3rd lowest) 2021. North American Arctic spring 2021 SCE anomalies were also below average (14th and 16th lowest, respectively).
- The summer 2020 snow-free period across Eurasia was the longest since at least 1999.
- Since 2006, North American June SCE has been below the long-term average every year, while Eurasian June SCE has been below the long-term average for every year but one.

Introduction

Many components of the Arctic land surface are directly influenced by snow cover from autumn through spring, including the surface energy budget (Flanner et al. 2011), ground thermal regime (with implications on the carbon cycle; Natali et al. 2019), permafrost (Walvoord and Kurylyk 2016), and terrestrial and freshwater ecosystems (Bokhorst et al. 2016). Even following the snow cover season, the influence of spring snow melt timing persists through impacts on river discharge timing and magnitude, surface water, soil moisture, vegetation phenology, and fire risk (Meredith et al. 2019). The assessment provided here is based on multiple datasets derived from satellite observations and snowpack models driven by atmospheric reanalyses. Collectively, this approach provides a reliable picture of Arctic snow cover variability over the last five decades.

We characterize snow conditions across the Arctic land surface using three quantities: how much total land area is covered by snow (snow cover extent - SCE), how much of the year snow covers the land surface (snow cover duration - SCD), and how much total water is stored in solid form in the snowpack. This last quantity is determined from the snow water equivalent (SWE), which is the product of snow depth and density. SWE can be aggregated across the Arctic land surface to provide an estimate of the total mass of water stored by snow. We examine each of these quantities in turn for the Arctic snow season spanning autumn 2020 through spring 2021.

Snow cover extent and duration

SCE anomalies (relative to the 1981-2010 climatology) in spring 2021 are shown separately for the North American and Eurasian terrestrial sectors of the Arctic in Fig. 1. Eurasian Arctic anomalies were strongly negative in May (5th lowest in the record since 1967) and June (3rd lowest). North American Arctic spring SCE anomalies in 2021 were also below average (14th and 16th lowest, respectively).

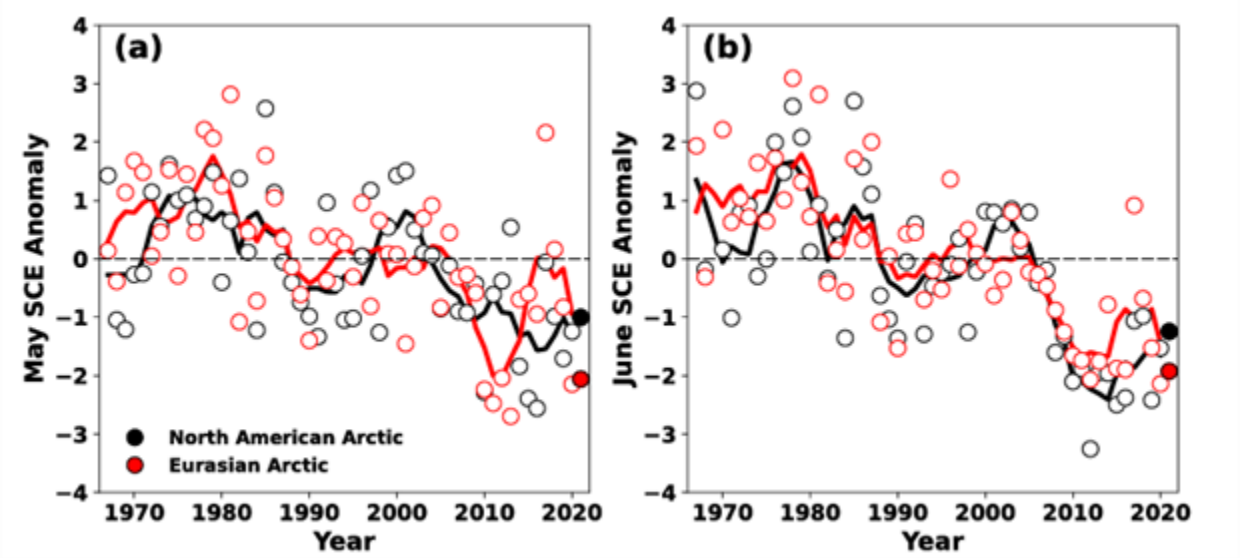

Fig. 1. Standardized monthly snow cover extent anomalies for Arctic land areas (>60° N) for (a) May, and (b) June from 1967 to 2021. Solid black and red lines depict 5-year running means for North America and Eurasia, respectively. Filled circles are used to highlight 2021 anomalies. Source: NOAA snow chart Climate Data Record (CDR).

Snow cover duration (SCD) anomalies across the Arctic region for the 2020-2021 snow season are shown in Fig. 2 for both snow onset and snow melt periods of the year (see Methods and data). Onset anomalies indicate snow cover during autumn 2020 began later than normal over much of Eurasia, particularly in eastern Siberia, as well as over much of Alaska and the western Canadian Arctic (Fig. 2a). Coupled with the early spring melt in 2020 (see last year's Arctic Report Card: Mudryk et al. 2020a), the complete 2020 snow-free period was the longest since the start of the database in 1998 across Eurasia and the second longest across the entire Arctic, with implications for Arctic vegetation (see essay *Tundra Greenness*). Spring 2021 (Fig. 2b) also had early snow melt and hence shorter SCD over almost the entire Arctic. In particular, across broad expanses of Eurasia the duration of the spring snow-free period was 30-50% longer than normal. As during the spring 2020 snow season, the early Eurasian melt in 2021 was driven by persistent, above-average temperatures during April-June (see essay *Surface Air Temperature*). While the early melt during 2021 was more extensive across Eurasia than the previous year, it was slightly less intense, resulting in near—but not record—low Eurasian Arctic SCE during June 2021.

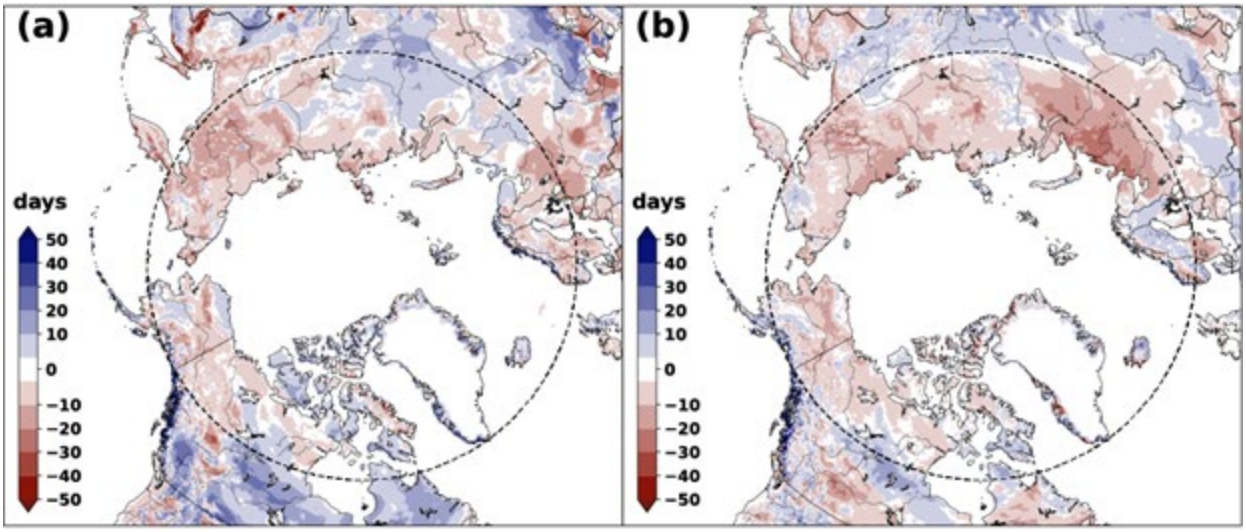

Fig. 2. Snow cover duration anomalies (% difference relative to normal number of snow-free days) for the 2020-21 snow year: (a) snow onset (Aug-Jan), and (b) snow melt (Feb-Jul). Red (blue) indicates increased (decreased) snow-free days compared to the 1999-2018 mean. The grey circle marks the latitude 60° N; land north of this defines Arctic land areas considered in this study. Source: NOAA IMS data record.

Snow mass and snow water equivalent

For Arctic regions as a whole, snow mass tends to peak seasonally during April, when snowfall has accumulated since the preceding autumn but before increasing temperatures during May and June lead to snow melt. Snow mass anomalies for April 2021 (Fig. 3) indicate above normal total snow accumulation in the North American Arctic and slightly below average accumulation over the Eurasian Arctic. Figure 4 illustrates SWE varied regionally from just before peak (March) through the end of the melt period (June). The above normal April snow mass in North America (Fig. 3) is already apparent in March SWE across much of the region (except for parts of the mainland adjacent to the Beaufort Sea). Over Eurasia, snow accumulation through March was near-normal: above average SWE in central and eastern Siberia was balanced by below average SWE in western Russia and Scandinavia. The high spring temperatures previously mentioned drove SWE reductions across western Eurasia in April (see April-June temperature anomaly pattern Fig. 2c in essay *Surface Air Temperature*). By May, SWE was below normal across most of the continent. In contrast to Eurasia, SWE across North America generally remained above normal amounts through June particularly in the Canadian Arctic Archipelago. However, even where SWE was seasonally above average, complete snow melt tended to occur slightly earlier than usual over most of the region (apparent by comparing Fig. 2b with Figs. 4c and 4d). This combination of increased snow accumulation (expressed as April SWE in Fig. 4b) but early snow melt (expressed by shorter SCD in Fig. 2b) is consistent with the expected changes to Arctic snow cover in a warmer Arctic (Meredith et al. 2019), reflected also in earlier and larger peak river discharge as observed over Eurasia during spring 2020 (see essay *River Discharge*).

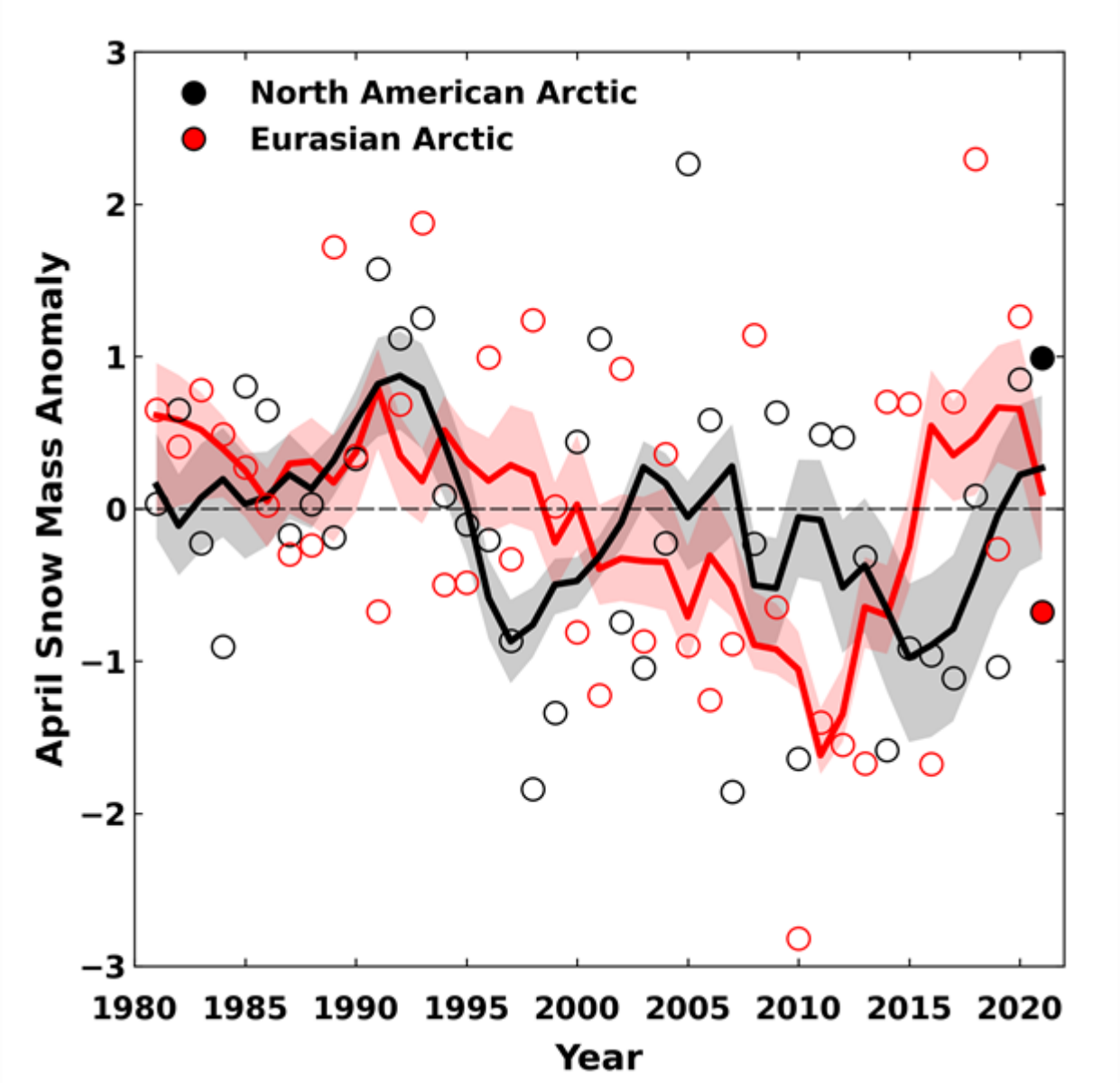

Fig. 3. Standardized April snow mass anomalies for Arctic land areas across the North American (black) and Eurasian (red) sectors. Anomalies represent the ensemble mean from a suite of four independent snow analyses (see Methods and data). Filled circles are used to highlight 2021 anomalies. Solid black and red lines depict 5-yr running means; shading depicts the spread among the running means of individual datasets. Source: snow analyses as described in Methods and data.

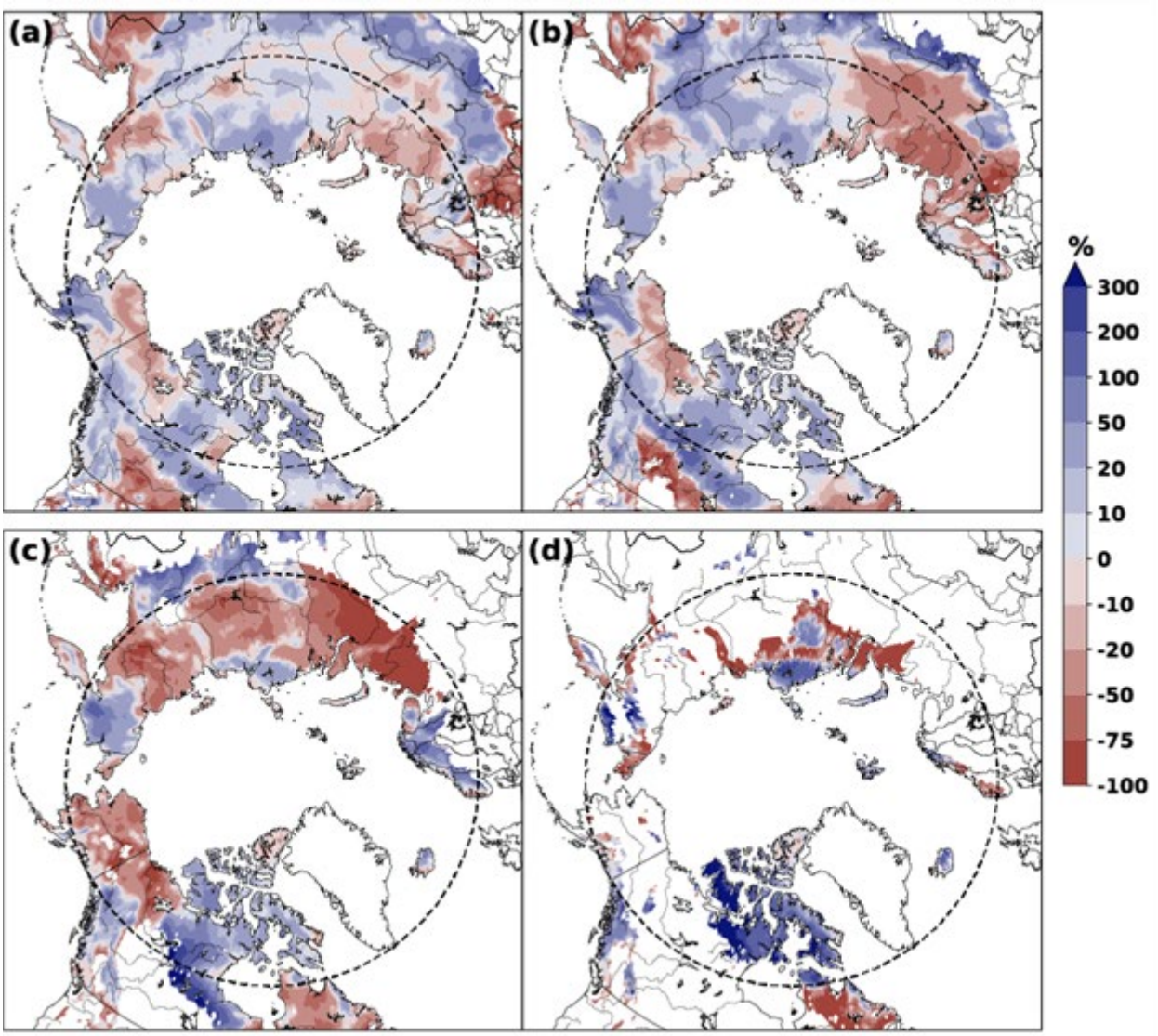

Fig. 4. Snow water equivalent (SWE) anomalies (% difference from the 1981-2010 average) in 2021 for (a) March, (b) April, (c) May, and (d) June. Anomalies represent the ensemble mean from a suite of four independent snow analyses (see Methods and data). The grey circle marks the latitude 60° N.

Summary and long-term trends

In summary, snow accumulation during the 2020/21 winter was near normal across the Eurasian Arctic and above normal across the North American Arctic. Regardless of the seasonal accumulation, spring snow extent has been persistently below normal for the last 15 years. Since 2006, North American June SCE has been below the long-term average every year, while Eurasian June SCE has been below the long-term average for all but one year. Long-term trends for total Arctic SCE, derived from the data presented in Fig. 1, are -3.8 ± 1.9% decade^{-1}, and -15.5 ± 5.8% decade^{-1} for May and June, respectively (1981-2021). These trends are more negative compared to a range of other sources, as discussed in Mudryk et al. (2017, 2020b). The April trend in Arctic snow mass over the 1981-2021 period is more moderate, reflecting larger interannual variability. Calculated from the data presented in Fig. 3, the snow mass

trend is -2.0 ± 1.7% decade^{-1}, representing a decrease in seasonally stored water of close to 10% over the entire Arctic since 1981.

Methods and data

Snow cover extent (SCE) anomalies are derived from the NOAA snow chart climate data record, which extends from 1967 to present (Estilow et al. 2015; Robinson et al. 2012). Monthly anomalies of total areal snow cover over land for a given Arctic sector (North America or Eurasia, > 60° N) are computed and standardized relative to the 1981-2010 period (each observation differenced from the mean and divided by the standard deviation and thus unitless).

Snow cover duration (SCD) fields are derived from the NOAA daily Interactive Multisensor Snow and Ice Mapping System (IMS) snow cover product (U.S. National Ice Center 2008). Anomalies in the total number of days with snow cover were computed separately for each half of the snow season: August 2020 to January 2021, referred to as "onset period," and February 2021 to July 2021, referred to as "melt period." IMS availability starts in 1998, so a 1999-2018 climatological period is used (including information from August-December 1998 for snow onset). Anomalies for each season are presented as percent differences from the climatological number of snow-free days. In the Arctic, this varies from approximately three months near 60° N, to approximately two months at 70° N, and decreases to less than a month over the Canadian Arctic Archipelago. Because the Arctic is generally always snow covered between November and April, Arctic region snow onset anomalies are indicative of conditions during September and October, while Arctic region snow melt anomalies are indicative of conditions during May and June.

Four snow water equivalent (SWE) analyses were used to generate multi-dataset SWE fields from March-June for the 1981-2021 period: (1) the European Space Agency Snow CCI SWE version1 product derived through a combination of satellite passive microwave brightness temperatures and climate station snow depth observations (Luojus et al. 2020); (2) the Modern-Era Retrospective Analysis for Research and Applications version 2 (MERRA-2, GMAO 2015; Gelaro et al. 2017) daily SWE fields; (3) SWE output from the ERA5-Land analysis (Muñoz Sabater 2019); and (4) the physical snowpack model Crocus (Brun et al. 2013) driven by ERA5 meteorological forcings. Reduced availability of climate station snow depth measurements limits the accuracy of the Snow CCI SWE product during May and June, hence we only use it during March and April. An approach using gridded products is required because in situ observations alone are too sparse to be representative of hemispheric snow conditions, especially in the Arctic where stations are particularly sparse. We consider multiple datasets because averaging multiple SWE products has been shown to be more accurate when validated with in situ observations (Mortimer et al. 2020). The ensemble-mean SWE field is used to calculate monthly SWE anomalies relative to the 1981-2010 period, and present them as percent differences. For April, the SWE fields for each product are also aggregated across Arctic land regions (> 60° N) for both North American and Eurasian sectors to produce multiple estimates of April snow mass. These monthly snow mass values are used to calculate standardized anomalies relative to the 1981-2010 period for each data product. The standardized anomalies are then averaged to produce an ensemble-mean time series.

Acknowledgments

ERA5-Land data (Muñoz Sabater 2019) were downloaded from the Copernicus Climate Change Service (C3S) Climate Data Store. The results contain modified Copernicus Climate Change Service information

2020. Neither the European Commission nor ECMWF is responsible for any use that may be made of the Copernicus information or data it contains.

References

Bokhorst, S., and Coauthors, 2016: Changing Arctic snow cover: A review of recent developments and assessment of future needs for observations, modelling, and impacts. *Ambio*, **45**, 516-537, https://doi.org/10.1007/s13280-016-0770-0.

Brun, E., V. Vionnet, A. Boone, B. Decharme, Y. Peings, R. Valette, F. Karbou, and S. Morin, 2013: Simulation of Northern Eurasian local snow depth, mass, and density using a detailed snowpack model and meteorological reanalyses. *J. Hydrometeor.*, **14**, 203-219, https://doi.org/10.1175/JHM-D-12-012.1.

Estilow, T. W., A. H. Young, and D. A. Robinson, 2015: A long-term Northern Hemisphere snow cover extent data record for climate studies and monitoring. *Earth Syst. Sci. Data*, **7**, 137-142, https://doi.org/10.5194/essd-7-137-2015.

Flanner, M. G., K. M. Shell, M. Barlage, D. K. Perovich, and M. A. Tschudi, 2011: Radiative forcing and albedo feedback from the Northern Hemisphere cryosphere between 1979 and 2008. *Nat. Geosci.*, **4**, 151-155, https://doi.org/10.1038/ngeo1062.

Gelaro, R., and Coauthors, 2017: The Modern-era retrospective analysis for research and applications, Version 2 (MERRA-2). *J. Climate*, **30**, 5419-5454, https://doi.org/10.1175/JCLI-D-16-0758.1.

GMAO (Global Modeling and Assimilation Office), 2015: MERRA-2tavg1_2d_lnd_Nx:2d, 1-Hourly, Time-Averaged, Single-Level, Assimilation, Land Surface Diagnostics V5.12.4, Goddard Earth Sciences Data and Information Services Center (GESDISC), accessed: 11 Aug 2021, https://doi.org/10.5067/RKPHT8KC1Y1T.

Luojus, K., and Coauthors, 2020: ESA Snow Climate Change Initiative (Snow_cci): Snow Water Equivalent (SWE) level 3C daily global climate research data package (CRDP) (1979-2018), version 1.0. Centre for Environmental Data Analysis, accessed: 19 Jul 2021, https://doi.org/10.5285/fa20aaa2060e40cabf5fedce7a9716d0.

Meredith, M., and Coathors, 2019: Polar Regions. IPCC Special Report on the Ocean and Cryosphere in a Changing Climate, H. -O. Pörtner, and co-editors, in press, https://www.ipcc.ch/srocc/.

Mortimer, C., L. Mudryk, C. Derksen, K. Luojus, R. Brown, R. Kelly, and M. Tedesco, 2020: Evaluation of long-term Northern Hemisphere snow water equivalent products. *Cryosphere*, **14**, 1579-1594, https://doi.org/10.5194/tc-14-1579-2020.

Mudryk, L. R., P. J. Kushner, C. Derksen, and C. Thackeray, 2017: Snow cover response to temperature in observational and climate model ensembles. *Geophys. Res. Lett.*, **44**, 919-926, https://doi.org/10.1002/2016GL071789.

Mudryk, L., A. Elias Chereque, R. Brown., C. Derksen, K., Luojus, and B. Decharme, 2020a: Terrestrial Snow Cover. *Arctic Report Card 2020*, R. L. Thoman, J. Richter-Menge, and M. L. Druckenmiller, Eds., https://doi.org/10.25923/p6ca-v923.

Mudryk, L., M. Santolaria-Otín, G. Krinner, M. Ménégoz, C. Derksen, C. Brutel-Vuilmet, M. Brady, and R. Essery, 2020b: Historical Northern Hemisphere snow cover trends and projected changes in the CMIP6 multi-model ensemble. *Cryosphere*, **14**, 2495-2514, https://doi.org/10.5194/tc-14-2495-2020.

Muñoz Sabater, J., 2019: ERA5-Land hourly data from 1981 to present. Copernicus Climate Change Service (C3S) Climate Data Store (CDS), accessed 11 Aug 2021, https://doi.org/10.24381/cds.e2161bac.

Natali, S. M., and Coauthors, 2019: Large loss of CO_2 in winter observed across the northern permafrost region. *Nat. Climate Change*, **9**, 852-857, https://doi.org/10.1038/s41558-019-0592-8.

Robinson, D. A., T. W. Estilow, and NOAA CDR Program, 2012: NOAA Climate Data Record (CDR) of Northern Hemisphere (NH) Snow Cover Extent (SCE), Version 1 [r01]. NOAA National Centers for Environmental Information, accessed: 8 Jul 2021, https://doi.org/10.7289/V5N014G9.

U.S. National Ice Center, 2008: IMS Daily Northern Hemisphere Snow and Ice Analysis at 1 km, 4 km, and 24 km Resolutions, Version 1. Boulder, Colorado USA. NSIDC: National Snow and Ice Data Center, accessed: 11 Aug 2021, https://doi.org/10.7265/N52R3PMC.

Walvoord, M. A., and B. L. Kurylyk, 2016: Hydrologic impacts of thawing permafrost—a review. *Vadose Zone J.*, **15**, vzj2016.01.0010, https://doi.org/10.2136/vzj2016.01.0010.

December 1, 2021

Greenland Ice Sheet

DOI: 10.25923/546g-ms61

T. A. Moon[1,2], M. Tedesco[3,4], J. E. Box[5], J. Cappelen[6], R. S. Fausto[5], X. Fettweis[7], N. J. Korsgaard[5], B. D. Loomis[8], K. D. Mankoff[5], T. L. Mote[9], A. Wehrlé[10], and Ø. A. Winton[5]

[1]Cooperative Institute for Research in Environmental Sciences, University of Colorado Boulder, Boulder, CO, USA
[2]National Snow and Ice Data Center, Boulder, CO, USA
[3]Lamont-Doherty Earth Observatory, Columbia University, Palisades, NY, USA
[4]Goddard Institute of Space Studies, NASA, New York, NY, USA
[5]Geological Survey of Denmark and Greenland, Copenhagen, Denmark
[6]Danish Meteorological Institute, Copenhagen, Denmark
[7]SPHERES Research Unit, University of Liège, Liège, Belgium
[8]Goddard Space Flight Center, NASA, Greenbelt, MD, USA
[9]Department of Geography, University of Georgia, Athens, GA, USA
[10]Institute of Geography, University of Zurich, Zurich, Switzerland

Highlights

- Greenland ice sheet total mass change for 1 September 2020 to 31 August 2021 was -85 ± 16 Gt, 179 Gt less than the 2002-21 average of -264 ± 12 Gt yr^{-1}.
- High variability characterized 2021 surface melting with a two-week long August period of increased melt and bare ice exposure contrasting with low June and July melt conditions. An overall average melt obscured strongly contrasting spatial and temporal melt patterns.
- On 14 August 2021, Greenland experienced the latest date of an extreme melt event (>50% area) within the 43-year satellite record, including the first reported rainfall at Summit Station, Greenland.

Introduction

The Greenland ice sheet covers ~1.63 million km^2 and contains ice equivalent to 7.4 m of eustatic sea level rise (Morlighem et al. 2017). Following decades of relative stability, the ice sheet has now lost mass almost every year since 1998, with tied years of record ice loss in 2012 and 2019 (Mankoff et al. 2021). Ice loss is exposing land, adding substantial freshwater into the ocean, and raising sea levels globally (Moon et al. 2020; Mankoff et al. 2020a; IMBIE Team 2020).

Total Greenland ice sheet mass balance is the sum of 1) the surface mass balance, which combines accumulated snow across the ice sheet with ice loss via surface melt and runoff, and 2) solid ice discharge via calving at tidewater glaciers. Surface melt in particular is sensitive to atmospheric and ice sheet surface conditions, and is a major component of ice loss (ablation). During the 2020-21 ice sheet balance year, spanning 1 September to 31 August, the total Greenland ice sheet mass change was -85 ± 16 Gt of ice as measured by the GRACE-FO satellite (Fig. 1). This is equivalent to ~0.2 mm of

sea level rise, not including ongoing thermal expansion (IPCC 2021). The 2020-21 total mass balance year had 179 Gt less mass loss than the 2002-21 average of -264 ± 12 Gt yr^{-1}.

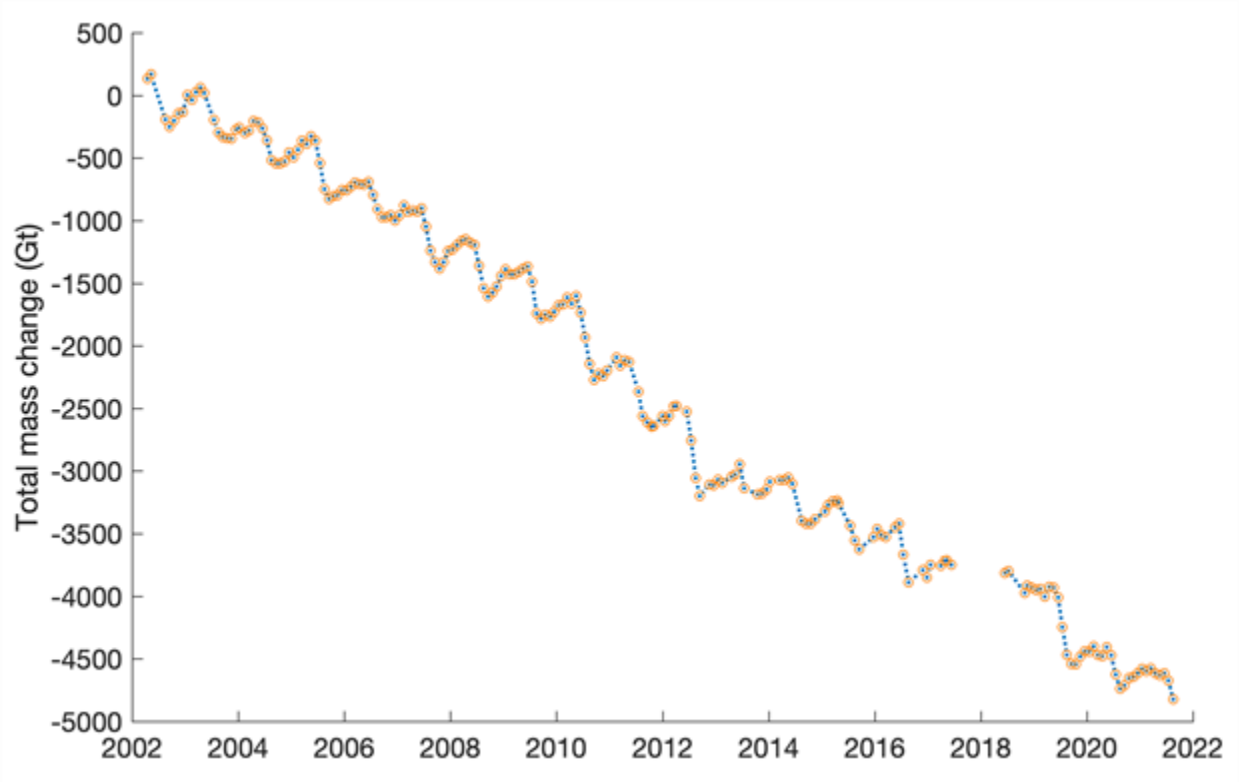

Fig. 1. Total mass change (Gt) of the Greenland ice sheet from April 2002 to August 2021 determined from GRACE (2002-17) and GRACE-FO (2018-Present) satellite data.

Surface temperature, melt, and ablation

Surface temperature observations at 15 terrestrial DMI weather stations (with record start dates spanning from 1784 to 1991) recorded near or above average temperatures throughout the balance year. Temperature anomalies were generally highest in winter (December-February), exceeding one standard deviation at 11 of the 15 stations. A new summer (June-August) high temperature record was set at the Danmarkshavn station in northeast Greenland and July-only heat records were set at several other northeast stations. Tasiilaq, in southeastern Greenland, set a new August high temperature.

Except for an above-average melt event on 27 April, the ice sheet daily melt extent as measured by satellites remained low until 26 May and through mid-summer remained mostly within the 1981-2010 10th to 90th percentiles (Fig. 2). In situ, on-ice PROMICE automated weather stations recorded temperatures within ±1 standard deviation for June and July. Late July and August, however, included three extreme melt episodes. The first, on 19 July, had melt across 702,000 km^2 (~43%) of the ice sheet surface. A second melt event on 28 July extended across 54% of the ice sheet surface, and a third melt episode concentrated on 14 August had 53% melt area and reached the highest ice sheet elevations (National Science Foundation's (NSF) Summit Station, 3216 m). All PROMICE weather stations along the ice sheet periphery recorded above-average air temperatures during all three events.

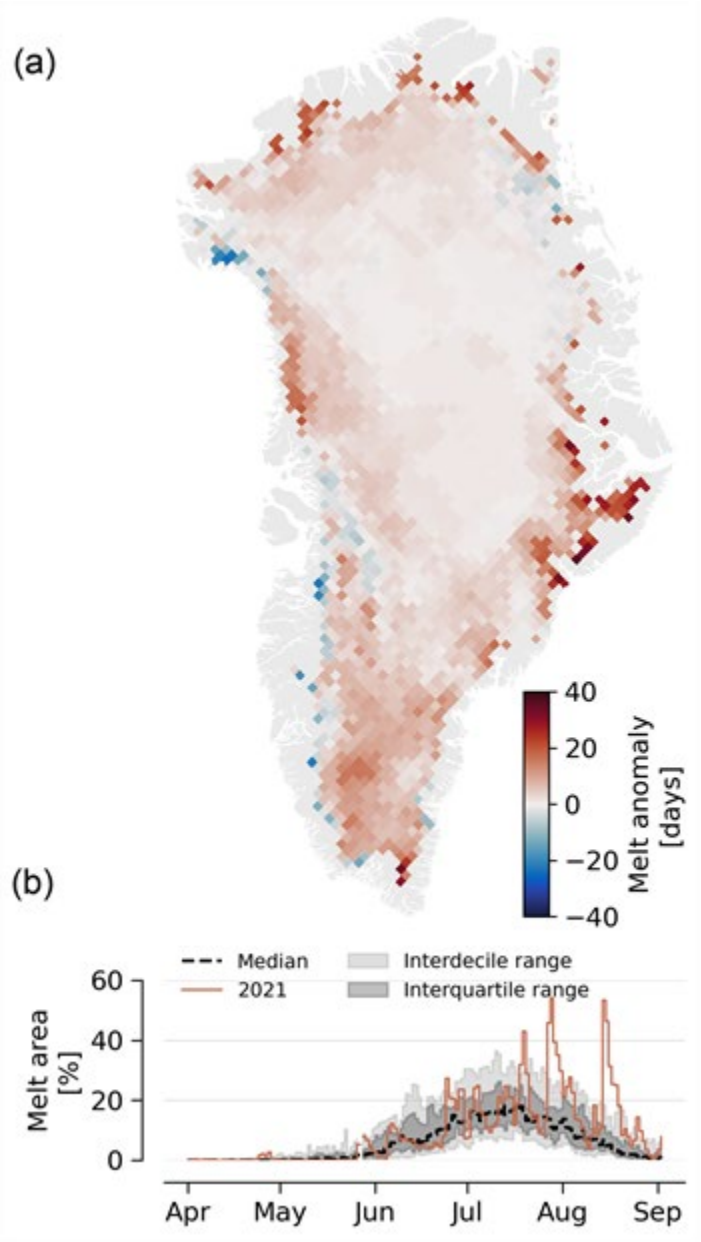

Fig. 2. (a) 2021 melt anomaly (in number of melting days) with respect to the 1981-2010 reference period, (b) Surface melt extent as a percentage of the ice sheet area during 2021 (solid red). Data derived from SSMIS satellite data.

For the full ablation season, PROMICE ablation measurements around the ice sheet margin indicate significantly above-average ablation along the central western and eastern coasts (Fig. 3).

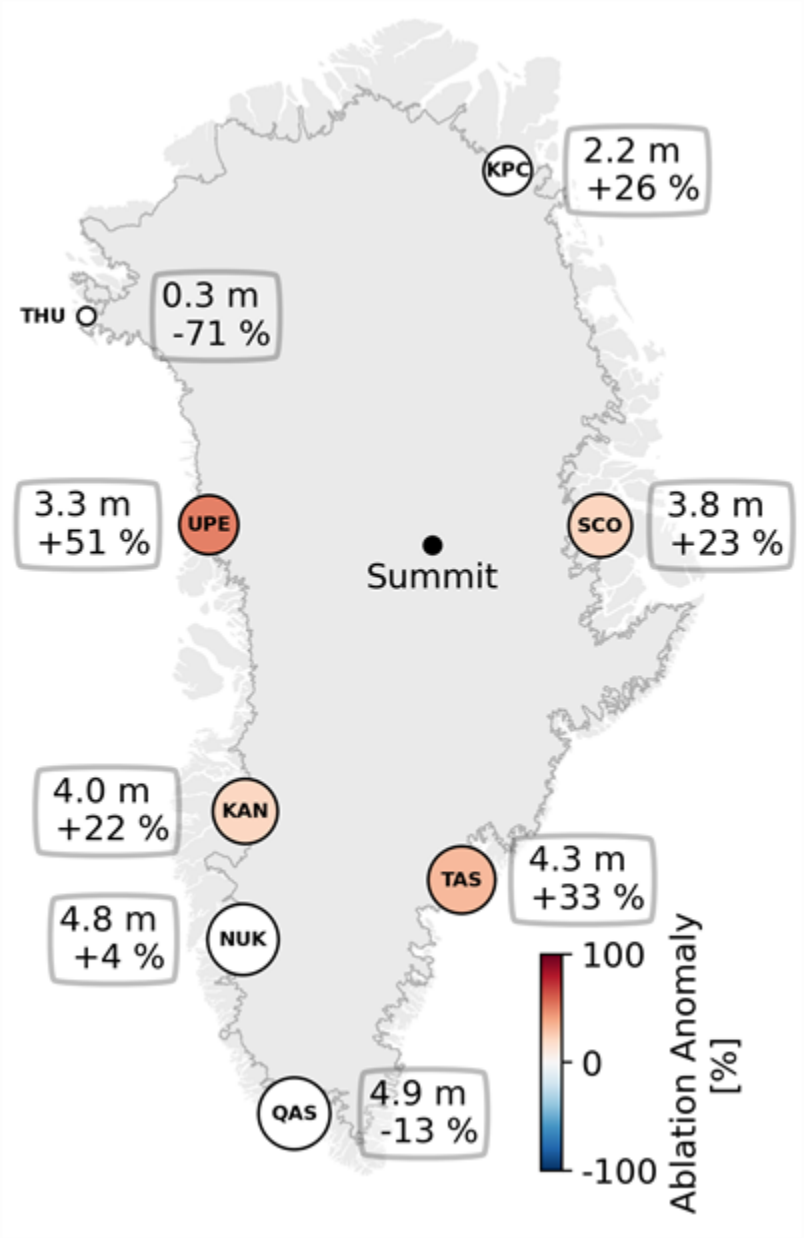

Fig. 3. Net ablation in 2021 measured by PROMICE weather transects and referenced to the 1981-2010 standard period. Circle size is scaled to the ablation in meters (m) of ice equivalent, and color scaled with anomaly value. White circles indicate anomaly values not exceeding methodological and measurement uncertainty. Stations are: Thule (THU), Upernavik (UPE), Kangerlussuaq (KAN), Nuuk (NUK), Qassimuit (QAS), Tasiliiq (TAS), Scorebysund (SCO), and Kronprins Christians Land (KPC). NSF Summit Station is also marked.

Albedo and bare ice area

Ice sheet reflectivity (albedo) strongly modulates surface melt. When the ice sheet surface is dark (low albedo) the surface absorbs more sunlight, leading to the possibility of earlier melt onset and/or enhanced melting. Contributors to low albedo include loss of snow cover revealing bare ice, snow grain growth, and organic and inorganic surface material like microbes or black carbon. In contrast, a bright surface, for example from fresh snow, increases albedo and reduces melt potential. The snow-covered

to bare glacial ice transition produces a strong albedo shift, making bare ice area a useful observational metric (Wehrlé et al. 2021).

The average June through August 2021 ice sheet albedo was at the 2000-21 average, due in part to an above-average (bright) July, offset by a below-average (dark) August. Regionally, the southwest was brighter than normal from delayed melting (Fig. 4a,b) and darker than normal across the northern ice sheet. During mid-August, bare ice area (Fig. 4c) reached extremely low values equal to those in 2019, a record-tying ice loss year. August 2021 also had the latest peak in bare ice area during the past five years (2017-21). Note that local ablation (Fig. 3) and albedo anomalies (Fig. 4a) may not intuitively align due to factors such as summer snowfall, surface atmospheric conditions, extreme melt events, etc.

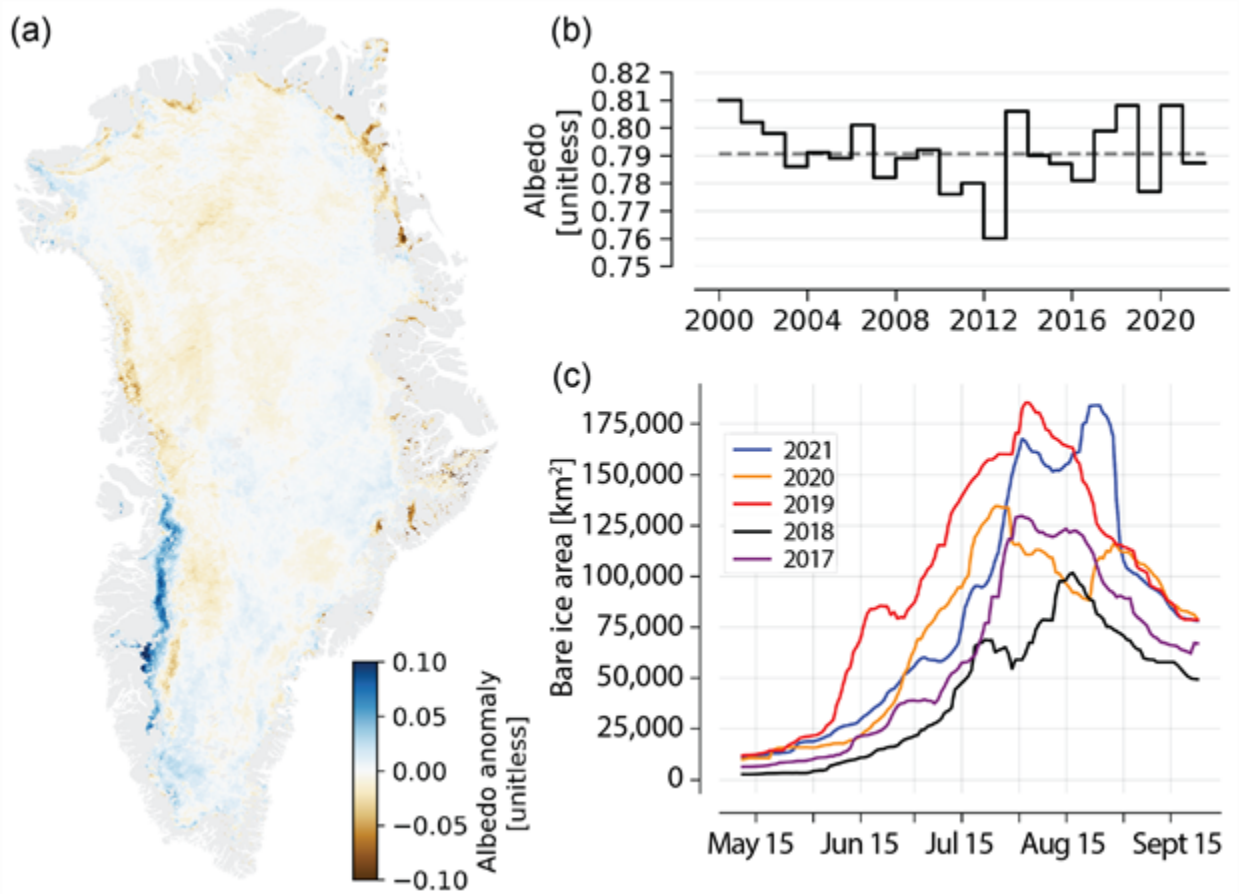

Fig. 4. (a) Albedo anomaly for summer 2021, relative to a 2000-09 reference period, (b) Time series for average Greenland ice sheet summer albedo, (c) Bare ice area from Sentinel-3. Data for (a) and (b) from MODIS.

Solid ice loss and tidewater area change

Year-to-year variability in ice loss from calving is lower than surface melt variability (Mankoff et al. 2020b). Nonetheless, an inter-decadal ~10% discharge increase is apparent. For 1981-2010, the average total discharge was ~444 ± 47 Gt yr^{-1}, while average discharge during 2010-19 was ~487 ± 46 Gt yr^{-1}. As of November, solid ice discharge for 2021 reached an average of 497 ± 48 Gt yr^{-1}, with the largest contributions from the southeast, followed by the northwest (Fig. 5a,c).

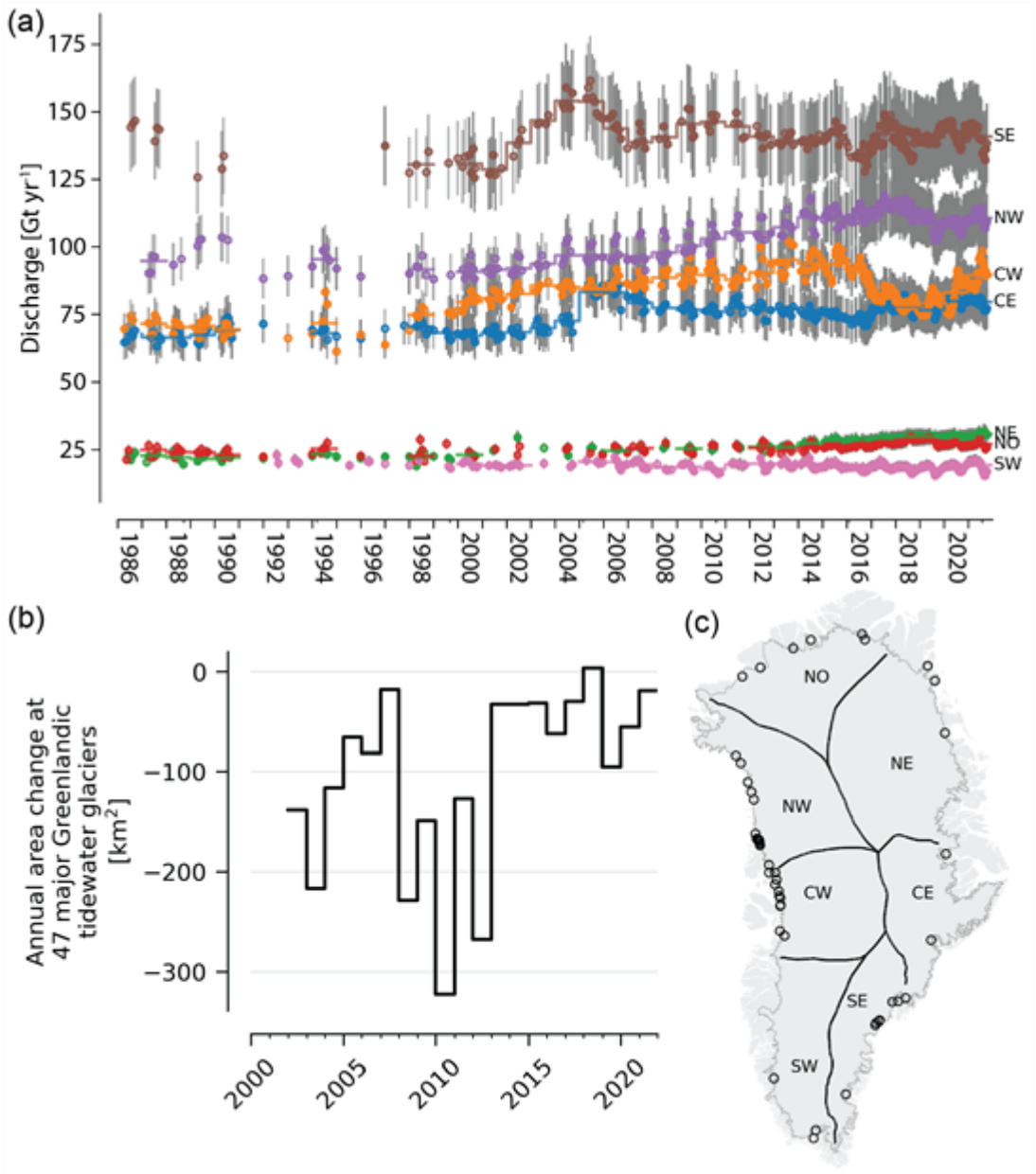

Fig. 5. (a) Solid ice discharge (Gt yr^{-1}; gray bars show ±10% uncertainty range), (b) Total area change at 47 major Greenland tidewater glaciers, (c) Regions for solid ice discharge for (a): north (NO), northeast (NE), central east (CE), southeast (SE), southwest (SW), central west (CW), and northwest (NW), and sampled glaciers for (b) indicated with open circles.

If solid ice loss through calving is more rapid than replacement from ice flow, the glacier front retreats and glacier area is lost. For 2020-21, net tidewater glacier surface area loss due to glacier front retreat was -18.9 km^2 for 47 major and representative Greenland tidewater glaciers (Fig. 5b,c), substantially lower than the mean annual loss of -103.3 km^2 for these glaciers since 2002 (Andersen et al. 2019).

Extreme August melt event

Atmospheric circulation strongly modulates surface melt via the thermal and radiative budgets. August 2021 had two notable atmospheric anomalies. In early August, persistent high-pressure conditions centered over the ice sheet promoted enhanced melting (see essay *Surface Air Temperature*). These conditions were similar to those that generated the 2012 and 2019 melt records but did not produce a 2021 extreme melt event. In mid-August, an atmospheric event associated with the transport of moisture at high elevations promoted the exceptional rainfall event at Summit. In this case, it was not an increase in solar radiation promoting melting but the heat and moisture influx. Though the near-surface processes that led to enhanced melting in early and mid-August 2021 were different, enhanced melting in both cases was associated with a disruption and increased sinuosity of the polar vortex.

Based on the 1978-present satellite record, the melt event centered on 14 August 2021 was the latest time during the ablation season that more than half of the ice sheet (>815,000 km^2) experienced surface melt. Summer 2021 is only the second year on record (along with 2012) with more than one melt event exceeding this threshold. This was also the first time that rainfall was reported at NSF's Summit Station (3216 m above sea level) since its operation started in 1989, though surface melt (without rainfall) was observed in 1995, 2012, and 2019. The 1995-to-present melt event frequency at Summit (4 events in 27 years) is in contrast to the average of one event per 153 years for the 10,000 years prior to 1950, derived from ice core data (Alley and Anandakrishnan 1995). Scientists are now installing rain gauges at interior ice sheet weather stations; rain gauges on a new-generation GC-Net station at South Dome (2850 m) recorded three distinct summer 2021 rainfall events.

Methods

Total mass change is measured indirectly by the GRACE (Gravity Recovery and Climate Experiment, 2002-17) and GRACE-FO (Follow On, 2018-present) satellite missions by detecting gravity anomalies. Technical Notes (TN) are hosted at https://podaac-tools.jpl.nasa.gov/drive/files/allData.

Direct weather observations are provided via 15 Danish Meteorological Institute (DMI) weather stations with records beginning from 1784 (Nuuk) to 1991 (Summit) and 8 automatic weather station transects from the Programme for Monitoring of the Greenland Ice Sheet (PROMICE) at the Geological Survey of Greenland and Denmark (GEUS). DMI stations are located on land, with most coastal and some within fjords, with Summit data provided by NOAA GEOSummit. PROMICE transects, located on the ice sheet, also provide surface ablation (following van As et al. 2016). Surface melt duration and extent measurements are derived from daily Special Sensor Microwave Imager/Sounder (SSMIS) 37 GHz, horizontally polarized passive microwave radiometer satellite data (Mote 2007).

NASA MODIS satellite data provide multi-decadal albedo monitoring (Box et al. 2017). The Sentinel-3 SICE product is now being used to monitor bare ice area (Kokhanovsky et al. 2020; Wehrlé et al. 2021).

PROMICE combines ice thickness estimates with ice velocity measurements based on Sentinel-1 satellite data to create a high temporal resolution solid ice discharge product integrated over Greenland (following Mankoff et al. 2020b).

Acknowledgments

Data from the Programme for Monitoring of the Greenland Ice Sheet (PROMICE) were provided by the Geological Survey of Denmark and Greenland (GUES) at http://www.promice.dk. T. Moon was supported by the University of Colorado Boulder Cooperative Institute for Research in Environmental Sciences (CIRES). M. Tedesco was supported by National Science Foundation ANS #1713072, National Science Foundation PLR-1603331, NASA MAP #80NSSC17K0351, NASA #NNX17AH04G, and the Heising-Simons Foundation. T. Mote was supported by National Science Foundation #1900324. Sentinel-3 SICE data processing via PolarView.org is made possible by the European Space Agency (ESA) Network of Resources. Summit Station is owned and operated by the National Science Foundation Office of Polar Programs with permission from the Government of Greenland.

References

Alley, R. B., and S. Anandakrishnan, 1995: Variations in melt-layer frequency in the GISP2 ice core: implications for Holocene summer temperatures in central Greenland. *Ann. Glaciol.*, **21**, 64-70, https://doi.org/10.3189/S0260305500015615.

Andersen, J. K., and Coauthors, 2019: Update of annual calving front lines for 47 marine terminating outlet glaciers in Greenland (1999-2018). *GEUS Bull.*, **43**, http://doi.org/10.34194/GEUSB-201943-02-02.

Box, J. E., D. van As, and K. Steffen, 2017: Greenland, Canadian and Icelandic land ice albedo grids (2000-2016). *GEUS Bull.*, **38**, 53-56, https://doi.org/10.34194/geusb.v38.4414.

IMBIE Team, 2020: Mass balance of the Greenland Ice Sheet from 1992 to 2018. *Nature*, **579**, 233-239, http://doi.org/10.1038/s41586-019-1855-2.

IPCC, 2021: Climate Change 2021: The Physical Science Basis. Contribution of Working Group I to the Sixth Assessment Report of the Intergovernmental Panel on Climate Change [V. Masson-Delmotte and Co-editors], Cambridge University Press, in press.

Kokhanovsky, A., J. E. Box, B. Vandecrux, K. D. Mankoff, M. Lamare, A. Smirnov, and M. Kern, 2020: The determination of snow albedo from satellite measurements using fast atmospheric correction technique. *Remote Sens.*, **12**, 234, https://doi.org/10.3390/rs12020234.

Mankoff, K. D., and Coauthors, 2020a: Greenland liquid water discharge from 1958 through 2019. *Earth Syst. Sci. Data*, **12**, 2811-2841, https://doi.org/10.5194/essd-12-2811-2020.

Mankoff, K. D., A. Solgaard, W. Colgan, A. P. Ahlstrøm, S. A. Khan, and R. S. Fausto, 2020b: Greenland ice sheet solid ice discharge from 1986 through March 2020. *Earth Syst. Sci. Data*, **12**, 1367-1383, https://doi.org/10.5194/essd-12-1367-2020.

Mankoff, K. D., and Coauthors, 2021: Greenland ice sheet mass balance from 1840 through next week. *Earth Syst. Sci. Data*, **13**, 5001-5025, https://doi.org/10.5194/essd-13-5001-2021.

Moon, T. A., A. S. Gardner, B. Csatho, I. Parmuzin, and M. A. Fahnestock, 2020: Rapid reconfiguration of the Greenland ice sheet coastal margin. *J. Geophys. Res.-Earth*, **125**, e2020JF005585, https://doi.org/10.1029/2020JF005585.

Morlighem, M., and Coauthors, 2017: BedMachine v3: Complete bed topography and ocean bathymetry mapping of Greenland from multibeam echo sounding combined with mass conservation. *Geophys. Res. Lett.*, **44**(21), 11051-11061, https://doi.org/10.1002/2017GL074954.

Mote, T. L., 2007: Greenland surface melt trends 1973-2007: Evidence of a large increase in 2007. *Geophys. Res. Lett.*, **34**, L22507, https://doi.org/10.1029/2007GL031976.

van As, D., R. S. Fausto, J. Cappelen, R. S. van de Wa, R. J. Braithwaite, H. Machguth, and PROMICE project team, 2016: Placing Greenland ice sheet ablation measurements in a multi-decadal context. *GEUS Bull.*, **35**, 71-74, https://doi.org/10.34194/geusb.v35.4942.

Wehrlé, A., J. E. Box, A. M. Anesio, and R. S. Fausto, 2021: Greenland bare ice albedo from PROMICE automatic weather station measurements and Sentinel-3 satellite observations. *GEUS Bull.*, **47**, https://doi.org/10.34194/geusb.v47.5284.

November 17, 2021

Sea Ice

DOI: 10.25923/y2wd-fn85

W. N. Meier[1,2], D. Perovich[3], S. Farrell[4], C. Haas[5], S. Hendricks[5], A. A. Petty[6], M. Webster[7], D. Divine[8], S. Gerland[8], L. Kaleschke[5], R. Ricker[9], A. Steer[8], X. Tian-Kunze[5], M. Tschudi[10], and K. Wood[11,12]

[1]National Snow and Ice Data Center, Boulder, CO, USA
[2]Cooperative Institute for Research in Environmental Sciences, University of Colorado Boulder, Boulder, CO, USA
[3]Thayer School of Engineering, Dartmouth College, Hanover, NH, USA
[4]Department of Geographical Sciences, University of Maryland, College Park, MD, USA
[5]Alfred Wegener Institute, Helmholtz Centre for Polar and Marine Research, Bremerhaven, Germany
[6]Goddard Space Flight Center, NASA, Greenbelt, MD, USA
[7]Geophysical Institute, University of Alaska Fairbanks, Fairbanks, AK, USA
[8]Norwegian Polar Institute, Fram Centre, Tromsø, Norway
[9]Norwegian Research Centre, Tromsø, Norway
[10]Aerospace Engineering Sciences, University of Colorado, Boulder, CO, USA
[11]Cooperative Institute for Climate, Ocean, and Ecosystem Studies, University of Washington, Seattle, WA, USA
[12]Pacific Marine Environmental Laboratory, NOAA, Seattle, WA, USA

Highlights

- Winter maximum (March) and summer minimum (September) 2021 sea ice extents were less extreme compared to the last couple of years, but the 15 lowest minimum extents have all occurred in the last 15 years.
- An early onset of sea ice melt and retreat occurred in the Laptev Sea, leading to record-low extent in the region during May and June, while winter advection of thick, multiyear ice into the Beaufort and Chukchi Seas resulted in a late and limited spring retreat in that region.
- The amount of multiyear sea ice, based on available data since 1985, reached its second lowest level by the end of summer 2021, sea ice thickness was lower than recent years, and volume was at record low (since at least 2010) in April 2021.

Introduction

Arctic sea ice is the frozen interface between the ocean and atmosphere in the north, limiting ocean-atmosphere exchanges of energy and moisture and playing a critical role in the earth's climate and the regional ecosystem. The high albedo (reflectivity) of sea ice and overlying snow reflects most incoming solar radiation, which inhibits summer warming. A range of marine mammals depend on the ice as a platform for mating, feeding, birthing, and other activities. The cycle of ice formation and melt influences food web dynamics and the biogeochemical balance of the upper ocean. Humans are deeply connected to the ice as well. Sea ice both facilitates and threatens human activities in the Arctic, including Indigenous hunting and transportation, marine navigation, and national security

responsibilities. Overall, 2021 continued to demonstrate the profound changes underway in the Arctic sea ice system.

Arctic sea ice began 2021 catching up from record or near-record low extent and a notably late freeze-up in autumn 2020. Such low autumn ice extent can potentially influence stratospheric circulation and subsequent midlatitude cold outbreaks (see essay *Surface Air Temperature*). At the start of 2021, sea ice extent was lower than the 1981-2020 average in the Bering and Barents Seas, but near-average elsewhere. High pressure in January and February persisted in the Siberian sector of the Arctic, resulting in divergence from and new ice formation along the Siberian coast and strong advection of thicker, multiyear ice into the Beaufort and Chukchi Seas. It also advected icebergs that were calved from the Canadian Archipelago into the coastal region of Utqiaġvik, Alaska. This multiyear ice in the Beaufort and Chukchi Seas delayed the retreat of ice on the North American side of the Arctic. On the Siberian side, strong pressure gradients during April and May facilitated early melt onset and local ice retreat in spring, leading to a record-low extent in the Laptev Sea during May and June.

Summer 2021 was marked by general low pressure over the Arctic Ocean. This brought relatively cloudier conditions and divergent ice circulation that, along with the thicker Beaufort and Chukchi Seas ice, slowed the decline in ice extent. Summer (JJA) air temperatures at the 925 mb level ranged from 1° to 2°C above normal over the Arctic Ocean, with the exception of near-normal temperatures for the Beaufort and Chukchi Seas (see essay *Surface Air Temperature*). The older ice in the Beaufort and Chukchi Seas resulted in a near-normal ice edge location throughout most of the summer, breaking the regional pattern of low ice extents seen in recent years. The summer circulation also limited ice export through Fram Strait, resulting in the unusual occurrence of a nearly ice-free East Greenland Sea during much of the summer.

Sea ice extent

Sea ice extent is defined as the total area covered by at least 15% ice concentration. Extent is a common and useful metric to assess seasonal and long-term Arctic sea ice changes, for which there is now a 43-year record derived from consistent satellite-borne passive microwave sensor observations. The substantial decline in Arctic ice extent since 1979 is one of the most iconic indicators of climate change.

The seasonal cycle of Arctic sea ice is characterized by the maximum annual extent in March, decreasing through spring and summer to an annual minimum extent in September. March and September 2021 total extent negative anomalies were not as extreme as in recent years, but still ranked among the lowest in the satellite record (Table 1). September trends are steeper than March (Fig. 1, Table 1) and the steepest of any month, though statistically significant declines in extent are seen in all months throughout the satellite record. The 15 lowest September extents in the satellite record have all occurred in the last 15 years. March 2021 was characterized by lower-than-average extent in the Bering Sea, Baffin Bay, and the Gulf of St. Lawrence and near-normal extent elsewhere (Fig. 2). September 2021 average extent was characterized by particularly lower-than-average coverage in the Siberian and East Greenland Seas and closer-to-normal coverage in the Beaufort and Chukchi Seas (Fig. 2).

Table 1. March and September monthly averages and annual daily maximum and minimum extent for 2021 and related statistics. The rank is from least ice to most ice of the 43 years (1 = least, 43 = most).

	March		September	
	Monthly Average	**Daily Maximum**	**Monthly Average**	**Daily Minimum**
Extent (10^6 km^2)	14.64	14.77	4.92	4.72
Rank (out of 43 years)	9	7	12	12
1981-2010 average (10^6 km^2)	15.43	15.65	6.41	6.22
Anomaly rel. 1981-2010 average (10^6 km^2)	-0.79	-0.88	-1.49	-1.50
Trend, 1979-2021 (km^2 yr^{-1})	-0.40	-0.43	-0.81	-0.81
Trend, 1979-2021 (% dec^{-1})	-2.6	-2.7	-12.7	-13.0

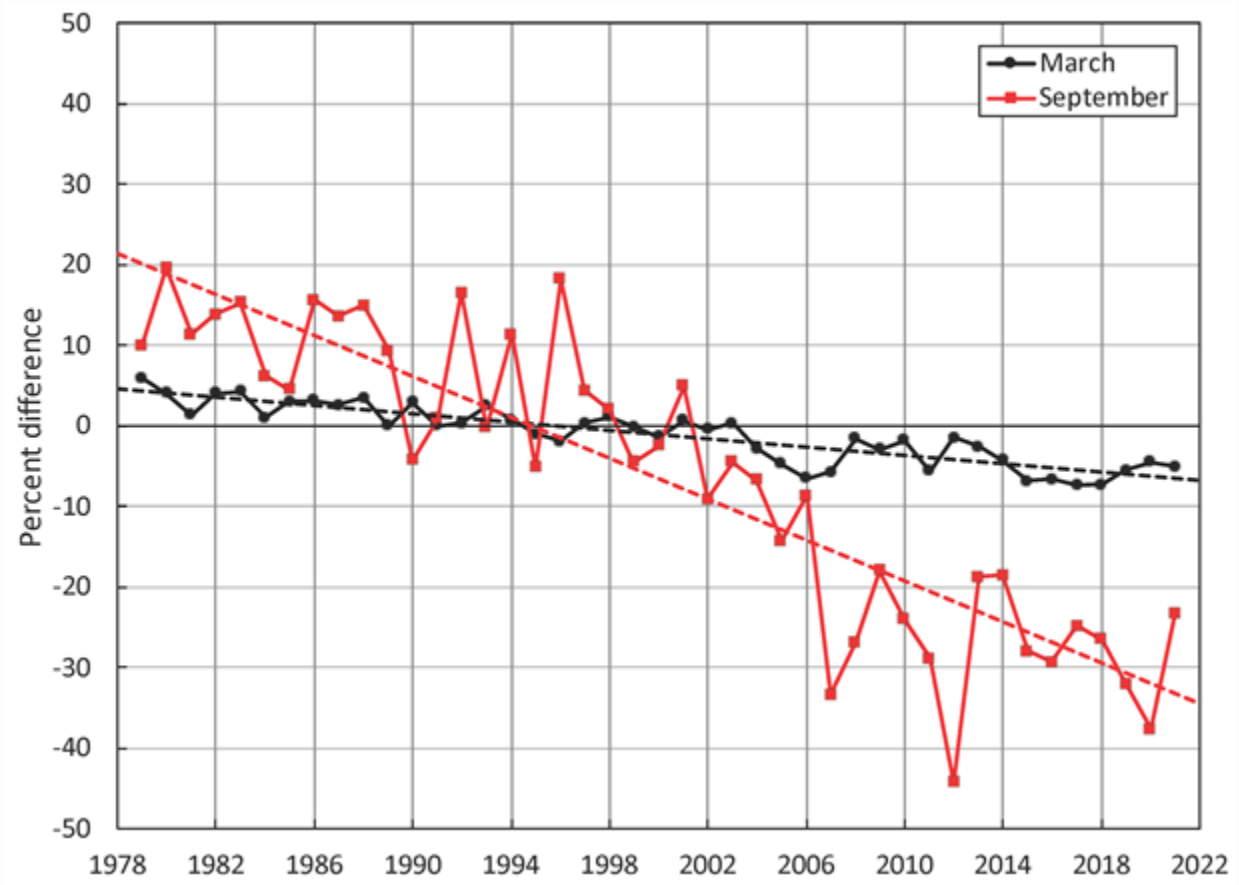

Fig. 1. Monthly sea ice extent anomalies (solid lines) and linear trend lines (dashed lines) for March (black) and September (red) 1979 to 2021. The anomalies are relative to the 1981 to 2010 average for each month (see Table 1).

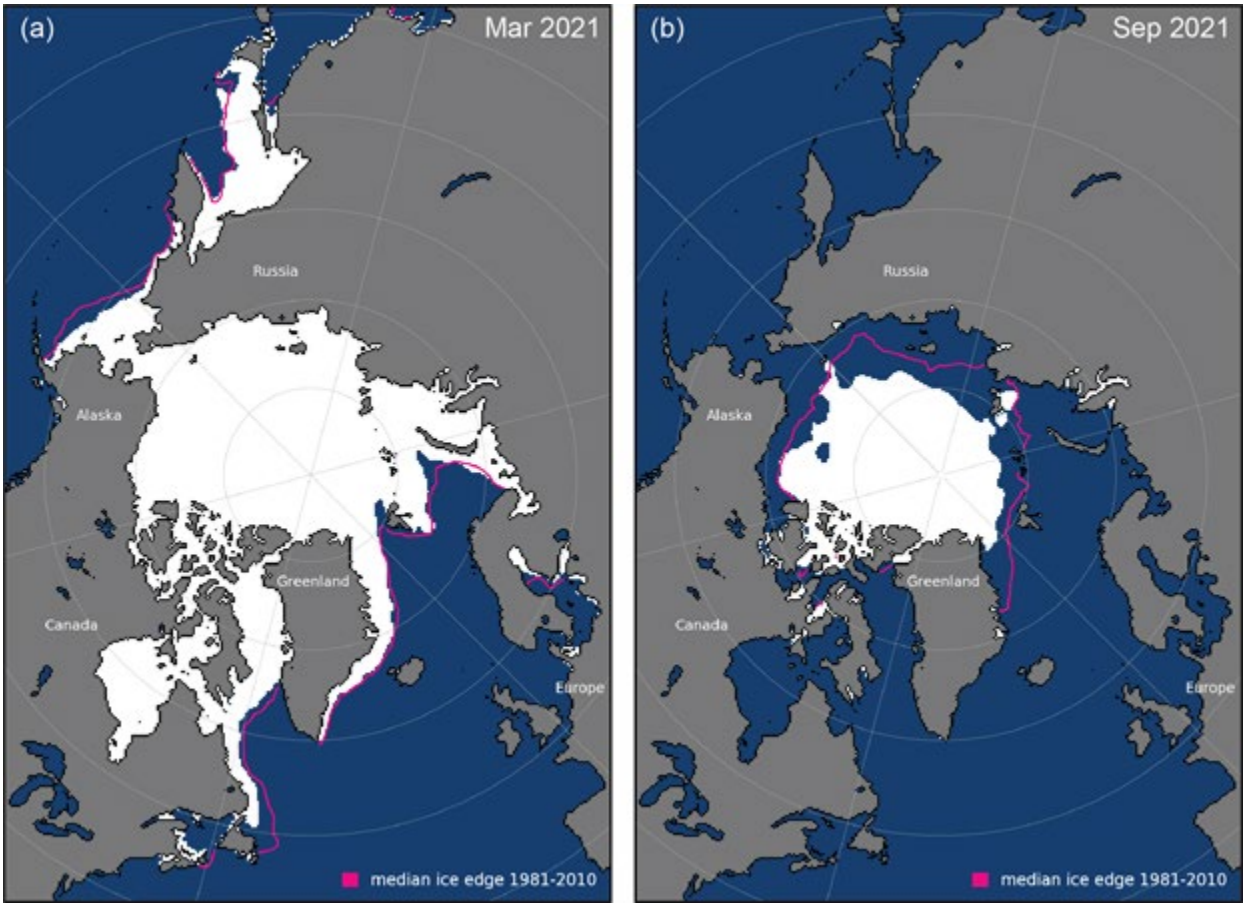

Fig. 2. Monthly average sea ice extent for (a) March 2021, and (b) September 2021. The median extent for 1981-2010 is shown by the magenta contour.

Sea ice age

Sea ice drifts around the Arctic Ocean, forced by winds and ocean currents, growing and melting thermodynamically. Ice convergence can also lead to dynamic thickening (i.e., ridging and rafting) while ice divergence during winter exposes open water within which new ice can form. Age is a proxy for thickness as multiyear ice (ice that survives at least one summer melt season) grows thicker over successive winter periods. Age is here presented over the Arctic Ocean domain (Fig. 3, inset) for the period 1985-2021. In the week before the 2021 annual minimum extent, when the age values of the remaining sea ice are incremented by one year, the amount of multiyear ice remaining in the Arctic Ocean was the second lowest on record (above only 2012). The September multiyear sea ice extent declined from 4.40 million km^2 in 1985 to 1.29 million km^2 in 2021 (Fig. 3). Over the same period, the oldest ice (>4 years old) declined from 2.36 million km^2 to 0.14 million km^2. In the 37 years since records began in 1985, the Arctic Ocean has changed from a domain dominated by multiyear ice to one where first-year ice prevails. A younger ice cover implies a thinner, less voluminous ice pack.

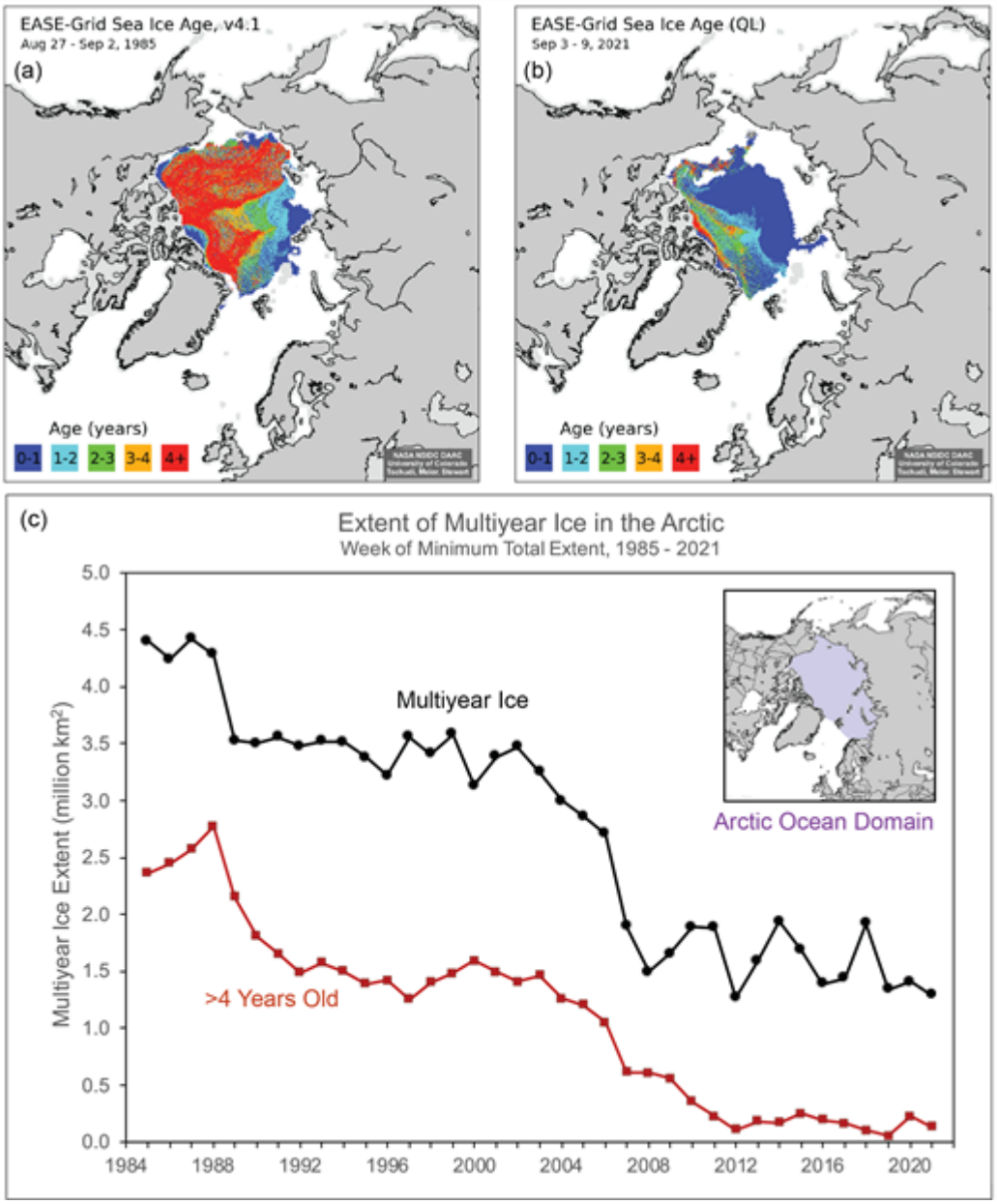

Fig. 3. Sea ice age coverage map for the week before minimum total extent (when age values are incremented to one year older) in (a) 1985, and (b) 2021; (c) extent of multiyear ice (black) and ice >4 years old (red) within the Arctic Ocean for the week of the minimum total extent.

Sea ice thickness and volume

Sea ice thickness is an important indicator of overall ice conditions because it provides the third dimension of the ice cover. The ICESat-2 and CryoSat-2/SMOS satellites tracked the seasonal October to April growth over the past three years in which both products were available (Fig. 4a). The 2020/21 winter sea ice was the thinnest of the three years in both products, and the thinnest in the full CryoSat-2/SMOS record (starting in the 2010/11 winter, not shown). April 2021 sea ice thickness fields from ICESat-2 and CryoSat-2/SMOS (Fig. 4b,c) are generally consistent, but with some regional differences. Both show a typical geographic pattern with the thickest ice along the Canadian Archipelago and

northern Greenland. However, comparing April 2021 to the average of previous years (2010-20) in the CryoSat-2/SMOS record (Fig. 4d), the ice along the Canadian Archipelago and northern Greenland is thinner than average, indicating a thinning of the thickest-ice region of the Arctic. Thicker-than-average ice in April 2021 is found in coastal areas, particularly along the Beaufort and Chukchi Seas coasts, likely due to the aforementioned advection of multiyear ice into the region. Differences in snow depth relative to the snow climatology used in the CryoSat-2/SMOS product may also account for some of the difference between years.

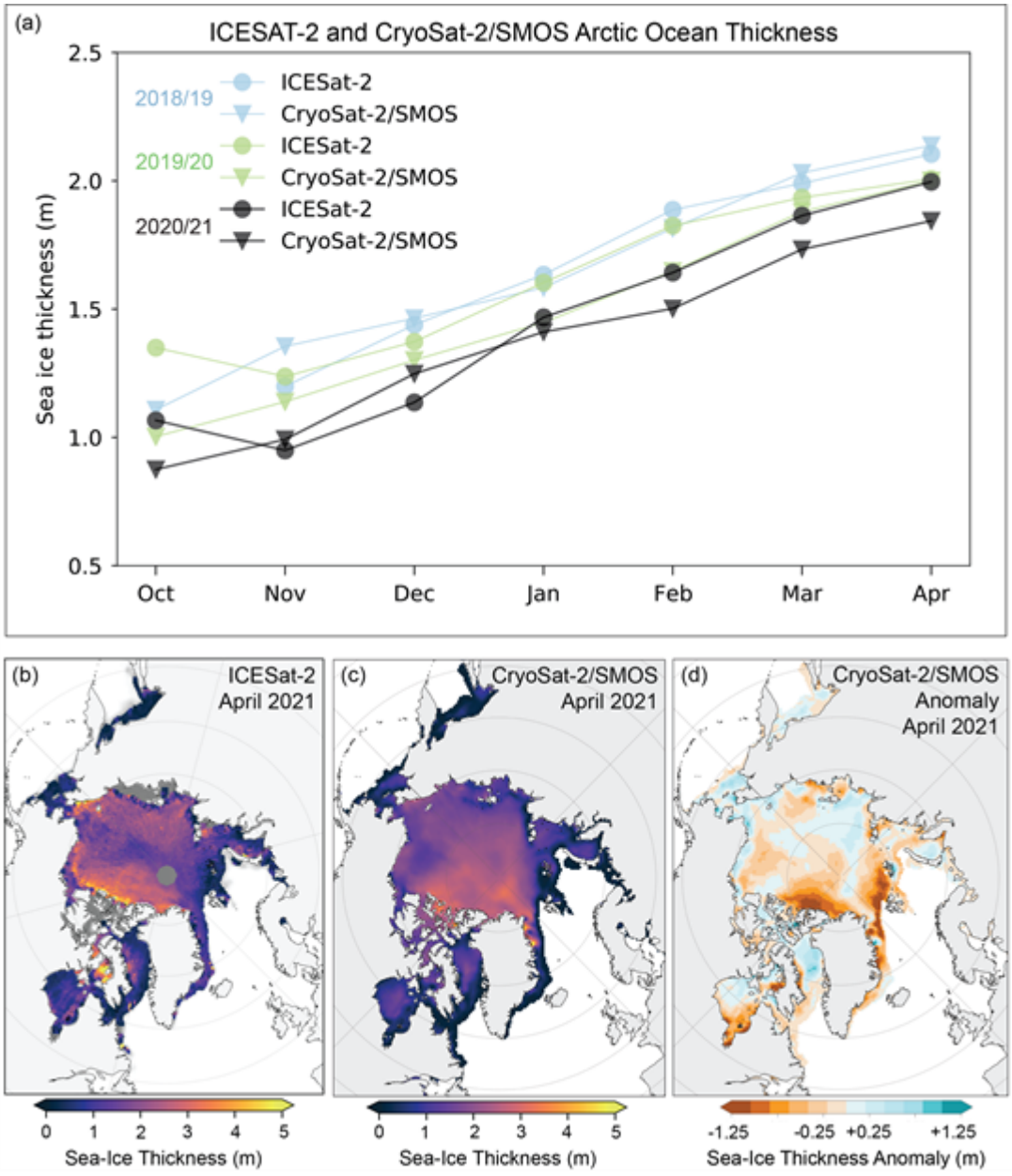

Fig. 4. (a) October through April monthly average sea ice thickness, calculated over an Inner Arctic Ocean Domain (see Methods and data section), from ICESat-2 (circles) and CryoSat-2/SMOS (triangles) for 2018-19 (blue), 2019-20 (green), and 2020-21 (dark gray). Average April 2021 sea ice thickness maps from (b) ICESat-2 (dark gray areas have no data) and (c) CryoSat-2/SMOS; (d) CryoSat-2/SMOS thickness anomaly (relative to the 2010-20 average). Note that ICESat-2 thickness estimates outside the Arctic Ocean Domain are not as reliable due to uncertainties in snow cover.

Sea ice thickness is integrated with ice concentration to provide winter volume estimates for the CryoSat-2/SMOS measurement time period. The seasonal time series (Fig. 5) indicates lower-than-average ice volume throughout the 2020/21 winter, with record-low conditions spanning from October to mid-November. Volume growth typically slows by early March as spring warming begins. In 2021, the volume growth was nearly flat for much of March and then experienced a slight decrease in volume during early April. While there may be regionally different reasons for this, a localized manifestation of this phenomenon was observed during the Nansen Legacy research cruises (direct observation from authors) in the northern Barents Sea where, despite continuous cold conditions during March, persistent presence of warm Atlantic water close to the sea surface prevented further ice growth. By the end of winter, ice volume in April 2021 was the lowest April volume within the 11-year record. This record suggests that while the rate of decline in September sea ice extent over the 2010-20 period has slowed compared to previous decades, the ice has continued to thin.

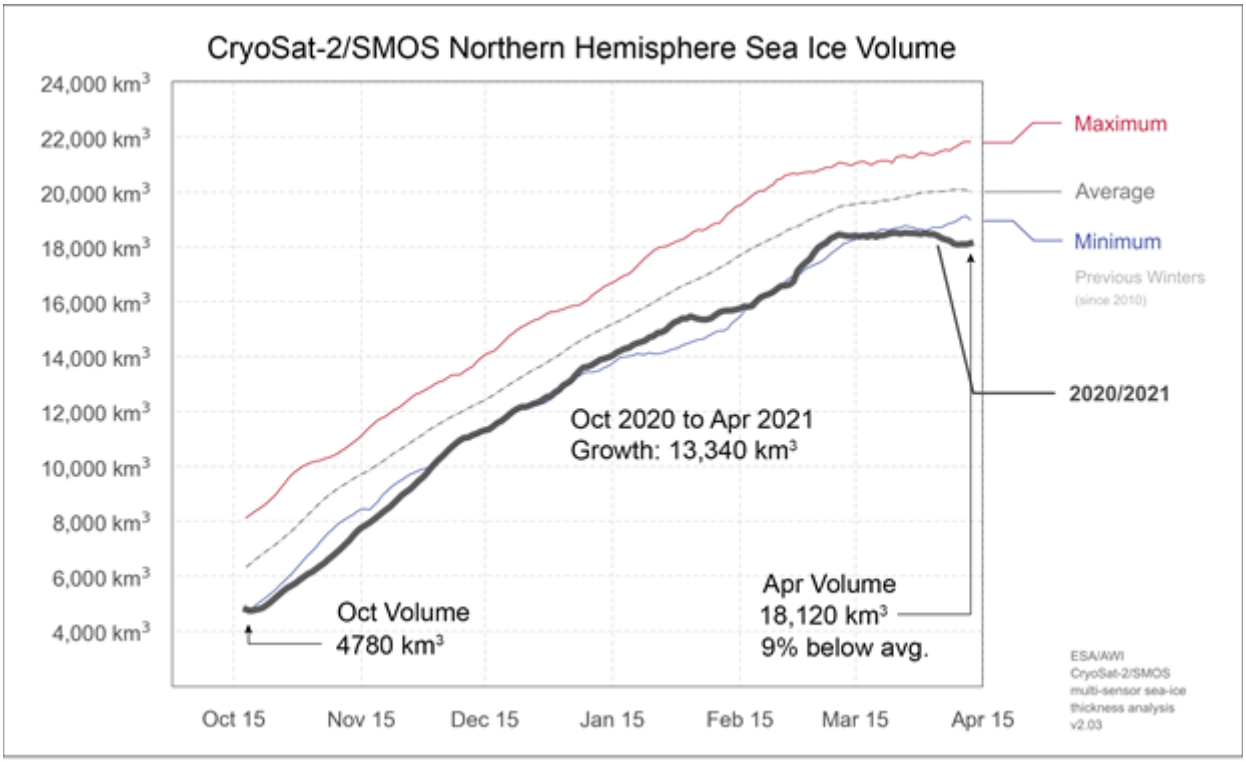

Fig. 5. CryoSat-2/SMOS Northern Hemisphere sea ice volume from 15 October to 15 April for the 2020-21 season. The maximum (red line), minimum (blue line), and average (dashed gray line) volume over the 11-year (2010-20) record are also provided.

Methods and data

Sea ice extent values are from the NSIDC Sea Ice Index (Fetterer et al. 2017), based on passive microwave derived sea ice concentrations from the NASA Team algorithm (Cavalieri et al. 1996; Maslanik and Stroeve 1999). There are several other passive microwave derived products available (e.g., Ivanova et al. 2014), including the EUMETSAT OSI-SAF CCI climate data record (Lavergne et al. 2019). All products have some limitations and uncertainties (e.g., Kern et al. 2019), but overall, the trends agree well (Comiso et al. 2017).

Sea ice age data are from the EASE-Grid Sea Ice Age, Version 4 (Tschudi et al. 2019a) and Quicklook Arctic Weekly EASE-Grid Sea Ice Age, Version 1 (Tschudi et al. 2019b) archived at the NASA Snow and Ice Distributed Active Archive Center (DAAC) at NSIDC. Age is calculated via Lagrangian tracking of ice parcels using weekly sea ice motion vectors. Age is generally a proxy for thickness because older ice is typically thicker, via thermodynamic growth and potential dynamic thickening (i.e., ridging and rafting). Only the oldest age category is preserved for each grid cell.

Satellite altimetry has enabled the continuous retrieval of sea ice thickness and volume estimates over the entire Arctic basin during the freezing season, starting with the ESA CryoSat-2 radar altimeter, launched in 2010. This was followed in September 2018 by the launch of the NASA Ice, Cloud, and land Elevation 2 (ICESat-2) laser altimeter. Thus, there are now two independent altimetry-based estimates of thickness and volume.

Altimeter measurements have higher relative errors for thin ice because of the achievable precision of the elevation. Weekly CryoSat-2 estimates have been combined with thin ice (<1 m) estimates from the ESA Soil Moisture Ocean Salinity (SMOS) instrument, launched in 2009, to obtain an optimal estimate across thin and thick ice regimes (Ricker et al. 2017) on a 25 km resolution EASE2 grid. Optimal interpolation is used to fill in data gaps in the weekly CryoSat-2 fields and to merge the CryoSat-2 and SMOS estimates. When combined with sea ice concentration, the CryoSat-2/SMOS record of ice thickness is used to compute sea ice volume; data are available at ftp://ftp.awi.de/sea_ice/product/cryosat2_smos/.

ICESat-2 estimates here focus on an Inner Arctic Domain (Central Arctic, Beaufort, Chukchi, Laptev, E. Siberian Seas—the same domain as for Fig. 3 except without the Barents and Kara Seas) due to poorer knowledge of snow conditions in the more peripheral seas. The data used here are the gridded 25 km x 25 km monthly data produced in Petty et al. (2020), now using rel004 ATL10 freeboard and v1.1 NESOSIM snow loading (depth and density). Data are available at NSIDC: https://nsidc.org/data/IS2SITMOGR4/versions/1.

Acknowledgments

W. Meier thanks the NSIDC DAAC and the NASA ESDIS project for support. Sea ice age data were processed by J. S. Stewart (NSIDC). Thanks to J. Belter and T. Krumpen (Alfred Wegener Institute), and Nansen Legacy project members for information on winter/spring ice conditions from the IceBird and Nansen Legacy field campaigns, respectively.

References

Cavalieri, D. J., C.L. Parkinson, P. Gloersen, and H. J. Zwally, 1996 (updated yearly): Sea Ice Concentrations from Nimbus-7 SMMR and DMSP SSM/I-SSMIS Passive Microwave Data, Version 1. NASA National Snow and Ice Data Center Distributed Active Archive Center, Boulder, CO, USA, https://doi.org/10.5067/8GQ8LZQVL0VL. [Accessed 27 August 2021]

Comiso, J. C., W. N. Meier, and R. Gersten, 2017: Variability and trends in the Arctic sea ice cover: Results from different techniques. *J. Geophys. Res.*, **122**, 6883-6900, https://doi.org/10.1002/2017JC012768.

Fetterer, F., K. Knowles, W. N. Meier, M. Savoie, and A.K. Windnagel, 2017 (updated daily): Sea Ice Index, Version 3. NSIDC: National Snow and Ice Data Center, Boulder, CO, USA, https://doi.org/10.7265/N5K072F8. [Accessed 27 August 2021]

Ivanova, N., O. M. Johannessen, L. T. Pedersen, and R. T. Tonboe, 2014: Retrieval of Arctic sea ice parameters by satellite passive microwave sensors: A comparison of eleven sea ice concentration algorithms. *IEEE Trans. Geosci. Rem. Sens.*, **52**(11), 7233-7246, https://doi.org/10.1109/TGRS.2014.2310136.

Kern, S., T. Lavergne, D. Notz, L. T. Pedersen, R. T. Tonboe, R. Saldo, and A. M. Sørensen, 2019: Satellite passive microwave sea-ice concentration data set intercomparison: closed ice and ship-based observations. *Cryosphere*, **13**, 3261-3307, https://doi.org/10.5194/tc-13-3261-2019.

Lavergne, T., and Coauthors, 2019: Version 2 of the EUMETSAT OSI SAF and ESA CCI sea-ice concentration climate data records. *Cryosphere*, **13**, 49-78, https://doi.org/10.5194/tc-13-49-2019.

Maslanik, J., and J. Stroeve, 1999: Near-Real-Time DMSP SSMIS Daily Polar Gridded Sea Ice Concentrations, Version 1. NASA National Snow and Ice Data Center Distributed Active Archive Center, Boulder, CO, USA, https://doi.org/10.5067/U8C09DWVX9LM. [Accessed 27 August 2021]

Petty, A. A., N. T. Kurtz, R. Kwok, T. Markus, and T. A. Neumann, 2020: Winter Arctic sea ice thickness from ICESat-2 freeboards. *J. Geophys. Res.-Oceans*, **125**, e2019JC015764, https://doi.org/10.1029/2019JC015764.

Ricker, R., S. Hendricks, L. Kaleschke, X. Tian-Kunze, J. King, and C. Haas, 2017: A weekly Arctic sea-ice thickness data record from merged CryoSat-2 and SMOS satellite data. *Cryosphere*, **11**, 1607-1623, https://doi.org/10.5194/tc-11-1607-2017.

Tschudi, M., W. N. Meier, J. S. Stewart, C. Fowler, and J. Maslanik, 2019a: EASE-Grid Sea Ice Age, Version 4. [March, 1984-2020]. NASA National Snow and Ice Data Center Distributed Active Archive Center, Boulder, CO, USA, https://doi.org/10.5067/UTAV7490FEPB. [Accessed 1 September 2021]

Tschudi, M., W. N. Meier, and J. S. Stewart, 2019b: Quicklook Arctic Weekly EASE-Grid Sea Ice Age, Version 1. [March, 2021]. NASA National Snow and Ice Data Center Distributed Active Archive Center, Boulder, CO, USA, https://doi.org/10.5067/2XXGZY3DUGNQ. [Accessed 1 September 2021]

November 19, 2021

Sea Surface Temperature

DOI: 10.25923/2y8r-0e49

M. -L. Timmermans[1] and Z. Labe[2]

[1]Yale University, New Haven, CT, USA
[2]Colorado State University, Fort Collins, CO, USA

Highlights

- August 2021 mean sea surface temperatures (SSTs) were ~1.0-3.5°C warmer than 1982-2010 August mean values in the Kara and Laptev Seas, and off the east coast of Greenland.
- Anomalously cooler August 2021 SSTs (~0.5-1.0°C cooler) were observed in the Chukchi and Northern Barents Seas and in Baffin Bay.
- Although there is considerable interannual variability in spatial SST patterns, August mean SSTs show statistically significant warming trends for 1982-2021 in most regions of the Arctic Ocean that are ice-free in August.

Arctic Ocean sea surface temperatures (SSTs) in the summer (June-August) are driven by the amount of incoming solar radiation absorbed by the sea surface and by the flow of warm waters into the Arctic from the North Atlantic and North Pacific Oceans. Solar warming of the Arctic Ocean surface is influenced by the distribution of sea ice (with greater warming occurring in ice-free regions), cloud cover, and upper-ocean stratification. Discharge of relatively warm Arctic river waters can provide an additional source of heat to the surface of marginal seas.

Arctic SST is an essential indicator of the role of the ice-albedo feedback mechanism in any given summer sea-ice melt season. As the area of sea ice cover decreases, more incoming solar radiation is absorbed by the ocean and, in turn, the warmer ocean melts more sea ice. In addition, higher SSTs are associated with delayed autumn freeze-up and increased ocean heat storage throughout the year. Marine ecosystems are influenced by SSTs, which affect the timing and development of primary and secondary production cycles (e.g., see essay *Primary Productivity* for further context), as well as available habitat for upper-trophic and temperature-sensitive species. With respect to carbon cycling, warmer SSTs are associated with reduced ocean uptake of carbon dioxide from the atmosphere, and thus represent another positive feedback loop (i.e., amplifying cycle) in a changing climate.

The SST data presented here are monthly mean values for August (1982-2021) (see Reynolds et al. 2002, 2007). August mean SSTs provide the most appropriate representation of Arctic Ocean summer SSTs because they are not affected by the cooling and subsequent sea-ice growth that typically takes place in the latter half of September.

August 2021 mean SSTs ranged from 6° to 10°C in the southeast Chukchi and Barents Seas to around 0° to 3°C in the East Siberian, Kara and Laptev Seas, Baffin Bay and in the ice-free waters east of Greenland (Fig. 1a). August 2021 mean SSTs were notably warm (around 1°-3.5°C warmer than the 1982-2010 August mean) in the Kara and Laptev Seas (Fig. 1b). This is consistent with early-season sea-ice retreat in these regions, and anomalously warm spring 2021 air temperatures over northern Eurasia (see essays *Sea Ice* and *Surface Air Temperature*). SSTs in the waters east of Greenland were also warmer (by around

1°-3°C) than the 1982-2010 August mean. It is notable that in the same region, summer 2021 surface air temperatures were about 2°-5°C warmer than the 1981-2010 mean (see essay *Surface Air Temperature*).

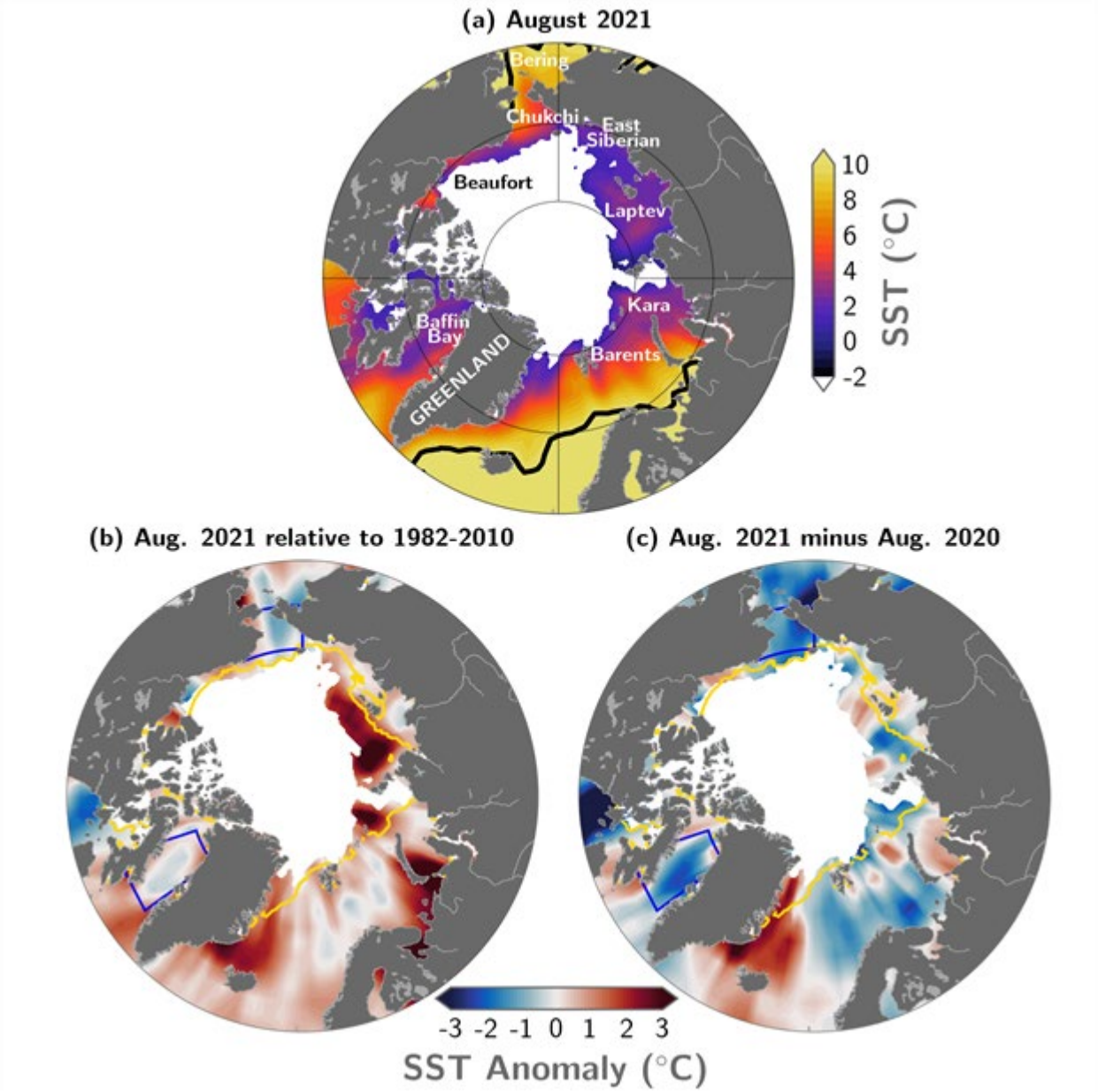

Fig. 1. (a) Mean sea surface temperature (SST; °C) in August 2021. Black contours indicate the 10°C SST isotherm, (b) SST anomalies (°C) in August 2021 relative to the August 1982-2010 mean, (c) Difference between August 2021 SSTs and August 2020 SSTs (negative values indicate where 2021 was cooler). White shading in all panels is the August 2021 mean sea-ice extent. The yellow lines in (b) and (c) indicate the median ice edge for August 1982-2010. The two regions marked by blue boxes in panels (b) and (c) indicate regions of Baffin Bay and the Chukchi Sea, and relate to data presented in Fig. 2b,c. See Methods and data for source information.

The northern Barents Sea, Baffin Bay, and the Chukchi Sea were marked by anomalously cool SSTs in August 2021 with SSTs around 0.5° to 1°C cooler than the mean (Fig. 1b). Surface air temperatures in summer (June-August 2021) were anomalously cold in the Beaufort and Chukchi Sea regions, and conditions were cloudy, limiting solar fluxes to the surface ocean (see essays *Sea Ice* and *Surface Air*

Temperature). Cooler SSTs are also consistent with greater sea-ice extents (closer to normal) in the Chukchi and Beaufort Sea regions compared to recent past years, related to wind-driven transport of thick multiyear ice into the region in early 2021 (see essay *Sea Ice*).

There is significant variability from year-to-year in the particular regions that exhibit anomalously cool or warm SSTs (e.g., see the *2020 Arctic Report Card Sea Surface Temperature* essay). The strong interannual variability in spatial patterns of SST is evident in the differences between August 2021 and August 2020 SSTs (Fig. 1c). August 2021 SSTs were around 0.5°C (and up to 2°C) cooler than in August 2020 over a significant portion of the ice-free regions, with some exceptions, including warmer SSTs off east Greenland (Fig. 1c).

Mean August SST warming trends from 1982 to 2021 persist over much of the Arctic Ocean, with statistically significant (at the 95% confidence interval) linear warming trends of up to +0.1°C yr^{-1} (Fig. 2a). The cooling trend (~-0.06°C yr^{-1}) in mean August SSTs in the northern Barents Sea region remains a notable exception, although the cooling trend is not observed for most other months (see e.g., Lind et al. 2018). Anomalously cool SSTs in Baffin Bay and the Chukchi Sea distinguished the August 2021 SST field (Fig. 1b; Fig. 2b,c). Overall, however, Baffin Bay SSTs are becoming warmer in August with a linear warming trend over 1982-2021 of 0.05 ± 0.01°C yr^{-1} (Fig. 2b). Similarly, Chukchi Sea August mean SSTs are warming, with a linear trend of 0.06 ± 0.03°C yr^{-1} (Fig. 2c). Mean August SSTs for the entire Arctic (the Arctic Ocean and marginal seas north of 67° N) exhibit a linear warming trend of 0.03 ± 0.01°C yr^{-1}.

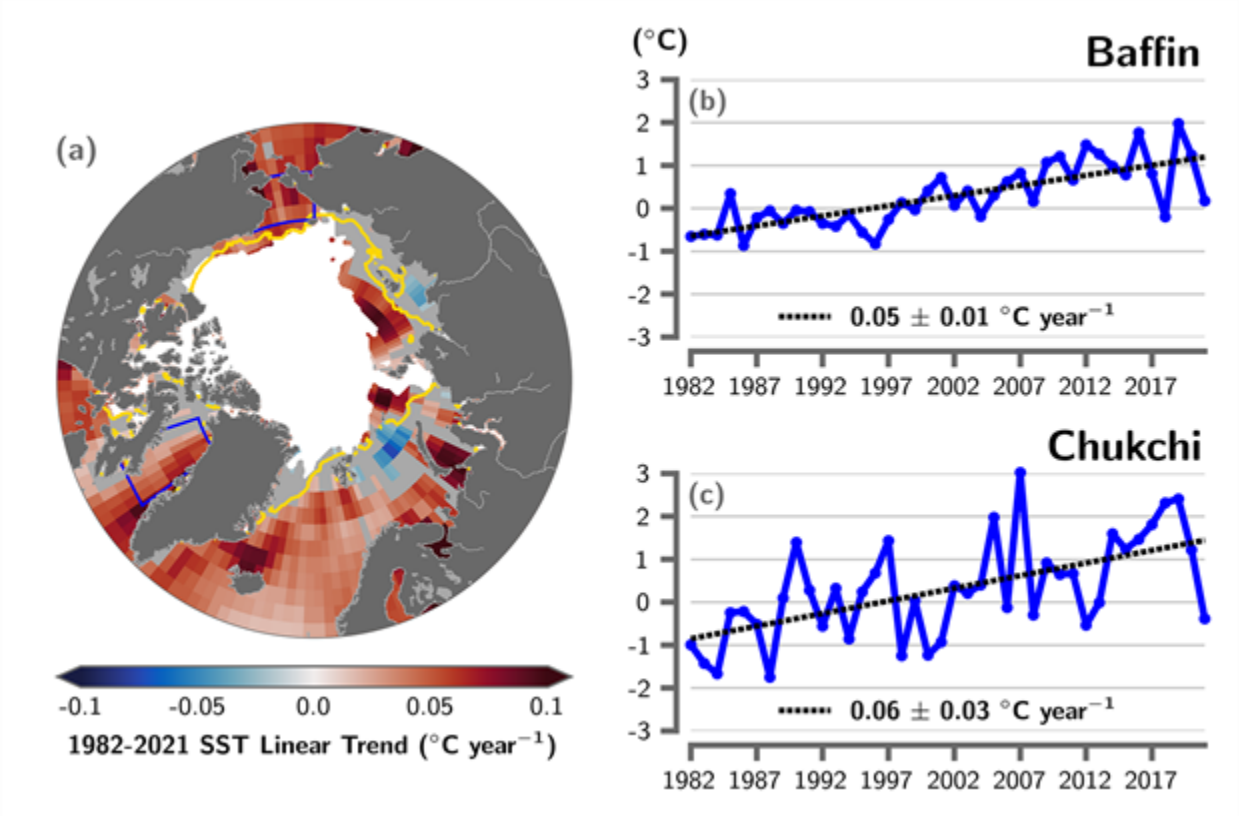

Fig. 2. (a) Linear SST trend (°C yr^{-1}) for August of each year from 1982 to 2021. The trend is only shown for values that are statistically significant at the 95% confidence interval; the region is shaded gray otherwise. White shading is the August 2021 mean sea ice extent, and the yellow line indicates the median ice edge for Aug 1982-2010, (b, c) Area-averaged SST anomalies (°C) for August of each year (1982-2021) relative to the 1982-2010 August mean for (b) Baffin Bay and (c) Chukchi Sea regions shown by blue boxes in (a). The dotted lines show the linear SST anomaly

trends over the period shown and trends in °C yr^{-1} (with 95% confidence intervals) are shown on the plots. See Methods and data for source information.

Methods and data

The SST data presented here are a blend of in situ and satellite measurements from August 1982 to August 2021, taken from the monthly mean NOAA Optimum Interpolation (OI) SST Version 2 product (OISSTv2; Reynolds et al. 2002, 2007). OISSTv2 data were provided by the NOAA/OAR/ESRL PSD, Boulder, Colorado, USA, from their Website at http://www.esrl.noaa.gov/psd [accessed Sept. 7, 2021] (Reynolds et al. 2007). In the Arctic Ocean overall, the OISSTv2 product has been found to exhibit a cold bias (i.e., underestimate SST) of up to 0.5°C compared to in situ measurements (Stroh et al. 2015). The OISSTv2 product uses a simplified linear relationship with sea-ice concentration to infer SST under sea ice (Reynolds et al. 2007), which means SSTs may be too cool by up to 0.2°C where there is sea-ice cover. We focus primarily on waters that are ice free in August, although this uncertainty can be reflected in trends and variability in the vicinity of the ice edge. The period 1982-2010 is used as the climatological reference for the August mean.

Sea-ice extent and ice edge data are from the NOAA/NSIDC Climate Data Record of Passive Microwave Sea Ice Concentration, Version 4 and Near-Real-Time NOAA/NSIDC Climate Data Record of Passive Microwave Sea Ice Concentration, Version 2 (Peng et al. 2013; Meier et al. 2021a,b.).

References

Lind, S., R. B. Ingvaldsen, and T. Furevik, 2018: Arctic warming hotspot in the northern Barents Sea linked to declining sea-ice import. *Nat. Climate Change*, **8**, 634-639, https://doi.org/10.1038/s41558-018-0205-y.

Meier, W. N., F. Fetterer, A. K. Windnagel, and J. S. Stewart, 2021a: NOAA/NSIDC Climate Data Record of Passive Microwave Sea Ice Concentration, Version 4. [1982-2021]. Boulder, Colorado USA. NSIDC: National Snow and Ice Data Center, https://doi.org/10.7265/efmz-2t65.

Meier, W. N., F. Fetterer, A. K. Windnagel, and J. S. Stewart, 2021b: Near-Real-Time NOAA/NSIDC Climate Data Record of Passive Microwave Sea Ice Concentration, Version 2. [1982-2021], https://doi.org/10.7265/tgam-yv28.

Peng, G., W. N. Meier, D. J. Scott, and M. H. Savoie, 2013: A long-term and reproducible passive microwave sea ice concentration data record for climate studies and monitoring. *Earth Syst. Sci. Data*, **5**, 311-318, https://doi.org/10.5194/essd-5-311-2013.

Reynolds, R. W., N. A. Rayner, T. M. Smith, D. C. Stokes, and W. Wang, 2002: An improved in situ and satellite SST analysis for climate. *J. Climate*, **15**, 1609-1625, https://doi.org/10.1175/1520-0442(2002)015<1609:AIISAS>2.0.CO;2.

Reynolds, R. W., T. M. Smith, C. Liu, D. B. Chelton, K. S. Casey, and M. G. Schlax, 2007: Daily high-resolution-blended analyses for sea surface temperature. *J. Climate*, **20**, 5473-5496, https://doi.org/10.1175/2007JCLI1824.1, and see http://www.esrl.noaa.gov/psd/data/gridded/data.noaa.oisst.v2.html.

Stroh, J. N., G. Panteleev, S. Kirillov, M. Makhotin, and N. Shakhova, 2015: Sea-surface temperature and salinity product comparison against external in situ data in the Arctic Ocean. *J. Geophys. Res.-Oceans*, **120**, 7223-7236, https://doi.org/10.1002/2015JC011005.

November 17, 2021

Arctic Ocean Primary Productivity: The Response of Marine Algae to Climate Warming and Sea Ice Decline

DOI: 10.25923/kxhb-dw16

K. E. Frey[1], J. C. Comiso[2], L. W. Cooper[3], J. M. Grebmeier[3], and L. V. Stock[2]

[1]Graduate School of Geography, Clark University, Worcester, MA, USA
[2]Cryospheric Sciences Laboratory, Goddard Space Flight Center, NASA, Greenbelt, MD, USA
[3]Chesapeake Biological Laboratory, University of Maryland Center for Environmental Science, Solomons, MD, USA

Highlights

- Satellite estimates of ocean primary productivity (i.e., the rate at which marine algae transform dissolved inorganic carbon into organic material) showed higher values for 2021 (relative to the 2003-20 mean) for seven of the nine regions investigated across the Arctic.
- All regions continue to exhibit positive trends over the 2003-21 period, with the strongest trends in the Eurasian Arctic and Barents Sea.
- During May 2021, a ~1700 km long region from the Greenland Sea in the west to the eastern boundary of the Barents Sea showed much lower (10-20%) chlorophyll-*a* concentrations compared with the same month of the multiyear average (2003-20), likely associated with cooler than average sea surface temperatures.

Introduction

Autotrophic single-celled algae living in sea ice (ice algae) and the water column (phytoplankton) are the main primary producers in the Arctic Ocean, although there is also increased scientific interest in the role of marine macroalgae in the Arctic (e.g., kelp forests; Filbee-Dexter et al. 2019). Recent projections indicate that range expansions of non-polar, boreal kelps are likely, while endemic Arctic species may become much more limited in distribution as water temperatures increase (Goldsmit et al. 2021). Through photosynthesis, all of these autotrophs transform dissolved inorganic carbon into organic material. Consequently, primary production provides a key ecosystem service by providing energy to the entire food web in the oceans. Primary productivity is strongly dependent upon light availability and the presence of nutrients, and thus is highly seasonal in the Arctic. The melting and retreat of sea ice during spring are strong drivers of primary production in the Arctic Ocean and its adjacent shelf seas, owing to enhanced light availability and stratification (Ardyna et al. 2017). Recent studies have emphasized that primary production occurs earlier in the season than previously recognized and even under unusually low light conditions (Randelhoff et al. 2020). Other studies suggest that increased nutrient supply has also influenced overall production (Henley et al. 2020; Lewis et al. 2020), although there are indications that increases in nutrients and primary production are not universal across the Arctic (Yun et al. 2016). In addition to upwelling of nutrients, high winds and glacial runoff are regionally important in helping to drive Arctic marine productivity (Crawford et al. 2020; Hopwood et al. 2020). While declines in Arctic sea ice extent (see essay on *Sea Ice*) and increases in seawater temperatures (see essay on *Sea Surface*

Temperature) over the past several decades have contributed substantially to shifts in primary productivity throughout the Arctic Ocean, the response of primary production to sea ice loss has varied both seasonally and spatially (e.g., Hill et al. 2018).

Chlorophyll-*a*

Here we present satellite-based estimates of algal chlorophyll-*a* (occurring in all species of phytoplankton), based on ocean color, and subsequently provide calculated primary production estimates. These results are shown for ocean areas with less than 10% sea ice concentration and, therefore, do not include production by sea ice algae or under-ice phytoplankton blooms, which can be significant (e.g., Lalande et al. 2019; Kim et al. 2021). The data presented in Fig. 1 show mean monthly ratios of chlorophyll-*a* concentrations for 2021 as percentages of the multiyear average from 2003 to 2020. Observed patterns, which are spatially and temporally heterogeneous across the Arctic Ocean, are often associated with the timing of the seasonal break-up and retreat of the sea ice cover (Fig. 2) (see essay on *Sea Ice*): high percentages tend to occur in regions where the break-up is relatively early, while low percentages tend to occur in regions where the break-up is delayed. Some of the most notable patterns in 2021 occurred in the Barents Sea, with widespread lower-than-average concentrations of chlorophyll-*a* in May (Fig. 1a) and several pockets of higher-than-average concentrations in June and July (Figs. 1b and 1c), linked with relatively cool sea surface temperatures across the region in May that may have delayed the spring phytoplankton bloom. In particular, this regional low in May chlorophyll-*a* concentrations extended ~1700 km from the Greenland Sea in the west to the eastern boundary of the Barents Sea. Additional lower-than-average chlorophyll-*a* concentrations occurred in the northern Bering Sea during May and June (Figs. 1a and 1b) associated with an above-average sea ice cover (Fig. 2a), as well as in the Kara Sea during July and August (Figs. 1c and 1d). Higher-than-average chlorophyll-*a* concentrations occurred in the Barents Sea during June and July (as noted above; Figs. 1b and 1c); the Laptev Sea, Baffin Bay, and Greenland Sea during July and August (Figs. 1c and 1d); and the northern Bering and Beaufort Seas during August (Fig. 1d).

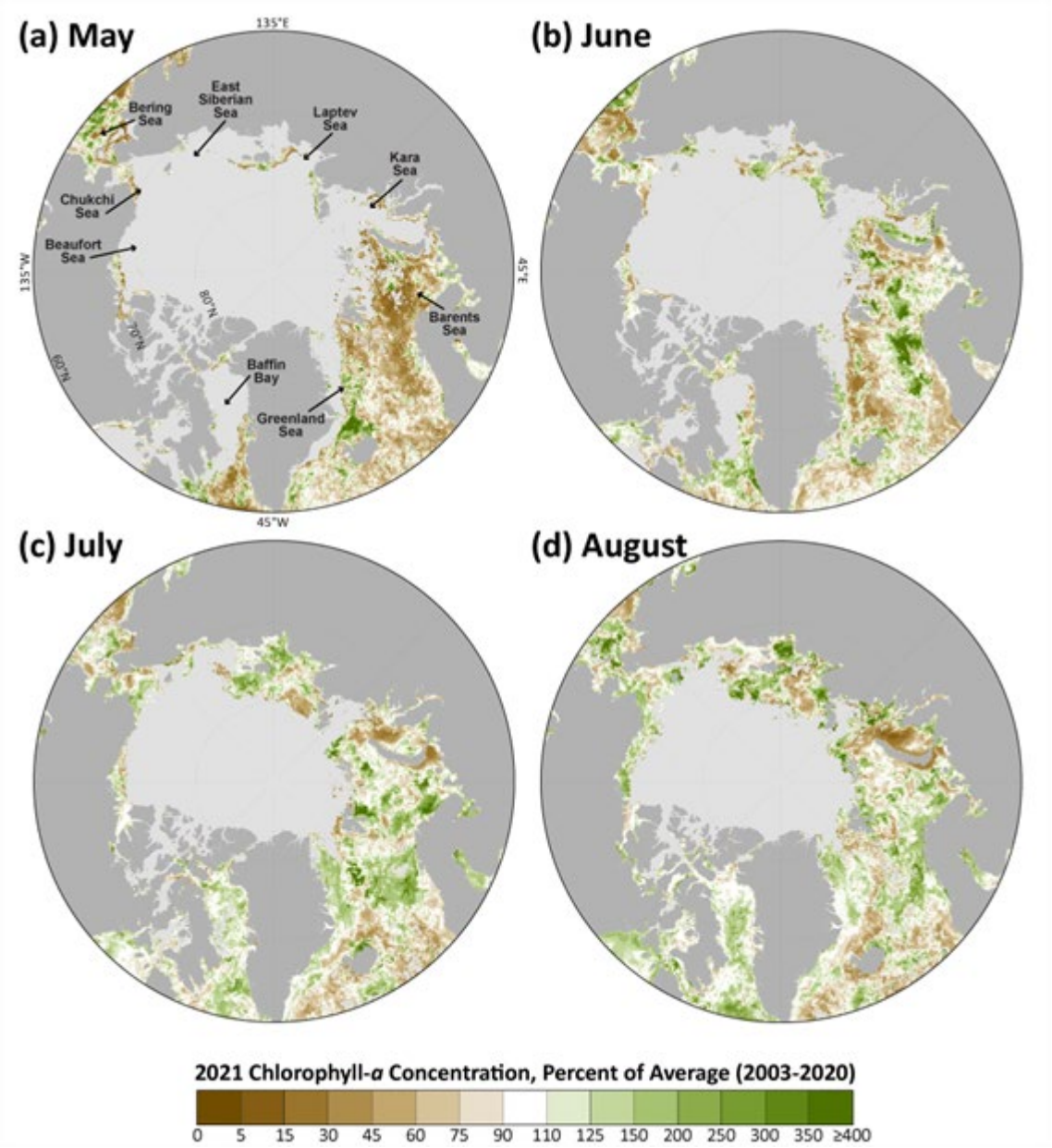

Fig. 1. Mean monthly chlorophyll-*a* concentrations during 2021, shown as a percent of the 2003-20 average for (a) May, (b) June, (c) July, and (d) August. The light gray regions represent areas where no data are available (owing to either the presence of sea ice or cloud cover). Data source: MODIS-Aqua Reprocessing 2018.0, chlor_a algorithm: https://oceancolor.gsfc.nasa.gov/.

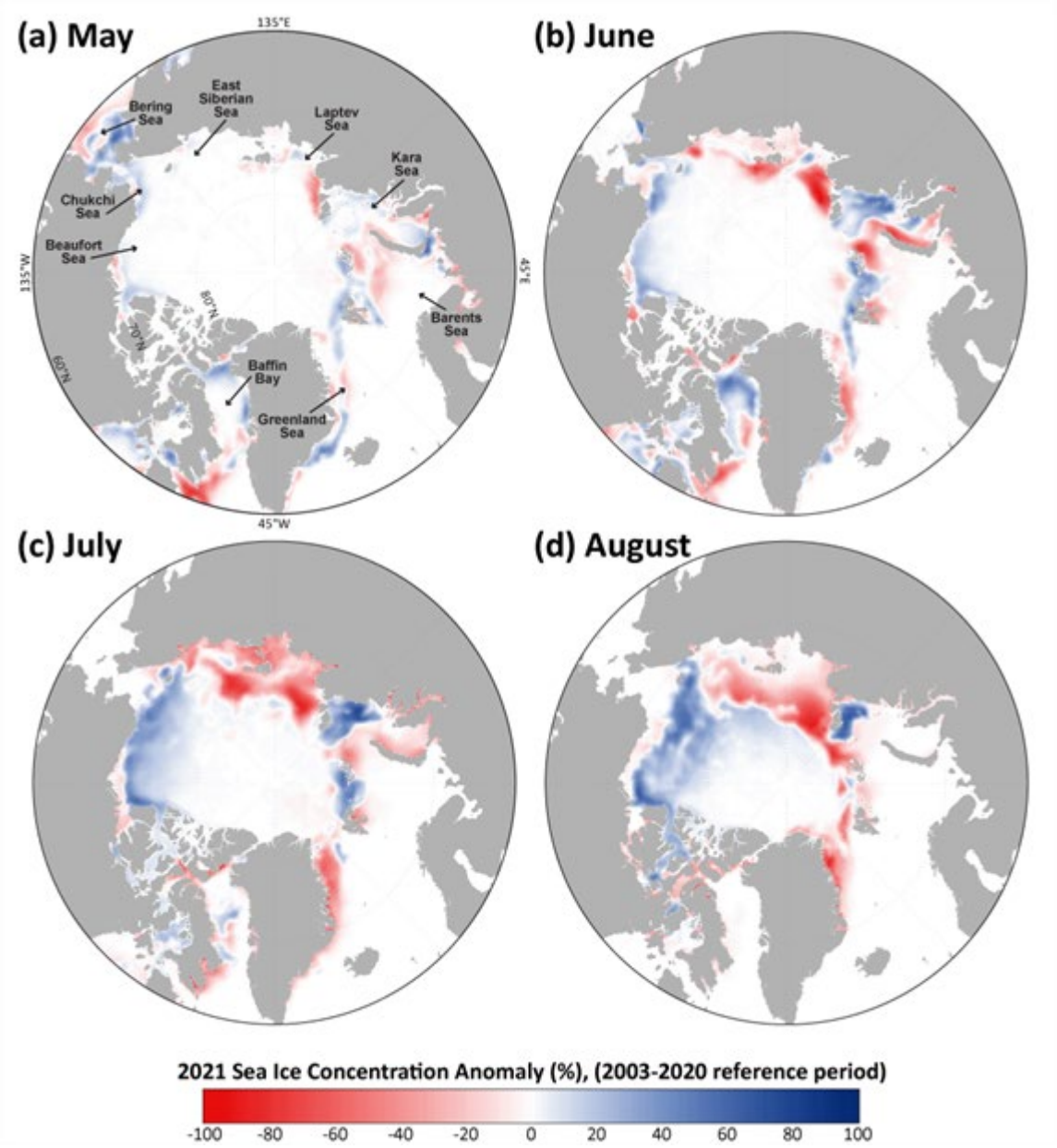

Fig. 2. Sea ice concentration anomalies (%) in 2021 (compared to a 2003-20 mean reference period) for (a) May, (b) June, (c) July, and (d) August. Data source: SSM/I and SSMIS passive microwave, calculated using the Goddard Bootstrap (SB2) algorithm (Comiso et al. 2017).

While many of these observed patterns in chlorophyll-*a* concentrations are directly linked to sea ice variability (and therefore light availability), there are other important factors at play that add to the complexity of observed chlorophyll-*a* concentrations, such as seawater temperatures, the distribution and availability of nutrients (e.g., Rijkenberg et al. 2018; Giesbrecht et al. 2019; Lewis et al. 2020), and sea surface salinity (Garcia-Eidell et al. 2021). The impacts of sea ice decline on specific water column phytoplankton properties, such as community composition and carbon biomass (Neeley et al. 2018) as well as broader ecosystem responses (Duffy-Anderson et al. 2019), are also critical to monitor as we continue to understand the responses of Arctic marine food web dynamics to climate warming. Furthermore, it is important to reiterate that the satellite ocean color data do not account for early-

season under-ice blooms that may contribute substantially to annual primary productivity estimates in these regions (e.g., Ardyna et al. 2020). Furthermore, under stratified conditions, it is well known that satellite observations can underestimate production when a deep chlorophyll maximum is present (see recent review by Bouman et al. 2021). The variable distribution of sediments and chromophoric dissolved organic matter (CDOM), owing to riverine delivery (Lewis et al. 2016) (see essay on *River Discharge*) and sea ice dynamics (Logvinova et al. 2016, Hölemann et al. 2021), can also affect the accuracy of satellite-based estimations of chlorophyll-*a* and primary productivity in Arctic waters. As such, in situ observations will continue to be important to provide overall context for changes to and drivers of primary productivity across Arctic marine ecosystems. For example, deployment of a new sediment trap array (together with a mooring array) in the northern Bering Sea in autumn 2020 should help to improve understanding of seasonal carbon production and export in this region, just as new year-round results reported from the Chukchi Ecosystem Observatory in the northern Chukchi Sea (Lalande et al. 2020) and across the Distributed Biological Observatory in the Pacific Arctic (Lalande et al. 2021) have improved understanding of annual production.

Primary production

Chlorophyll-*a* concentrations give an estimate of the total standing stock of algal biomass. However, rates of primary production (i.e., the production of organic carbon via photosynthesis) provide a different perspective since not all algae present in the water column are necessarily actively producing. The mean annual primary productivity across the Arctic shows important spatial patterns, most notably the overall decreases moving northward as sea ice cover is present for a greater fraction of the year (Fig. 3a). Spatial trends in annual primary productivity (Fig. 3b) are a particularly useful tool for understanding hotspots of change. Statistically significant positive trends are primarily clustered in the Bering/Chukchi, Laptev, Barents, and Greenland Seas. Those trends that are positive and the largest are located in the Laptev Sea, reaching into the 100-150 g $C/m^2/yr/decade$ range (Fig. 3b). This is consistent with the Eurasian Arctic region as a whole, which exhibited the greatest increases in primary productivity compared to all other Arctic regions (Fig. 4, Table 1). Investigation of 2021 annual primary productivity (Fig. 3c), as well as 2021 compared to the 2003-20 average (Fig. 3d), shows greater-than-average annual productivity in the western Greenland and northern Bering Seas, but lower-than-average annual productivity in the Beaufort and Chukchi Seas as well as localized areas throughout the Arctic region. The Laptev Sea shows subregions of both greater-than-average and lower-than-average annual primary productivity, which is also similarly reflected in spatial heterogeneity of chlorophyll-*a* concentrations during July (Fig. 1c) and August (Fig. 1d).

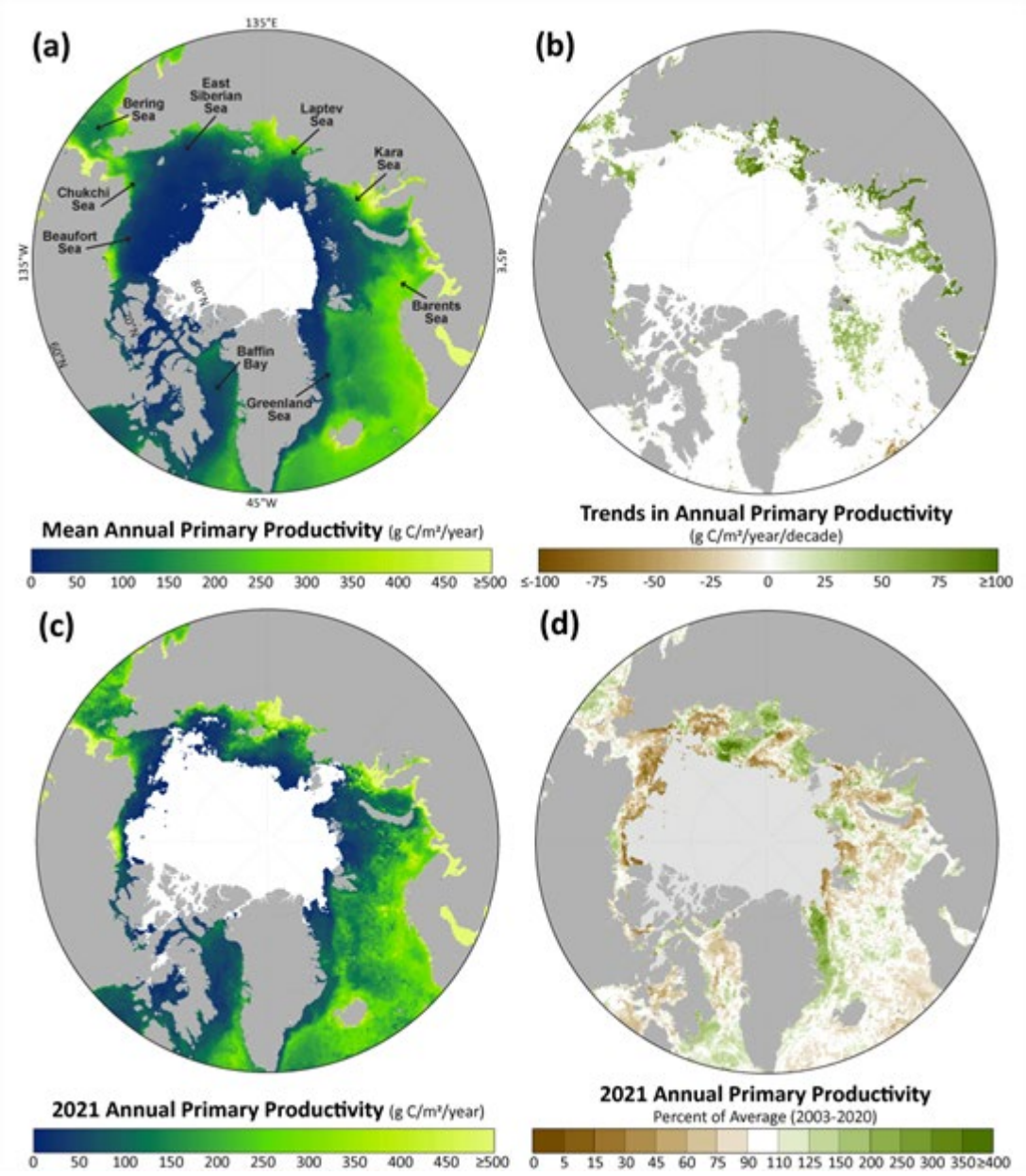

Fig. 3. For the pan-Arctic region: (a) mean annual (March-September only) primary productivity (2003-21) where white indicates no data owing to the presence of sea ice; (b) trends in annual productivity (over 2003-21) where only those trends that are statistically significant (p<0.05) are shown; (c) annual primary productivity for 2021 only where white indicates no data owing to the presence of sea ice; and (d) 2021 annual primary productivity anomalies (shown as a percent of the 2003-20 average) where light gray indicates no data owing to the presence of sea ice. Additional information regarding these data can be found in Table 1. See Methods and data section for details of how primary productivity was calculated.

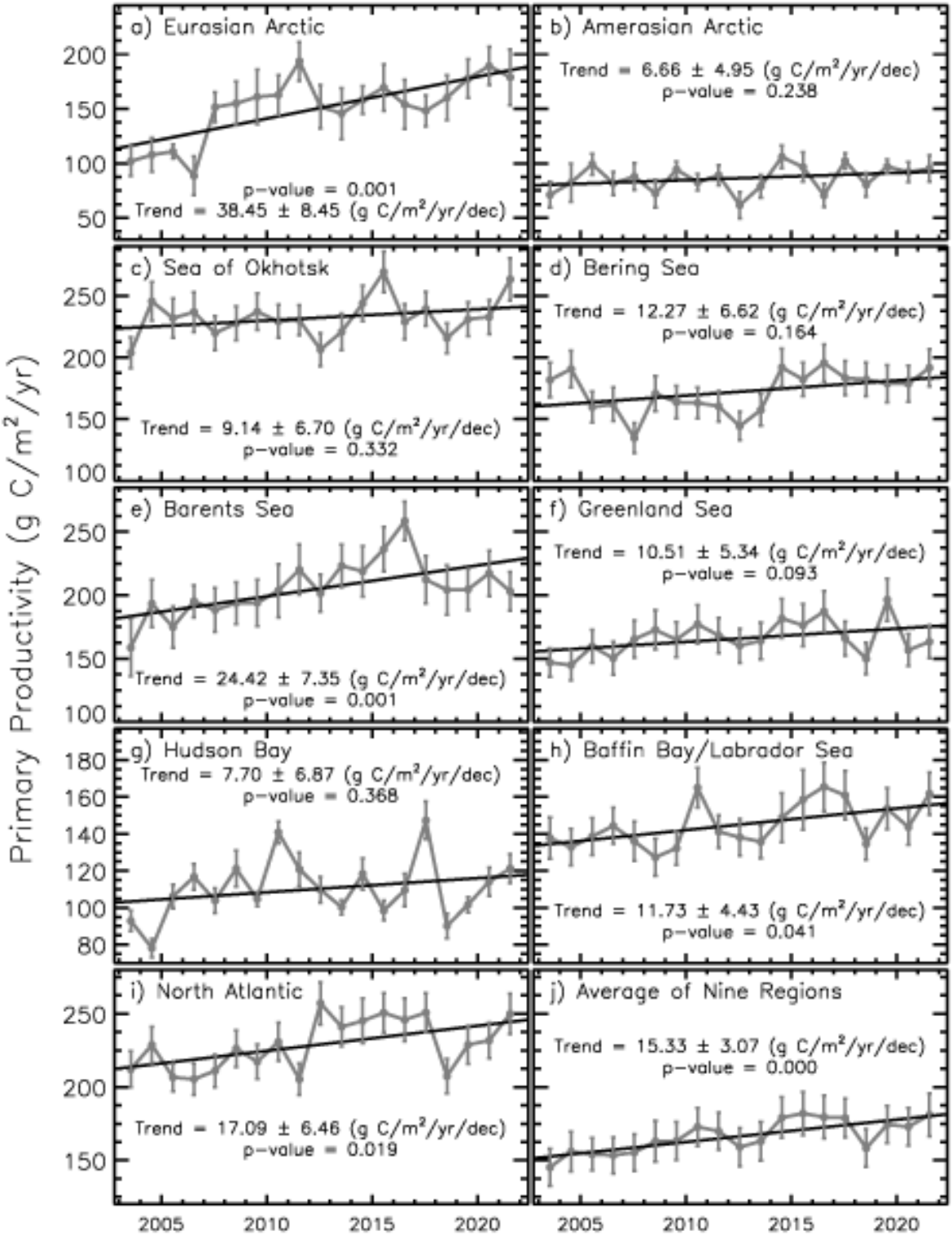

Fig. 4. Primary productivity (2003-21, March-September only) in nine different regions of the Northern Hemisphere (for a definition of the regions see Comiso, 2015), as well as the average of these nine regions. The *p*-values shown indicate the statistical significance of the trend (based on the Mann-Kendall test). Additional information regarding these data can be found in Table 1. See Methods and data section for details of how primary productivity was calculated.

Table 1. Linear trends, statistical significance, and percent change in primary productivity (2003-21) and primary productivity anomalies for 2021 (March-September) in the nine regions (and overall average) as shown in Fig. 4. Values in bold are statistically significant (p<0.05) using the Mann-Kendall test for trend. The percent change was estimated from the linear regression of the 18-year time series.

Region	2003-2021			2021	
	Trend (g C/m^2/yr/decade)	Mann-Kendall p -value	% Change	Anomaly (g C/m^2/yr) from a 2003-20 reference period	Primary Productivity (% of the 2003-20 average)
Eurasian Arctic	**38.45**	0.001	59.5	29.72	119.9
Amerasian Arctic	6.66	0.238	14.9	9.31	110.8
Sea of Okhotsk	9.14	0.332	7.3	32.80	114.2
Bering Sea	12.27	0.164	13.7	20.44	111.9
Barents Sea	**24.42**	0.001	24.0	-2.47	98.8
Greenland Sea	10.51	0.093	12.1	-2.71	98.4
Hudson Bay	7.70	0.368	13.4	11.50	110.5
Baffin Bay/ Labrador Sea	**11.73**	0.041	15.7	17.66	112.3
North Atlantic	**17.09**	0.019	14.4	22.07	109.7
Average of nine regions	**15.33**	0.000	18.1	15.37	109.3

Estimates of ocean primary productivity for nine regions and across the Northern Hemisphere (relative to the 2003-20 reference period) were assessed (Fig. 4, Table 1). The Eurasian Arctic designation includes the Kara Sea, Laptev Sea, and East Siberian Sea. The Amerasian Arctic designation includes the Chukchi Sea, Beaufort Sea, and Canadian Archipelago region. The North Atlantic region in this categorization is south of 60° N and east of 45° W, and as such is not inclusive of the Labrador or Greenland Seas. Our results show above average primary productivity for 2021 in seven of the nine regions investigated; only the Barents and Greenland Seas exhibit lower-than-average values (Fig. 4, Table 1). Across the whole time series, positive trends in primary productivity occurred in all regions during the 2003-21 period. Statistically significant positive trends occurred in the Eurasian Arctic, Barents Sea, Baffin Bay/Labrador Sea, North Atlantic, as well as on average for the nine regions. The steepest trends over the 2003-21 period were in the Eurasian Arctic (a ~59.5% overall increase) and the Barents Sea (a ~24.0% overall increase). In summary, while observations of primary productivity have shown complex interannual and spatial patterns over the 2003-21 period, we observe overall increasing trends across all sectors of the Arctic Ocean.

Methods and data

Measurements of the algal pigment chlorophyll (specifically, chlorophyll-*a*) serve as a proxy for the amount of algal biomass present in the ocean (e.g., Behrenfeld and Boss 2006) as well as overall plant health. The complete, updated Moderate Resolution Imaging Spectroradiometer (MODIS)-Aqua satellite record of chlorophyll-*a* concentrations within northern polar waters for the years 2003-21 serves as a

time series against which individual years can be compared. Satellite-based chlorophyll-*a* data across the pan-Arctic region were derived using the MODIS-Aqua Reprocessing 2018.0, chlor_a algorithm: https://oceancolor.gsfc.nasa.gov/. For this reporting, we show mean monthly chlorophyll-*a* concentrations calculated as a percentage of the 2003-20 average, which was chosen as the reference period in order to maximize the length of the satellite-based time series. Satellite-based sea ice concentrations were derived from the Special Sensor Microwave/Imager (SSM/I) and Special Sensor Microwave Imager/Sounder (SSMIS) passive microwave instruments, calculated using the Goddard Bootstrap (SB2) algorithm (Comiso et al. 2017). Monthly sea ice concentration anomalies were additionally calculated for 2021 (compared to the 2003-20 average) in order to streamline comparisons with the variability in monthly chlorophyll-*a* satellite data. Primary productivity data were derived using chlorophyll-*a* concentrations from MODIS-Aqua data, the NOAA 1/4° daily Optimum Interpolation Sea Surface Temperature Version 2 dataset (or daily OISSTv2) that uses satellite sea surface temperatures from AVHRR, incident solar irradiance, mixed layer depths, and additional parameters. Primary productivity values were calculated based on the techniques described by Behrenfeld and Falkowski (1997). Chlorophyll-*a* and primary productivity data only incorporate pixels where sea ice is less than 10%, which is a compromise between potential pixel contamination with sea ice and an attempt to incorporate open water near the ice edge that typically exhibits high rates of primary production. We define annual productivity as productivity over the March-September time period. The 2021 annual primary productivity percent of average (compared to 2003-20) was calculated the same way as for chlorophyll-*a*, as described above. Lastly, Theil-Sen median trends were calculated spatially (Fig. 3b) and for the extracted time series for each geographic region (Table 1), where statistical significance ($p<0.05$) of the trends was determined using the Mann-Kendall trend test.

An erratum for past Arctic Report Card (ARC) primary production essays (2015-2020) can be found here. *This erratum identifies how the algorithm that produced primary production data for these years incorrectly incorporated sea surface temperatures, and presents a comparison of the previously reported data with corrected updated data.*

Acknowledgments

K. Frey would like to acknowledge financial support by the National Science Foundation (NSF) Arctic Observing Network (AON) Program (Grant 1917434). J. Comiso and L. Stock are also grateful for the support provided by the NASA Ocean Biology and Biogeochemistry Program. Support for J. Grebmeier and L. Cooper is provided through NSF AON (Grant 1917469) and the NOAA Arctic Research Program (CINAR 22309.07_UMCES_Grebmeier).

References

Ardyna, M., M. Babin, E. Devred, A. Forest, M. Gosselin, P. Raimbault, and J. -É. Tremblay, 2017: Shelf-basin gradients shape ecological phytoplankton niches and community composition in the coastal Arctic Ocean (Beaufort Sea). *Limnol. Oceanogr.*, **62**, 2113-2132, https://doi.org/10.1002/lno.10554.

Ardyna, M., and Coauthors, 2020: Under-ice phytoplankton blooms: Shedding light on the "invisible" part of Arctic primary production. *Front. Mar. Sci.*, **7**, 608032, https://doi.org/10.3389/fmars.2020.608032.

Behrenfeld, M. J., and E. Boss, 2006: Beam attenuation and chlorophyll concentration as alternative optical indices of phytoplankton biomass. *J. Mar. Res.*, **64**, 431-451, https://doi.org/10.1357/002224006778189563.

Behrenfeld, M. J., and P. G. Falkowski, 1997: Photosynthetic rates derived from satellite-based chlorophyll concentration. *Limnol. Oceanogr.*, **42**(1), 1-20, https://doi.org/10.4319/lo.1997.42.1.0001.

Bouman, H. A., T. Jackson, S. Sathyendranath, and T. Platt, 2020: Vertical structure in chlorophyll profiles: influence on primary production in the Arctic Ocean. *Philos. Trans. Roy. Soc. A*, **378**, 20190351, https://doi.org/10.1098/rsta.2019.0351.

Comiso, J. C., 2015: Variability and trends of the global sea ice covers and sea level: Effects on physicochemical parameters. Climate and Fresh Water Toxins, L. M. Botana, M. C. Lauzao, and N. Vilarino, Eds., De Gruyter, Berlin, Germany, https://doi.org/10.1515/9783110333596-003.

Comiso, J. C., W. N. Meier, and R. Gersten, 2017: Variability and trends in the Arctic Sea ice cover: Results from different techniques. *J. Geophys. Res.-Oceans*, **122**, 6883-6900, https://doi.org/10.1002/2017JC012768.

Crawford, A. D., K. M. Krumhardt, N. S. Lovenduski, G. L. Van Dijken, and K. R. Arrigo, 2020: Summer high-wind events and phytoplankton productivity in the Arctic Ocean. *J. Geophys. Res.-Oceans*, **125**, e2020JC016565, https://doi.org/10.1029/2020jc016565.

Duffy-Anderson, J. T., and Coauthors, 2019: Responses of the northern Bering Sea and southeastern Bering Sea pelagic ecosystems following record-breaking low winter sea ice. *Geophys. Res. Lett.*, **46**, 9833-9842, https://doi.org/10.1029/2019GL083396.

Filbee-Dexter, K., T. Wernberg, S. Fredriksen, K. M. Norderhaug, and M. F. Pedersen, 2019: Arctic kelp forests: Diversity, resilience and future. *Global Planet. Change*, **172**, 1-14, https://doi.org/10.1016/j.gloplacha.2018.09.005.

Garcia-Eidell, C., J. C. Comiso, M. Berkelhammer, and L. Stock, 2021: Interrelationships of sea surface salinity, chlorophyll-*a* concentration, and sea surface temperature near the Antarctic ice edge. *J. Climate*, **34**(15), 6069-6086, https://doi.org/10.1175/JCLI-D-20-0716.1.

Giesbrecht, K. E., D. E. Varela, J. Wiktor, J. M. Grebmeier, B. Kelly, and J. E. Long, 2019: A decade of summertime measurements of phytoplankton biomass, productivity and assemblage composition in the Pacific Arctic Region from 2006 to 2016. *Deep-Sea Res. Pt. II*, **162**, 93-113, https://doi.org/10.1016/j.dsr2.2018.06.010.

Goldsmit, J., and Coauthors, 2021: Kelp in the eastern Canadian Arctic: Current and future predictions of habitat suitability and cover. *Front. Mar. Sci.*, **18**, 742209, https://doi.org/10.3389/fmars.2021.742209.

Henley, S. F., M. Porter, L. Hobbs, J. Braun, R. Guillaume-Castel, E. J. Venables, E. Dumont, and F. Cottier, 2020: Nitrate supply and uptake in the Atlantic Arctic sea ice zone: seasonal cycle, mechanisms and drivers. *Philos. T. Roy. Soc. A*, **378**(2181), 20190361, http://doi.org/10.1098/rsta.2019.0361.

Hill, V., M. Ardyna, S. H. Lee, and D. E. Varela, 2018: Decadal trends in phytoplankton production in the Pacific Arctic Region from 1950 to 2012. *Deep-Sea Res. Pt. II*, **152**, 82-94, https://doi.org/10.1016/j.dsr2.2016.12.015.

Hölemann, J. A., B. Juhls, D. Bauch, M. Janout, B. P. Koch, and B. Heim, 2021: The impact of the freeze-melt cycle of land-fast ice on the distribution of dissolved organic matter in the Laptev and East Siberian Seas (Siberian Arctic). *Biogeosciences*, **18**, 3637-3655, https://doi.org/10.5194/bg-18-3637-2021.

Hopwood, M. J., and Coauthors, 2020: Review article: How does glacier discharge affect marine biogeochemistry and primary production in the Arctic? *Cryosphere*, **14**, 1347-1383, https://doi.org/10.5194/tc-14-1347-2020.

Kim, H. -J., and Coauthors, 2021: Temporal and spatial variations in particle fluxes on the Chukchi Sea and East Siberian Sea slopes from 2017 to 2018. *Front. Mar. Sci.*, **7**, 609748, https://doi.org/10.3389/fmars.2020.609748.

Lalande, C., J. M. Grebmeier, R. R. Hopcroft, and S. L. Danielson, 2020: Annual cycle of export fluxes of biogenic matter near Hanna Shoal in the northeast Chukchi Sea. *Deep-Sea Res. Pt. II*, **177**, 104730, https://doi.org/10.1016/j.dsr2.2020.104730.

Lalande, C., J. M. Grebmeier, A. M. P. McDonnell, R. R. Hopcroft, S. O'Daly, and S. L. Danielson, 2021: Impact of a warm anomaly in the Pacific Arctic region derived from time-series export fluxes. *PLoS ONE*, **16**(8), e0255837, https://doi.org/10.1371/journal.pone.0255837.

Lalande, C., E. -M. Nöthig, and L. Fortier, 2019: Algal export in the Arctic Ocean in times of global warming. *Geophys. Res. Lett.*, **46**, 5959-5967, https://doi.org/10.1029/2019gl083167.

Lewis, K. M., B. G. Mitchell, G. L. van Dijken, and K. R. Arrigo, 2016: Regional chlorophyll *a* algorithms in the Arctic Ocean and their effect on satellite-derived primary production estimates. *Deep-Sea Res. Pt. II*, **130**, 14-27, https://doi.org/10.1016/j.dsr2.2016.04.020.

Lewis, K. M., G. L. van Dijken, and K. R. Arrigo, 2020: Changes in phytoplankton concentration now drive increased Arctic Ocean primary production. *Science*, **369**, 198-202, https://doi.org/10.1126/science.aay8380.

Logvinova, C. L., K. E. Frey, and L. W. Cooper, 2016: The potential role of sea ice melt in the distribution of chromophoric dissolved organic matter in the Chukchi and Beaufort Seas. *Deep-Sea Res. Pt. II*, **130**, 28-42, https://doi.org/10.1016/j.dsr2.2016.04.017.

Neeley, A. R., L. A. Harris, and K. E. Frey, 2018: Unraveling phytoplankton community dynamics in the northern Chukchi Sea under sea-ice-covered and sea-ice-free conditions. *Geophys. Res. Lett.*, **45**, 7663–7671, https://doi.org/10.1029/2018GL077684.

Randelhoff, A., and Coauthors, 2020: Arctic mid-winter phytoplankton growth revealed by autonomous profilers. *Sci. Adv.*, **6**, eabc2678, https://doi.org/10.1126/sciadv.abc2678.

Rijkenberg, M. J., H. A. Slagter, M. Rutgers van der Loeff, J. van Ooijen, and L. J. A. Gerringa, 2018: Dissolved Fe in the deep and upper Arctic Ocean with a focus on Fe limitation in the Nansen Basin. *Front. Mar. Sci.*, **5**, 88, https://doi.org/10.3389/fmars.2018.00088.

Yun, M. S., and Coauthors, 2016: Primary production in the Chukchi Sea with potential effects of freshwater content. *Biogeosciences*, **13**, 737-749, https://doi.org/10.5194/bg-13-737-2016.

November 22, 2021

Tundra Greenness

DOI: 10.25923/8n78-wp73

G. V. Frost[1], M. J. Macander[1], U. S. Bhatt[2], L. T. Berner[3], J. W. Bjerke[4], H. E. Epstein[5], B. C. Forbes[6], S. J. Goetz[3], M. J. Lara[7,8], T. Park[9,10], G. K. Phoenix[11], S. P. Serbin[12], H. Tømmervik[4], D. A. Walker[13], and D. Yang[12,14]

[1]Alaska Biological Research, Inc., Fairbanks, AK, USA
[2]Geophysical Institute, University of Alaska Fairbanks, Fairbanks, AK, USA
[3]School of Informatics, Computing and Cyber Systems, Northern Arizona University, Flagstaff, AZ, USA
[4]Norwegian Institute for Nature Research, FRAM - High North Research Centre for Climate and the Environment, Tromsø, Norway
[5]Department of Environmental Sciences, University of Virginia, Charlottesville, VA, USA
[6]Arctic Centre, University of Lapland, Rovaniemi, Finland
[7]Department of Plant Biology, University of Illinois, Urbana, IL, USA
[8]Department of Geography, University of Illinois, Urbana, IL, USA
[9]Ames Research Center, NASA, Mountain View, CA, USA
[10]Bay Area Environmental Research Institute, Moffett Field, CA, USA
[11]School of Biosciences, University of Sheffield, Sheffield, UK
[12]Environmental and Climate Sciences Department, Brookhaven National Laboratory, Upton, NY, USA
[13]Institute of Arctic Biology, University of Alaska Fairbanks, Fairbanks, AK, USA
[14]Department of Ecology and Evolution, Stony Brook University, Stony Brook, NY, USA

Highlights

- 2021 continued a recent series of years with exceptionally high midsummer tundra productivity, or "greenness."
- The five highest circumpolar tundra greenness measurements in the long-term satellite record (1982-2020) have all been recorded in the last 10 years.
- Satellites provide unequivocal evidence of widespread tundra greening, but extreme events and other drivers of local-scale "browning" have also become more frequent, highlighting regional variability as an increasing component of Arctic change.

Introduction

Earth's northernmost continental landmasses and island archipelagos are home to the Arctic tundra biome, a 5.1 million km^2 region characterized by low-growing, treeless vegetation adapted to short, cool summers (CAVM Team 2003). The Arctic tundra biome has long been a "hotspot" of global environmental change, because vegetation and underlying permafrost soils are strongly influenced by warming air temperatures and the rapid decline of sea ice on the nearby Arctic Ocean (Bhatt et al. 2021; see essays *Surface Air Temperature* and *Sea Ice*). In the late 1990s, a pronounced increase in the productivity of tundra vegetation became evident in global satellite observations, a phenomenon that has come to be known as "the greening of the Arctic." Arctic greening is dynamically linked with Earth's changing climate, permafrost, seasonal snow, and sea-ice cover, and has continued to be a focal point of multi-disciplinary scientific research. Today, a growing constellation of spaceborne satellite sensors and

emerging airborne technologies such as unoccupied aerial systems (UAS), or "drones," provide increasingly detailed observations of Arctic ecosystems.

Satellite observations of tundra greenness

Arctic tundra greenness has been monitored from space since 1982 by the Advanced Very High Resolution Radiometer (AVHRR), and since 2000 by the Moderate Resolution Imaging Spectroradiometer (MODIS). Both satellite sensors monitor vegetation greenness using the Normalized Difference Vegetation Index (NDVI), a spectral metric that exploits the unique way in which green vegetation reflects light in the visible and infrared wavelengths. The AVHRR and MODIS records both indicate that the yearly maximum tundra greenness (MaxNDVI) has increased across most of the circumpolar Arctic during 1982-2020 and 2000-21, respectively (Figs. 1a,b). Several Arctic regions display particularly strong trends in both records. In North America, greening has been strongest in northern Alaska and mainland Canada, while flat or negative ("browning") trends are evident in parts of the Canadian Arctic Archipelago and southwestern Alaska. In Eurasia, strong greening has occurred in the Russian Far East (Chukotka), but browning is evident in the East Siberian Sea sector and parts of the Taymyr Peninsula. Trends in northwestern Siberia and the European Arctic provide mixed signals, which may be due to the different periods across the two satellite records. Regional contrasts in greenness highlight the complexity of Arctic change, and the rich web of interactions that exist between tundra ecosystems and the local properties of sea ice, permafrost, seasonal snow, soil composition and moisture, disturbance processes, wildlife, and human activities (Buchwal et al. 2020; Myers-Smith et al. 2020; Campbell et al. 2021).

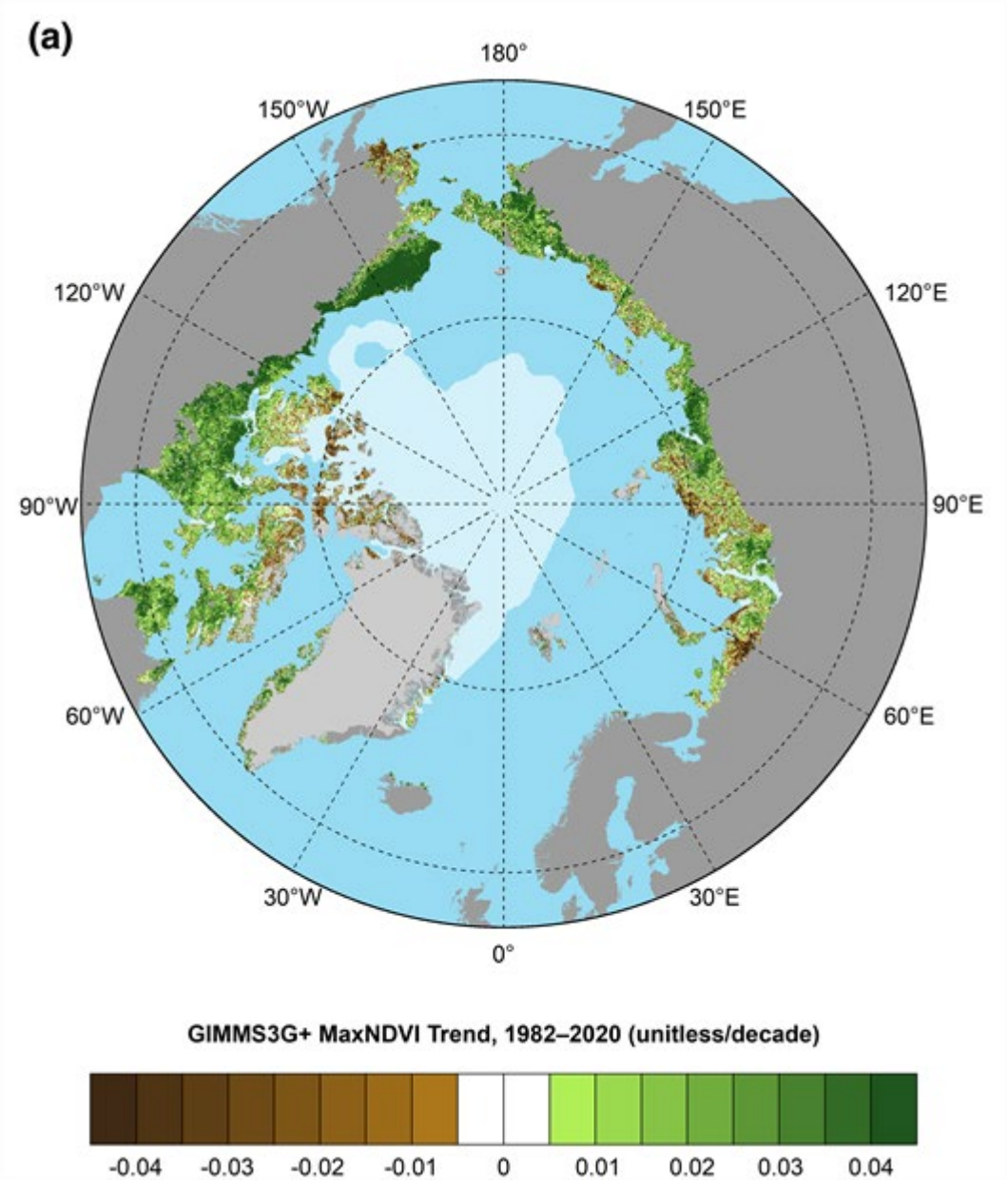

Fig. 1a. Magnitude of the trend in MaxNDVI (Maximum Difference Vegetation Index) for the 39-year period 1982-2020 based on the AVHRR GIMMS-3g+ dataset. GIMMS-3g+ data for 2021 were not available for this report due to data-processing requirements. The 2020 minimum sea-ice extent is indicated by light shading.

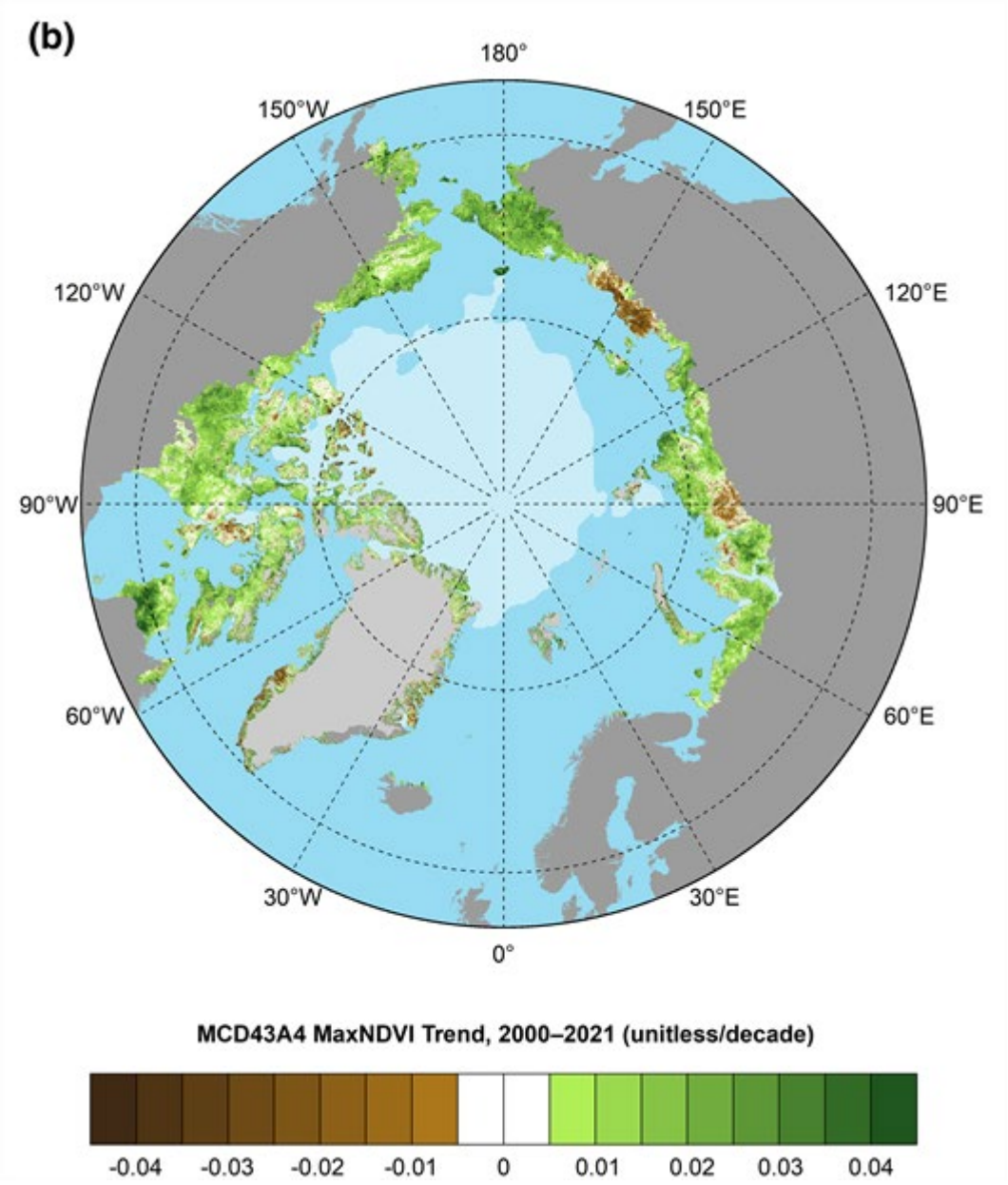

Fig. 1b. Magnitude of the trend in MaxNDVI (Maximum Difference Vegetation Index) for the 22-year period 2000-21 based on the MODIS MCD43A4 dataset. The 2021 minimum sea-ice extent is indicated by light shading.

In 2020—the most recent year with observations from both AVHRR and MODIS—both sensors observed record-high MaxNDVI values for Eurasia, North America, and the circumpolar region as a whole, concurrent with record-high Arctic surface temperatures and record-low snow cover that year (see essay *Terrestrial Snow Cover*). In 2021, the circumpolar MODIS-observed MaxNDVI value declined 2.7% from the previous year, but was still the second highest value in the 22-year record for that sensor. Further, the overall trend in MODIS-observed circumpolar MaxNDVI is strongly positive, and circumpolar values have exceeded the 22-year mean in 11 of the last 12 growing seasons (Fig. 2). The AVHRR record also indicates increasing annual mean circumpolar MaxNDVI for both the full record (1982-2020) and the period of overlap with MODIS (2000-20).

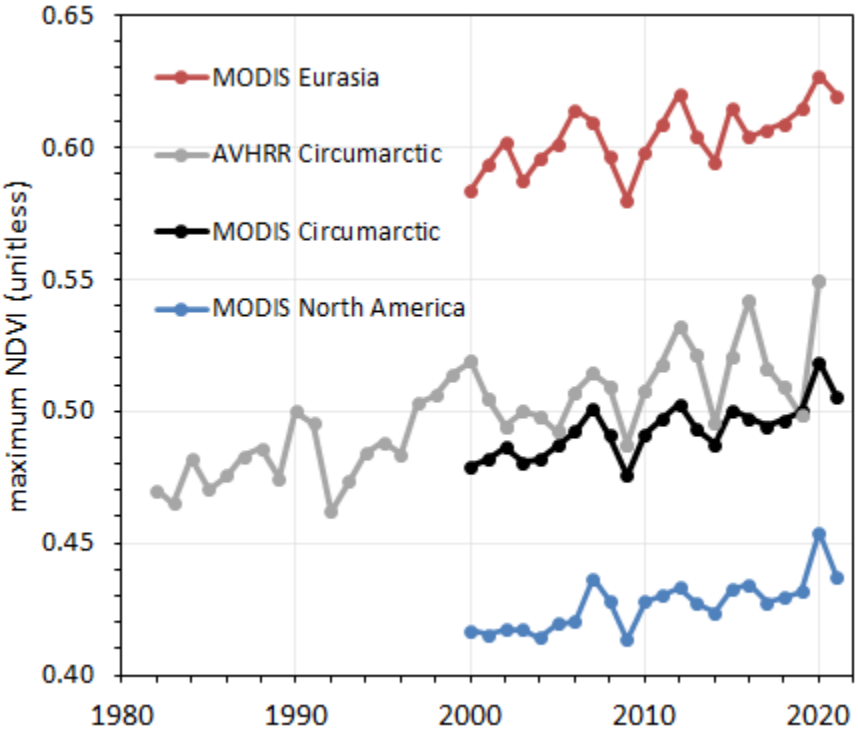

Fig. 2. Time series of MaxNDVI (Maximum Normalized Difference Vegetation Index) from the MODIS MCD43A4 (2000-21) dataset for the Eurasian Arctic (in red), North American Arctic (in blue), and the circumpolar Arctic (in black), and from the long-term AVHRR GIMMS-3g+ (1982-2020) dataset for the circumpolar Arctic (in gray).

Interpretation of greening trends

What are the drivers that underlie the greening trends observed from space, and what types of change might an observer see on the ground? Recent low-altitude remote sensing and field-based studies provide detail and context for understanding changes in vegetation and landscape features that underlie the greenness trends observed by satellites. Increases in the abundance and height of Arctic shrubs are a key driver of Arctic greening, and have important impacts on biodiversity, surface energy balance, permafrost temperatures, and biogeochemical cycling (Kropp et al. 2021; Mekonnen et al. 2021). However, many Arctic landscapes are a complex mosaic of lakes, ponds, marshes, and vegetated terrain, and this heterogeneity presents challenges in quantifying the drivers and impacts of shrub increase on tundra ecosystems. The emergence of UAS has opened new windows to study the influence of shrub increase both in the "big picture" of Arctic greening, and on the structure and function of ecosystems in specific tundra landscapes. For example, in western Alaska, Yang et al. (2021) observed a reduction in plant species richness in areas with higher abundance of tall shrubs. With these fine-scale UAS datasets, the scale-gap between field- and satellite-observed patterns of vegetation change will begin to close, enabling more detailed monitoring of vegetation composition, structure, and function to track changes across the Arctic.

The timing of phenological events and the duration of the Arctic growing season are useful indicators of Arctic climate change that can be tracked both on the ground and from space. Ground-based observation systems provide more frequent measurements beyond the capabilities of satellites, and effectively link the seasonality and spatial patterns of vegetation greenness with spaceborne

observations (Parmentier et al. 2021; Swanson 2021). For example, Hemming et al. (2021) used MODIS, time-lapse digital cameras, and field observations to evaluate changes in Northern Hemisphere phenology. They found that climate warming has led to earlier onset (-2.3 ± 0.7 days decade^{-1}) and a later end (1.3 ± 0.9 days decade^{-1}) of growing seasons during 2000-20. Additionally, in Svalbard, Karlsen et al. (2021) used high-resolution satellite data and a network of ground-based cameras to show that the onset of the 2018 growing season was 10 days earlier than in 2017, highlighting the variability in seasonality that can influence tundra greenness from year to year.

Although the satellite record provides unequivocal evidence of widespread tundra greening, there is substantial regional variability. Greening is not occurring everywhere; many parts of the Arctic exhibit little or no trend (Callaghan et al. 2021), and some regions, such as the East Siberian Sea sector, exhibit widespread browning, due in part to ground subsidence and increased surface water triggered by permafrost thaw (Veremeeva et al. 2021; see essay *Glacier and Permafrost Hazards*). Die-back or removal of vegetation can also be caused by ecological disturbances, including wildfire (Gaglioti et al. 2021), permafrost thaw (Magnússon et al. 2021), herbivory and pest outbreaks (Veselkin et al. 2021), and the construction of beaver dams (Jones et al. 2020; see *Beaver* essay). While warming is likely to continue to drive Arctic greening, extreme events and other causes of browning are also increasing in frequency (Christensen et al. 2021), highlighting the emergence of increased variability as a component of Arctic climate change.

Methods and data

The satellite record of Arctic tundra greenness began in 1982 using the Advanced Very High Resolution Radiometer (AVHRR), a sensor that collects daily observations and continues to operate onboard polar-orbiting satellites. As of September 2021, however, processed AVHRR data were only available through the 2020 growing season. Therefore, we also report observations from the Moderate Resolution Imaging Spectroradiometer (MODIS), a more modern sensor with improved calibration and spatial resolution that became operational in 2000. The long-term AVHRR dataset analyzed here for 1982-2020 is the Global Inventory Modeling and Mapping Studies 3g V1.2 dataset (GIMMS-3g+), which is based on corrected and calibrated AVHRR data with a spatial resolution of about 8 km (Pinzon and Tucker 2014). For MODIS, we computed tundra greenness trends for 2000-21 at a much higher spatial resolution of 500 m from daily Nadir Bidirectional Reflectance Distribution Function Adjusted Reflectance data (MCD43A4, version 6; Schaaf and Wang 2015). Data were masked to include only ice-free land within the extent of the Circumpolar Arctic Vegetation Map (CAVM Team 2003); MODIS data were further masked to exclude permanent water based on the 2015 MODIS Terra Land Water Mask (MOD44W, version 6). We summarize the GIMMS-3g+ and MODIS records for Maximum NDVI (MaxNDVI), the peak yearly value that is strongly correlated with the biomass of aboveground vegetation during midsummer (Raynolds et al. 2012). The seasonal timing of MaxNDVI varies from year to year and from place to place, but occurs during the months of July and August for most of the Arctic. MaxNDVI time-series for the two sensors show similar patterns and trends for the period of overlap (2000-20), but the AVHRR record displays higher variability (i.e., "noise"), particularly over the last 5 years of the record. This is likely due in part to AVHRR's lower spatial resolution and less advanced calibration compared to MODIS.

Acknowledgments

We thank Jorge Pinzon at the Biospheric Sciences Laboratory, NASA Goddard Space Flight Center for providing updates for the GIMMS-3g+ dataset.

References

Bhatt, U. S., and Coauthors, 2021: Climate drivers of Arctic tundra variability and change using an indicators framework. *Environ. Res. Lett.*, **16**, 055019, https://doi.org/10.1088/1748-9326/abe676.

Buchwal, A., and Coauthors, 2020: Divergence of Arctic shrub growth associated with sea ice decline. *Proc. Natl. Acad. Sci. USA*, **117**, 33334-33344, https://doi.org/10.1073/pnas.2013311117.

Callaghan, T. V., R. Cazzolla Gatti, and G. Phoenix, 2021: The need to understand the stability of arctic vegetation during rapid climate change: An assessment of imbalance in the literature. *Ambio*, https://doi.org/10.1007/s13280-021-01607-w.

Campbell, T. K. F., T. C. Lantz, R. H. Fraser, and D. Hogan, 2021: High Arctic vegetation change mediated by hydrological conditions. *Ecosystems*, **24**, 106-121, https://doi.org/10.1007/s10021-020-00506-7.

CAVM Team, 2003: Circumpolar Arctic vegetation map (1:7,500,000 scale). Conservation of Arctic Flora and Fauna (CAFF) Map No. 1. U.S. Fish and Wildlife Service, Anchorage, AK.

Christensen, T. R., and Coauthors, 2021: Multiple ecosystem effects of extreme weather events in the Arctic. *Ecosystems*, **24**, 122-136, https://doi.org/10.1007/s10021-020-00507-6.

Gaglioti, B. V., and Coauthors, 2021: Tussocks enduring or shrubs greening: Alternate responses to changing fire regimes in the Noatak River Valley, Alaska. *J. Geophys. Res.-Biogeosci.*, **126**, e2020JG006009, https://doi.org/10.1029/2020JG006009.

Hemming, D. L., J. Garforth, J. O'Keefe, T. Park, A. D. Richardson, T. Rutishauser, T. H. Sparks, and S. J. Thackeray, 2021: Phenology of primary producers [in "State of the Climate in 2020"]. *Bull. Amer. Meteor. Soc.*, **102**, S108-S111.

Jones, B. M., K. D. Tape, J. A. Clark, I. Nitze, G. Grosse, and J. Disbrow, 2020: Increase in beaver dams controls surface water and thermokarst dynamics in an Arctic tundra region, Baldwin Peninsula, northwestern Alaska. *Environ. Res. Lett.*, **15**, 075005, https://doi.org/10.1088/1748-9326/ab80f1.

Karlsen, S. R., L. Stendardi, H. Tømmervik, L. Nilsen, I. Arntzen, and E. J. Cooper, 2021: Time-series of cloud-free Sentinel-2 NDVI data used in mapping the onset of growth of central Spitsbergen, Svalbard. *Remote Sens.*, **13**, 3031, https://doi.org/10.3390/rs13153031.

Kropp, H., and Coauthors, 2021: Shallow soils are warmer under trees and tall shrubs across Arctic and Boreal ecosystems. *Environ. Res. Lett.*, **16**, 015001, https://doi.org/10.1088/1748-9326/abc994.

Magnússon, R. Í., J. Limpens, D. Kleijn, K. Huissteden, T. C. Maximov, S. Lobry, and M. M. P. D. Heijmans, 2021: Shrub decline and expansion of wetland vegetation revealed by very high resolution land cover change detection in the Siberian lowland tundra. *Sci. Total Environ.*, **782**, 146877, https://doi.org/10.1016/j.scitotenv.2021.146877.

Mekonnen, Z. A., and Coauthors, 2021: Arctic tundra shrubification: a review of mechanisms and impacts on ecosystem carbon balance. *Environ. Res. Lett.*, **16**, 053001, https://doi.org/10.1088/1748-9326/abf28b.

Myers-Smith, I. H., and Coauthors, 2020: Complexity revealed in the greening of the Arctic. *Nat. Climate Change*, **10**, 106-117, https://doi.org/10.1038/s41558-019-0688-1.

Parmentier, F. -J. W., L. Nilsen, H. Tømmervik, and E. J. Cooper, 2021: A distributed time-lapse camera network to track vegetation phenology with high temporal detail and at varying scales. *Earth Syst. Sci. Data*, **13**, 3593-3606, https://doi.org/10.5194/essd-13-3593-2021.

Pinzon, J. E., and C. J. Tucker, 2014: A non-stationary 1981-2012 AVHRR $NDVI_{3g}$ time series. *Remote Sens.*, **6**, 6929-6960, https://doi.org/10.3390/rs6086929.

Raynolds, M. K., D. A. Walker, H. E. Epstein, J. E. Pinzon, and C. J. Tucker, 2012: A new estimate of tundra-biome phytomass from trans-Arctic field data and AVHRR NDVI. *Remote Sens. Lett.*, **3**, 403-411, https://doi.org/10.1080/01431161.2011.609188.

Schaaf, C., and Z. Wang, 2015: MCD43A4 MODIS/Terra+Aqua BRDF/Albedo Nadir BRDF Adjusted Ref Daily L3 Global - 500m V006. NASA EOSDIS Land Processes DAAC [Nadir BRDF-Adjusted Reflectance (NBAR) Daily L3 Global 500 m SIN Grid], accessed 1 September 2021, https://doi.org/10.5067/MODIS/MCD43A4.006.

Swanson, D. K., 2021: Start of the green season and Normalized Difference Vegetation Index in Alaska's Arctic national parks. *Remote Sens.*, **13**, 2554, https://doi.org/10.3390/rs13132554.

Veremeeva, A., I. Nitze, F. Günther, G. Grosse, and E. Rivkina, 2021: Geomorphological and climatic drivers of thermokarst lake area increase trend (1999-2018) in the Kolyma Lowland yedoma region, north-eastern Siberia. *Remote Sens.*, **13**, 178, https://doi.org/10.3390/rs13020178.

Veselkin, D. V., L. M. Morozova, and A. M. Gorbunova, 2021: Decrease of NDVI values in the southern tundra of Yamal in 2001-2018 correlates with the size of domesticated reindeer population. Sovrem. Probl. Distantsionnogo Zondirovaniya Zemli Iz Kosmosa, **18**, 143-155, https://doi.org/10.21046/2070-7401-2021-18-2-143-155.

Yang, D., and Coauthors, 2021: Landscape-scale characterization of Arctic tundra vegetation composition, structure, and function with a multi-sensor unoccupied aerial system. *Environ. Res. Lett.*, **16**, 085005, https://doi.org/10.1088/1748-9326/ac1291.

November 17, 2021

Beaver Engineering: Tracking a New Disturbance in the Arctic

DOI: 10.25923/0jtd-vv85

K. D. Tape[1], J. A. Clark[1], B. M. Jones[2], H. C. Wheeler[3], P. Marsh[4], and F. Rosell[5]

[1]Geophysical Institute, University of Alaska Fairbanks, Fairbanks, AK, USA
[2]Water and Environmental Research Center, Institute of Northern Engineering, University of Alaska Fairbanks, Fairbanks, AK, USA
[3]School of Life Sciences, Anglia Ruskin University, Cambridge, UK
[4]Department of Geography, Wilfrid Laurier University, Waterloo, ON, Canada
[5]Department of Natural Sciences and Environmental Health, University of South-Eastern Norway, Bø, Norway

Highlights

- Recent satellite imagery and older aerial photography show that North American beavers (*Castor canadensis*) are colonizing the Arctic tundra of Alaska, with over 12,000 ponds thus far counted in western Alaska, a doubling of ponds since 2000.
- In Canada, beaver pond mapping is underway, complemented by scattered observations of recent changes. Eurasian beavers (*C. fiber*) are rebounding in Asia but remain south of the Arctic tundra in most locations.
- The Arctic Beaver Observation Network was established in 2020 to help integrate, guide, and disseminate information concerning beaver range expansion into tundra regions and implications for ecosystems and resources.

Introduction

Research on North American beaver (*Castor canadensis*) engineering in the Arctic has made great strides in recent years, but most of the work lies ahead. Over the last several decades, people in remote Alaska communities have observed an influx of beavers (ADF&G Reports 1965-2017). We quantified this trend by using satellite imagery to detect beaver pond formation in Alaska tundra regions, mapping approximately 12,000 beaver ponds (e.g., Fig. 1, right panel), including a doubling in most areas during the last 20 years (Tape et al. 2021). We showed that new beavers are controlling surface water increases, which affects underlying permafrost (Jones et al. 2020). Fieldwork is underway to characterize the impacts of beaver ponds on aquatic and terrestrial Arctic ecosystems, starting with hydrology and permafrost, and continuing downstream to methane flux, fish populations, and aquatic food webs. As a result of these efforts, most of the questions surrounding beaver engineering in the Arctic are presently being examined but are unanswered. To coordinate research and action among stakeholders in the circumarctic region, the Arctic Beaver Observation Network (A-BON) was formed in 2020 and a synthesis effort is underway to identify knowledge gaps and support the integration of different approaches and perspectives.

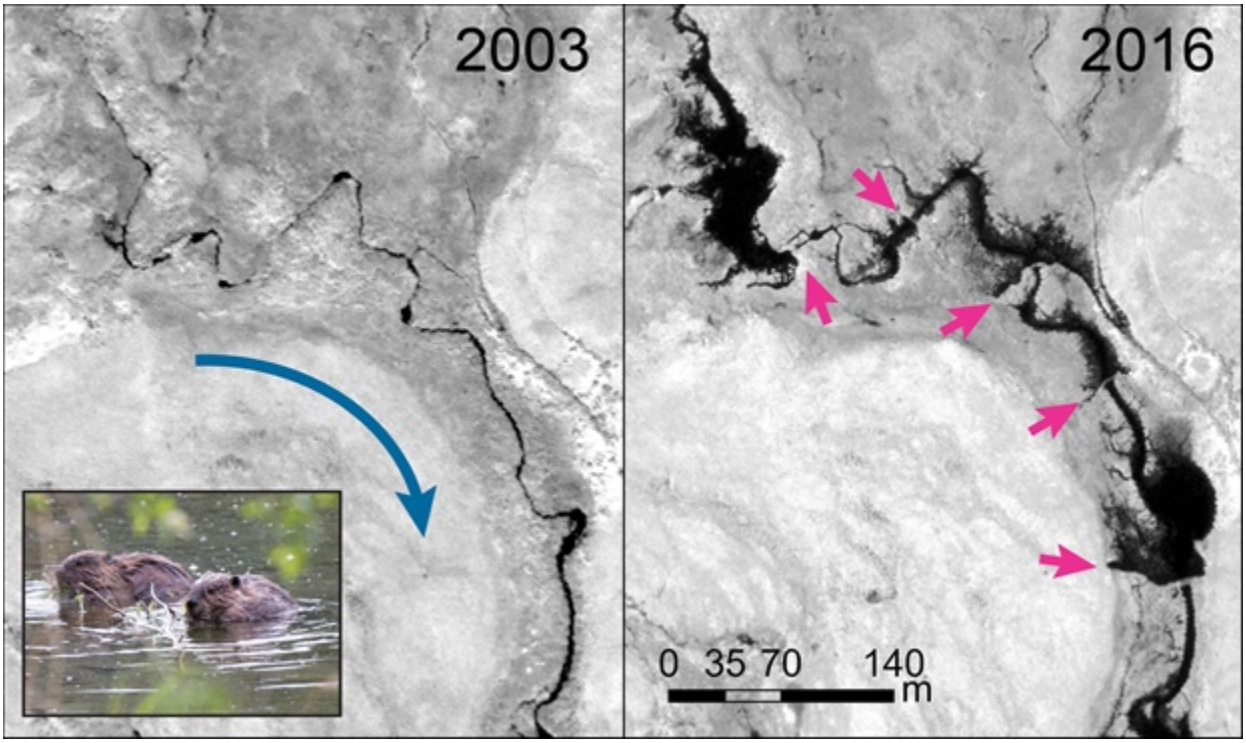

Fig. 1. Beaver engineering dramatically altered a tundra stream on the Seward Peninsula in western Alaska between 2003 and 2016. The enlarged black areas are new beaver ponds, the blue arrow shows flow direction, and magenta arrows denote dams. Ikonos satellite image: 6 Aug 2003, Worldview satellite image: 10 June 2016, 64° 33.52'N, 165° 50.12'W (Imagery © 2021 Maxar).

Tundra be dammed

In 2016 we imagined that beaver distribution and possible dispersal in the Arctic could be identified by mapping beaver ponds in satellite imagery and older aerial photography through time. Initial studies confirmed our suspicions (Tape et al. 2018), as did the observations of local people in northwest Alaska, who have been observing the influx of beavers for a half-century (ADF&G Reports 1965-2017). Yet the scale and magnitude of this new disturbance regime was unknown in Alaska and the circumarctic. We have since mapped approximately 12,000 beaver ponds (using 2015-19 imagery) in Arctic tundra of Alaska (e.g., Fig. 2). This mapping excludes southwest Alaska tundra and thus provides an underestimate of the total number of beaver ponds. Most areas show a doubling of beaver ponds in the last 20 years (Tape et al. 2021). In 1949-55 aerial photography covering coastal areas of western Alaska, there are no detectable beaver ponds. Stream by stream and floodplain by floodplain, beavers are transforming lowland tundra ecosystems. Increased vegetation productivity (see essay *Tundra Greenness*) and the expansion of woody shrubs (Myers-Smith et al. 2015) due to climate change has created more forage and dam construction materials, translating to more favorable habitat. The increase in winter stream discharge (St. Jacques and Sauchyn 2009) also implies greater aqueous habitat. Finally, the earlier end of winter and onset of spring (see essay *Terrestrial Snow Cover*), when beavers can again begin foraging, effectively shortens what is presumably the most challenging time in the annual life cycle of beavers. It remains unclear whether beaver colonization of the Arctic is occurring due to climate change ameliorating habitat or a decrease in trapping pressure, or some combination of both.

Fig. 2. Beaver lodge (center), dam (bottom center), and pond on the Seward Peninsula in western Alaska. (Credit: Ken Tape, Aug 2021)

In Canada, beaver distribution changes have also been observed both by local people and scientists. Concern over rising numbers of beavers in the Inuvialuit settlement region in the Northwest Territories in northwestern Canada was sufficient to instigate a harvesting incentive scheme in 2017. Although publications of academic studies of beavers in northern Canada have been sparse to date, there are reports of beavers north of the previously known range (Jung et al. 2016).

In Europe, Eurasian beavers (*C. fiber*) were widespread from the Arctic to the Mediterranean, before being substantially reduced around the twelfth century, and almost extinct by the sixteenth century. Today, the Eurasian beaver has restored a large area of its original range, and increased in numbers from around 1200 beavers a century ago to an estimated 1.5 million individuals today; beavers distribution reaches the northern coast throughout most of Europe (Halley et al. 2021). In Asia, beaver distribution remains well south of Arctic tundra regions, though recent northward range extensions have been observed (Halley et al. 2021). In general, research on beavers in Arctic tundra regions is in its early stages. A coordinated circumarctic beaver pond mapping effort is underway, which will hopefully establish the footprint, if not the nature, of this new disturbance regime in the Arctic.

Implications of beaver engineering in the Arctic

Beavers are a keystone species whose engineering is known to heavily influence streams, rivers, riparian corridors, and lakes in North America, Eurasia, and South America (Whitfield et al. 2015). Beavers are known to dramatically change the landscapes they inhabit by harvesting shrubs, saplings, and trees, which they use to construct dams, inundate the surrounding landscape, and create their watery world.

Beavers build lodges of mud and vegetation in water that is deep enough for an underwater entrance that remains unfrozen and permits access for them, but not predators. By constructing dams, beavers severely alter the stream flow regime, which facilitates the arrival of new species, including riverine plants, invertebrates, and fish (Bunn and Arthington 2002). Beaver ponds in temperate ecosystems enhance aquatic habitat complexity and biodiversity.

It remains unclear how these impacts will be manifest in the Arctic, where low water temperatures inhibit stream productivity and biodiversity, and where permafrost holds much of the soil together. People living in remote communities are concerned for resources such as fish, water quality, and boat access (Moerlein and Carothers 2012). In an area of northwest Alaska with exceptional satellite imagery coverage, we discovered that beavers are the dominant factor (66%) controlling increases in surface water extent (Jones et al. 2020), which thaws underlying permafrost as it inundates tundra vegetation. Beaver dams divert flow, sometimes catastrophically when they fail, and can thaw and destabilize the landscape (Lewkowicz and Coultish 2004) through fluvio-erosional and thermokarst processes (Fig. 3). Thawing of permafrost associated with new beaver ponds would initially release carbon and methane stored in permafrost, though the magnitude and fate of these fluxes are complex and unknown. Permafrost thaw, thermokarst, and the inception of a more dynamic lowland Arctic ecosystem suggest an exacerbation of effects due to warming air temperatures. As beavers create thermal and biological oases by the thousands, they could provide a foothold for boreal aquatic species, including fish and aquatic invertebrates. For now, however, these remain hypotheses that will spawn downstream studies involving field measurements and local knowledge to answer.

Fig. 3. Thermokarst terrain in western Alaska resulting from beaver damming, ponding, and redirecting of flow, occurring in less than 2 years. The original stream channel is marked by taller shrubs and flows right to left at the top of the picture. Beavers remain at the site and have rebuilt two dams. (Credit: Ken Tape, Aug 2021)

Arctic Beaver Observation Network (A-BON): Tracking a new disturbance

Recognizing an impending need to understand the scale, dynamics, and effects of beaver engineering in the tundra, individuals and organizations joined forces across Alaska, Canada, and Eurasia to identify key questions and involve stakeholders and land managers. A-BON involves natural scientists, social scientists, tribal entities and local observers, and agency land managers across the Arctic. A-BON has working groups in Alaska, Canada, Europe, and Asia.

The initial goals of A-BON are to (1) include diverse backgrounds and establish working relationships, (2) identify key questions for study, (3) align study designs and observation methods, (4) facilitate co-production of knowledge between scientists and local observers, (5) understand stakeholder land/resource management objectives, (6) assemble an expert steering committee to advise other Arctic science bodies (e.g., Conservation of Arctic Flora & Fauna, Circumpolar Biodiversity Monitoring Program), and (7) synthesize, archive, and disseminate relevant and co-produced data. These goals are actively being refined.

A synthesis effort underway within A-BON aims to identify key questions and knowledge gaps surrounding beaver colonization in the tundra across natural and social scientists, Indigenous organizations and observers, and land managers. Preliminary results demonstrate the breadth of interests and concerns, spanning beaver ecology, biophysical and socio-cultural impacts, local and Indigenous knowledge, management, and adapting to the evolving relationships with beavers. A-BON will discuss these and other efforts at the first meeting in March 2022 in Fairbanks, Alaska (could be virtual). We welcome participation in A-BON from anyone with interest in the topic.

Acknowledgments

K. Tape, J. Clark, and B. Jones acknowledge NSF OPP #1850578 and #2114051. H. Wheeler acknowledges the UK-Canada Arctic partnership bursary (NERC/BEIS) and Anglia Ruskin Next Steps QR fund.

References

ADF&G, 1965-2017: ADF&G (Furbearer) Reports. Alaska Department of Fish & Game, Division of Wildlife Conservation, Juneau, Alaska.

Bunn, S. E., and A. H. Arthington, 2002: Basic principles and ecological consequences of altered flow regimes for aquatic biodiversity. *Environ. Manage.*, **30**(4), 492-507, https://doi.org/10.1007/s00267-002-2737-0.

Halley, D. J., A. P. Saveljev, and F. Rosell, 2021: Population and distribution of beavers *Castor fiber* and *Castor canadensis* in Eurasia. *Mammal Rev.*, **51**, 1-24, https://doi.org/10.1111/mam.12216.

Jones, B. M., K. D. Tape, J. A. Clark, I. Nitze, G. Grosse, and J. Disbrow, 2020: Increase in beaver dams controls surface water and thermokarst dynamics in an Arctic tundra region, Baldwin Peninsula, northwestern Alaska. *Environ. Res. Lett.*, **15**(7), 075005, https://doi.org/10.1088/1748-9326/ab80f1.

Jung, T. S., J. Frandsen, D. C. Gordon, and D. H. Mossop, 2016: Colonization of the Beaufort coastal plain by Beaver (*Castor canadensis*): a response to shrubification of the Tundra? *Can. Field Nat.*, **130**(4), 332-335, https://doi.org/10.22621/cfn.v130i4.1927.

Lewkowicz, A. G., and T. L. Coultish, 2004: Beaver damming and palsa dynamics in a subarctic mountainous environment, Wolf Creek, Yukon Territory, Canada. *Arct. Antarct. Alp. Res.*, **36**, 208-218, https://doi.org/10.1657/1523-0430(2004)036[0208:bdapdi]2.0.co;2.

Moerlein, K. J., and C. Carothers, 2012: Total environment of change: impacts of climate change and social transitions on subsistence fisheries in northwest Alaska. *Ecol. Soc.*, **17**(1), 10, https://doi.org/10.5751/es-04543-170110.

Myers-Smith, I. H., and Coauthors, 2015: Climate sensitivity of shrub growth across the tundra biome. *Nat. Climate Change*, **5**(9), 887-891, https://doi.org/10.1038/nclimate2697.

St. Jacques, J. -M., and D. J. Sauchyn, 2009: Increasing winter baseflow and mean annual streamflow from possible permafrost thawing in the Northwest Territories, Canada. *Geophys. Res. Lett.*, **36**(1), L01401, https://doi.org/10.1029/2008gl035822.

Tape, K. D., B. M. Jones, C. D. Arp, I. Nitze, and G. Grosse, 2018: Tundra be dammed: Beaver colonization of the Arctic. *Glob. Change Biol.*, **24**(10), 4478-4488, https://doi.org/10.1111/gcb.14332.

Tape, K. D., J. A. Clark, and B. M. Jones, 2021: Beaver Pond Locations in Arctic Alaska, 1949 to 2020. Arctic Data Center. Accessed 15 September 2021, https://doi.org/10.18739/A2QR4NR6D.

Whitfield, C. J., H. M. Baulch, K. P. Chun, and C. J. Westbrook, 2015: Beaver-mediated methane emission: The effects of population growth in Eurasia and the Americas. *Ambio*, **44**(1), 7-15, https://doi.org/10.1007/s13280-014-0575-y.

December 2, 2021

Ocean Acidification

DOI: 10.25923/s5wq-8v05

J. N. Cross[1], A. Niemi[2], N. Steiner[3], and D. J. Pilcher[1,4]

[1]Pacific Marine Environmental Laboratory, NOAA, Seattle, WA, USA
[2]Freshwater Institute, Fisheries and Oceans Canada, Winnipeg, MB, Canada
[3]Institute of Ocean Sciences, Fisheries and Oceans Canada, Sidney, BC, Canada
[4]Cooperative Institute for Climate, Ocean, and Ecosystem Studies, University of Washington, Seattle, WA, USA

Highlights

- Recent work has shown that the Arctic Ocean is acidifying faster than the global ocean, but with high spatial variability.
- A growing body of research indicates that acidification in the Arctic Ocean could have implications for the Arctic ecosystem, including influences on algae, zooplankton, and fish.
- Cutting-edge tools like computational models are increasing our capacity to understand patterns, trends, and impacts of ocean acidification in the Arctic region.

The uptake of anthropogenic carbon dioxide (CO_2) causes a cascade of chemical reactions that decreases ocean pH and carbonate ion concentrations, a process known as ocean acidification (OA). While OA is a global process, some of the fastest rates of ocean acidification around the world have been observed in the Arctic Ocean (e.g., Qi et al. 2017, 2020). These extremely rapid rates of acidification reflect the Arctic's natural vulnerability to changes in pH, caused by cold temperatures, naturally higher baseline CO_2 concentrations resulting from global circulation processes, seasonal processes that rapidly concentrate CO_2 in some water masses, as well as unique land-sea interactions and hydrological mechanisms (circumpolar perspective broadly reviewed by AMAP 2018). Surface waters in some parts of the Arctic Ocean are already undersaturated with respect to some biologically important calcium carbonate minerals (e.g., aragonite and calcite) and most regions of the Arctic are likely to become corrosive (able to dissolve biologically important carbonate minerals) by the end of the century (AMAP 2018). These changes could have serious implications for the regional ecosystem, including detrimental impacts on local wildlife, cultural assets and practices, and subsistence resources.

Robust sampling programs that prioritize the collection of OA data (e.g., pH, partial pressure of CO_2, dissolved inorganic carbon (DIC), and total alkalinity (TA)) are extremely difficult to implement in the Arctic. The coastal sub-Arctic seas exhibit a highly dynamic spatial and temporal variability as the underlying biogeochemistry is impacted by a range of land, ocean, and atmosphere processes. Accordingly, mature OA monitoring systems must be highly resolved in both space and time to provide adequate information for decision support. Given the expansive area, the remote geographic location, and harsh winters, traditional monitoring tools are also challenging to deploy consistently in the Arctic region, although some of these time series are starting to mature (e.g., Beaufort Gyre: Zhang et al. 2020; Canadian Archipelago: Beaupré-Laperrière et al. 2020; Eurasian Basin: Ulfsbo et al. 2018; Fram Strait: Chierici et al. 2019; Svalbard: Jones et al. 2021).

Despite these advances, we do not have a synoptic understanding of OA across the pan-Arctic system. Accordingly, computational models grounded in observable data have emerged as a useful tool to help explore spatial-temporal variability due to their much finer spatial and temporal resolution. Using these outputs, researchers are better able to explore the intensity, duration, and extent of ecosystem exposure to OA processes. In recent years, regional and global modeling studies have been used to explore both long- and short-term aspects of OA in the Arctic (e.g., Bering Sea: Pilcher et al. 2019; pan-Arctic, Terhaar et al. 2020), as well as the processes leading to these trends that are notoriously difficult to observe (e.g., pan-Arctic sea-ice related impacts: Mortenson et al. 2020). However, there is substantial regional and seasonal variability especially where land processes can influence OA, highlighting potential problems with interpolating sparse measurements (e.g., Chierici et al. 2019; Jones et al. 2021). Better regional to local climate projections may provide key improvements. Model studies continue to be refined and will likely form a pivotal part of future Arctic OA research.

As the observational record of OA in the Arctic continues to grow, research on the possible impact of OA on Arctic ecosystems continues to progress both in the laboratory and in the field (Fig. 1). The primary concern is that the short food web linkages so characteristic of the Arctic may lead to widespread impacts of OA across the ecosystem, creating both winners and losers. This is evident at the very base of the food chain: for example, OA negatively affects the calcification of some Arctic phytoplankton (pan-Arctic: Ardyna and Arrigo 2020) and may shift the community toward smaller species (western Arctic: Sugie et al. 2020). Some primary producers may experience little impact; research syntheses indicate that OA likely has a limited effect on sea ice algae, given that the biogeochemistry of the ice matrix itself naturally undergoes extreme fluctuations that result in evolutionary resilience (central Arctic: Torstensson et al. 2021).

Fig. 1. Onboard laboratory setup for collection and filtering of Arctic seawater samples. Discrete sampling remains critical to understanding ocean chemistry. Photo by J. N. Cross.

At the zooplankton trophic level, the quintessential species for detrimental OA impacts is the pteropod (sea snail). These organisms are extremely sensitive to ocean pH and are often used around the world as indicators that can inform OA conditions. Both laboratory and field observations have shown that pteropod responses to OA include reduced juvenile survival, reduced shell growth and condition, as well as costly metabolic regulation. Arctic population connectivity and morphological characteristics of pteropods is a growing area of research. For example, recent studies of natural populations indicate a high occurrence of severe shell dissolution in the Bering Sea, Amundsen Gulf, and Svalbard margin (Niemi et al. 2021; Bednaršek et al. 2021; Anglada-Ortiz et al. 2021, respectively). While pteropods are an important biological indicator, research on other organisms specific to Arctic ecosystems will also support regional relevance. For example, fish show sensitivities to OA, including important species such as Arctic cod (e.g., western Arctic cod populations: Steiner et al. 2019; eastern Arctic cod: Hänsel et al. 2020). However, key questions remain to fully understand the mechanisms that produce individual and population-level responses to OA. Across species (fish, benthic and pelagic invertebrates) repair, adaptability, and associated tolerance have been linked to resource availability (e.g., Niemi et al. 2021; Hänsel et al. 2020; Duarte et al. 2020; Goethel et al. 2017), indicating the importance of a holistic ecosystem approach to understand OA biological responses (Fig. 2).

Fig. 2. A researcher processes Arctic sediment samples. Some benthic organisms that build shells out of calcium carbonate, like mussels and clams, may be susceptible to ocean acidification. Because these species commonly serve as prey for other parts of the Arctic food web, impacts could be felt through the entire Arctic ecosystem. Photo by J.N. Cross.

Seals, walrus, and marine birds may be impacted by the inherent vulnerability of their preferred foods to acidification. Calcifying bivalves are particularly sensitive to acidified conditions; weakly acidified waters can reduce growth, while severely corrosive waters can eventually begin to dissolve shells. Although laboratory experiments have identified resilience to acidification in Arctic invertebrates (Goethel et al.

2017), some model research suggests that they are likely to be among the most negatively impacted invertebrate populations in the world (Tai et al. 2021). Though the specifics remain uncertain, it is likely that the consequences of continuing OA will be detrimental for parts of the marine food web over the next decade. Warming and acidification are likely to become compounding stressors for the Arctic ecosystem by the end of the century. More research will be necessary to determine how acidification-stressed marine invertebrate populations may influence the Arctic ecosystem. This work will be especially important given that invertebrates as well as their predators are important commercial, cultural, and subsistence resources across the region.

Building ecosystem and human resilience to OA in the Arctic in part will require global solutions, given that OA is primarily caused by global carbon dioxide emissions. However, regional decision makers are likely to benefit from continually improving resolution of both data collection and regional modeling, which will provide additional support for Arctic decision makers and ecosystem management. Measurements from novel sensors, especially those collecting surface data are likely to improve the resolution of regional CO_2 flux products and provide a better understanding of the surface CO_2 sink for carbon across the Arctic. Additionally, short-term forecasting applications are likely to be developed for regional and pan-Arctic models in support of ecosystem management systems. Through this process, development of connections between biogeochemical and ecosystem models, based on empirical laboratory and in-situ data, are likely to allow researchers to continue to explore the impact of OA on regional ecosystems. The ultimate goal is to develop an interdisciplinary, hybridized approach that will allow the scientific community to develop annual OA products of the type now produced for temperature or sea ice extent for the Arctic Report Card. Given the high connectivity of processes leading to OA and its downstream effects, trans-national data access and collaboration will be essential for success.

In addition to improvements in data collection, it also seems likely that coastal marine CO_2 removal may scale inside coastal waters in the Arctic. The IPCC has acknowledged that achieving climate goals requires substantial changes to atmospheric greenhouse gas concentrations. While emissions-reduction approaches are an essential component of addressing this challenge, negative emissions strategies will be necessary for keeping global temperatures at recommended levels (IPCC 2021). Negative emissions strategies refer to a portfolio of techniques that are used to manually remove greenhouse gases from the atmosphere and store them away from the atmosphere. Carbon dioxide removal (CDR) specifically references techniques that remove legacy emissions of CO_2 from the atmosphere. Where these techniques involve the coastal oceans, there may be opportunities to remediate acidified ocean conditions in some instances. However, these marine CDR techniques are in their infancy and will require additional study to limit the risks associated with deployment, despite the potential benefits of atmospheric carbon sequestration and OA mitigation. It will also be essential to consider the ethical and climate justice ramifications of these techniques, especially regarding Arctic communities and peoples (Cassotta 2021).

References

AMAP, 2018: AMAP Assessment 2018: Arctic Ocean Acidification. Arctic Monitoring and Assessment Programme (AMAP), Tromsø, Norway. Vi+187 pp.

Anglada-Ortiz, G., K. Zamelczyk, J. Meilland, P. Ziveri, M. Chierici, A. Fransson, and T. L. Rasmussen, 2021: Planktic foraminiferal and pteropod contributions to carbon dynamics in the Arctic Ocean (North Svalbard Margin). *Front. Mar. Sci.*, **8**, 661158, https://doi.org/10.3389/fmars.2021.661158.

Ardyna, M., and K. R. Arrigo, 2020: Phytoplankton dynamics in a changing Arctic Ocean. *Nat. Climate Change*, **10**(10), 892-903, https://doi.org/10.1038/s41558-020-0905-y.

Beaupré-Laperrière, A., A. Mucci, and H. Thomas, 2020: The recent state and variability of the carbonate system of the Canadian Arctic Archipelago and adjacent basins in the context of ocean acidification. *Biogeosciences*, **17**, 3923-3942, https://doi.org/10.5194/bg-17-3923-2020.

Bednaršek, N., and Coauthors, 2021: Integrated assessment of ocean acidification risks to pteropods in the northern high latitudes: Regional comparison of exposure, sensitivity and adaptive capacity. *Front. Mar. Sci.*, **8**, 671497, https://doi.org/10.3389/fmars.2021.671497.

Cassotta, S., 2021: Ocean acidification in the Arctic in a multi-regulatory, climate-justice perspective. *Front. Climate*, **3**, 713644. https://doi.org/10.3389/fclim.2021.713644.

Chierici, M., M. Vernet, A. Fransson, and K. Y. Børsheim, 2019: Net community production and carbon exchange from winter to summer in the Atlantic Inflow to the Arctic Ocean. *Front. Mar. Sci.*, **6**, 528, https://doi.org/10.3389/fmars.2019.00528.

Duarte, C. M., A. B. Rodriguez-Navarro, A. Delgado-Huertas, and D. Krause-Jensen, 2020: Dense mytilus beds along freshwater-influenced Greenland shores: Resistance to corrosive waters under high food supply. *Estuar. Coast.*, **43**(2), 387-395, https://doi.org/10.1007/s12237-019-00682-3.

Goethel, C. L., J. M. Grebmeier, L. W. Cooper, and T. J. Miller, 2017: Implications of ocean acidification in the Pacific Arctic: experimental responses of three Arctic bivalves to decreased pH and food availability. *Deep-Sea Res. Pt. II*, **144**, 112-124, https://doi.org/10.1016/j.dsr2.2017.08.013.

Hänsel, M. C., J. O. Schmidt, M. H. Stiasny, M. T. Stöven, R. Voss, and M. F. Quaas, 2020: Ocean warming and acidification may drag down the commercial Arctic cod fishery by 2100. *PLoS One*, **15**(4), e0231589, https://doi.org/10.1371/journal.pone.0231589.

IPCC, 2021: Climate Change 2021: The Physical Science Basis. Contribution of Working Group I to the Sixth Assessment Report of the Intergovernmental Panel on Climate Change [V. Masson-Delmotte, and coeditors, (eds.)]. Cambridge University Press.

Jones, E. M., M. Chierici, S. Menze, A. Fransson, R. B. Ingvaldsen, and H. H. Lødemel, 2021: Ocean acidification state variability of the Atlantic Arctic Ocean around northern Svalbard. *Prog. Oceanogr.*, **199**, 102708, https://doi.org/10.1016/j.pocean.2021.102708.

Mortenson, E., N. Steiner, A. H. Monahan, H. Hayashida, T. Sou, and A. Shao, 2020: Modeled impacts of sea ice exchange processes on Arctic Ocean carbon uptake and acidification, 1980-2015. *J. Geophys. Res.-Oceans*, **125**(7), e2019JC015782, https://doi.org/10.1029/2019JC015782.

Niemi, A., N. Bednaršek, C. Michel, R. A. Feely, W. Williams, K. Azetsu-Scott, W. Walkusz, and J. D. Reist, 2021: Biological impact of ocean acidification in the Canadian Arctic: Widespread severe pteropod shell dissolution in Amundsen Gulf. *Front. Mar. Sci.*, **8**, 600184, https://doi.org/10.3389/fmars.2021.600184.

Pilcher, D. J., D. M. Naiman, J. N. Cross, A. J. Hermann, S. A. Siedlecki, G. A. Gibson, and J. T. Mathis, 2019: Modeled effect of coastal biogeochemical processes, climate variability, and ocean acidification

on aragonite saturation state in the Bering Sea. *Front. Mar. Sci.*, **5**, 508, https://doi.org/10.3389/fmars.2018.00508.

Qi, D., and Coauthors, 2017: Increase in acidifying water in the western Arctic Ocean. *Nat. Climate Change*, **7**, 195-199, https://doi.org/10.1038/NCLIMATE3228.

Qi, D., and Coauthors, 2020. Coastal acidification induced by biogeochemical processes driven by sea-ice melt in the western Arctic Ocean. *Polar Sci.*, **23**, 100504, https://doi.org/10.1016/j.polar.2020.100504.

Steiner, N. S., and Coauthors, 2019: Impacts of changing ocean-sea ice system on the key forage fish Arctic Cod (*Boreogadus saida*) and subsistence fisheries in the western Canadian Arctic—evaluating linked climate, ecosystem, and economic (CEE) models. *Front. Mar. Sci.*, **6**, 179, https://doi.org/10.3389/fmars.2019.00179.

Sugie, K., A. Fujiwara, S. Nishino, S. Kameyama, and N. Harada, 2020: Impacts of temperature, CO_2, and salinity on phytoplankton community composition in the western Arctic Ocean. *Front. Mar. Sci.*, **6**, 821, https://doi.org/10.3389/fmars.2019.00821.

Tai, T. C., U. R. Sumaila, and W. W. L. Cheung, 2021: Ocean acidification amplifies multi-stressor impacts on global marine invertebrate fisheries. *Front. Mar. Sci.*, **8**, 596644. https://doi.org/10.3389/fmars.2021.596644.

Terhaar, J., L. Kwiatkowski, and L. Bopp, 2020: Emergent constraint on Arctic Ocean acidification in the twenty-first century. *Nature*, **582**, 379-383, https://doi.org/10.1038/s41586-020-2360-3.

Torstensson, A., A. R. Margolin, G. M. Showalter, W. O. Smith Jr., E. H. Shadwick, S. D. Carpenter, F. Bolinesi, and J. W. Deming, 2021: Sea-ice microbial communities in the Central Arctic Ocean: Limited responses to short-term pCO_2 perturbations. *Limnol. Oceanogr.*, **66**(S1), S383-S400, https://doi.org/10.1002/lno.11690.

Ulfsbo, A., E. M. Jones, N. Casacuberta, M. Korhonen, B. Rabe, M. Karcher, and S. M. A. C. van Heuven, 2018: Rapid changes in anthropogenic carbon storage and ocean acidification in the intermediate layers of the Eurasian Arctic Ocean: 1996-2015. *Global Biogeochem. Cycles*, **32**(9), 1254-1275, https://doi.org/10.1029/2017GB005738.

Zhang, Y., M. Yamamoto-Kawai, W. J. Williams, 2020: Two decades of ocean acidification in the surface waters of the Beaufort Gyre, Arctic Ocean: Effects of sea ice melt and retreat from 1997-2016. *Geophys. Res. Lett.*, **47**(3), e60119, https://doi.org/10.1029/2019GL086421.

November 23, 2021

River Discharge

DOI: 10.25923/zevf-ar65

R. M. Holmes[1], A. I. Shiklomanov[2,3], A. Suslova[1], M. Tretiakov[3], J. W. McClelland[4], L. Scott[1], R. G. M. Spencer[5], and S. E. Tank[6]

[1]Woodwell Climate Research Center, Falmouth, MA, USA
[2]University of New Hampshire, Durham, NH, USA
[3]Arctic and Antarctic Research Institute, St. Petersburg, Russia
[4]Marine Science Institute, University of Texas at Austin, Port Aransas, TX, USA
[5]Florida State University, Tallahassee, FL, USA
[6]University of Alberta, Edmonton, AB, Canada

Highlights

- In 2021, the combined discharge (January through October) from the six Eurasian rivers was 1850 km^3, which was 81 km^3 or ~5% greater than during the 1981-2010 reference period.
- In 2020, the combined discharge of the eight largest Arctic rivers was 2623 km^3, ~12% greater than the average over the 1981-2010 reference period.
- In 2019, the combined discharge of the eight largest Arctic rivers was 2233 km^3, 5% less than the 1981-2010 average.
- In 2020, an extraordinarily high May discharge from Eurasian rivers of 443 km^3 (96% above average) was followed by an extraordinarily low June discharge of 432 km^3 (21% below average), indicating a shift of the freshet to earlier in the season.
- The long-term observations for Eurasian and North American Arctic river discharges demonstrate an upward trend, providing evidence for the intensification of the Arctic hydrologic cycle.

Introduction

Arctic river discharge is a key indicator reflecting changes in the hydrologic cycle associated with widespread environmental change in the Arctic. It is the most accurately measured component of the Arctic water cycle (Shiklomanov et al. 2006). Records of Arctic river discharge since the early 1930s reveal a long-term increase of freshwater flux to the Arctic Ocean, providing compelling evidence of intensification of the Arctic water cycle (Peterson et al. 2002; McClelland et al. 2006). This hydrologic and associated biogeochemical change has significant ramifications for the Arctic Ocean, which contains only about 1% of global ocean water yet receives 11% of the global river discharge (Aagaard and Carmack 1989; McClelland et al. 2012).

Of the eight largest Arctic rivers by annual discharge, six lie in Eurasia (Kolyma, Yenisey, Lena, Ob', Pechora, and Severnaya Dvina) and two are in North America (Mackenzie and Yukon). Collectively, the watersheds of these eight rivers cover approximately 70% of the pan-Arctic drainage area and account for the majority of river water input to the Arctic Ocean (Fig. 1). In this report we present river discharge values for these eight rivers for 2019 and 2020, and for the Eurasian portion of these same rivers for the first ten months of 2021, updating the 2018 Arctic Report Card (Holmes et al. 2018). 2021 data are not

available for the two North American rivers at the time of this report. Here, we use a common baseline period of 1981-2010 to compare and contextualize recent observations.

Fig. 1. Watersheds of the eight largest Arctic rivers that are featured in this analysis. Collectively, these rivers cover approximately 70% of the 16.8 million km^2 pan-Arctic watershed (indicated by the red boundary line). The red dots show the locations of the discharge monitoring stations (see Table 2).

Discharge records

In 2021, the combined discharge (January through October) from the six Eurasian rivers was 1850 km^3, which was 81 km^3 or ~5% greater than during 1981-2010 reference period. The majority of this increase was driven by the Yenisey River. The Pechora and Severnaya Dvina showed below average discharge, 26% and 28%, respectively (Fig. 2).

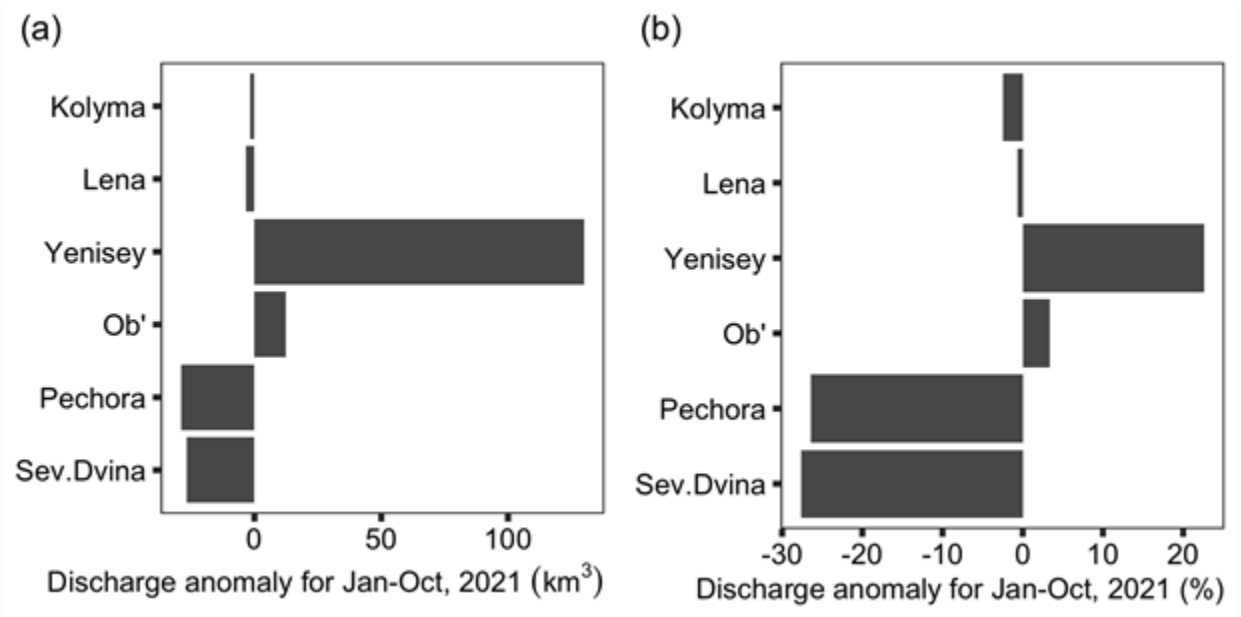

Fig. 2. Discharge anomalies relative to the 1981-2010 reference period for the six Eurasian rivers in 2021, January through October. Panel (a) shows the anomalies in absolute terms (km^3), whereas panel (b) shows the anomalies as percent deviations.

In 2020, the combined annual discharge of the eight largest Arctic rivers was 2623 km^3, which was 272 km^3 or ~12% greater than the 30-year average. This increase is greater than the annual average discharge of the Yukon River. Discharge from the two North American rivers combined was 630 km^3, ~28% greater than their 1981-2010 average. Discharge from the six Eurasian rivers combined was 1992 km^3, ~7% greater than the average over the 1981-2010 reference period, or ~10% greater than average for whole period of record from 1936 to 2020 (Table 1).

Table 1. Annual discharge for the eight largest Arctic rivers (km^3) for 2019 and 2020, compared to the 1981-2010 reference period and to the all-time averages (1936-2021 for the six Eurasian rivers; 1973-2020 for the Mackenzie River, and 1976-2020 for the Yukon River). Italicized values indicate provisional data and are subject to modification until official data are published.

	River Basin								
Year	**Yukon**	**Mackenzie**	**S. Dvina**	**Pechora**	**Ob'**	**Yenisey**	**Lena**	**Kolyma**	**SUM**
2020	*251*	*379*	*152*	*116*	*464*	*620*	*581*	*59*	*2623*
2019	210	*236*	*122*	*146*	*437*	*557*	*463*	*63*	*2233*
Average 1981-2010	205	288	104	114	398	612	557	70	2348
All time average	*206*	*286*	*101*	*110*	*404*	*586*	*541*	*73*	*2307*

High annual discharge of the North American rivers in 2020 was primarily driven by the high discharge values in July, August, and September (+2.1, +2.6, +2.8 std. dev. above average, respectively; Fig. 3). This is attributed to an unusually wet summer, the wettest summer since 1985 based on analysis of precipitation aggregated over the Mackenzie and Yukon watersheds (Hersbach et al. 2020).

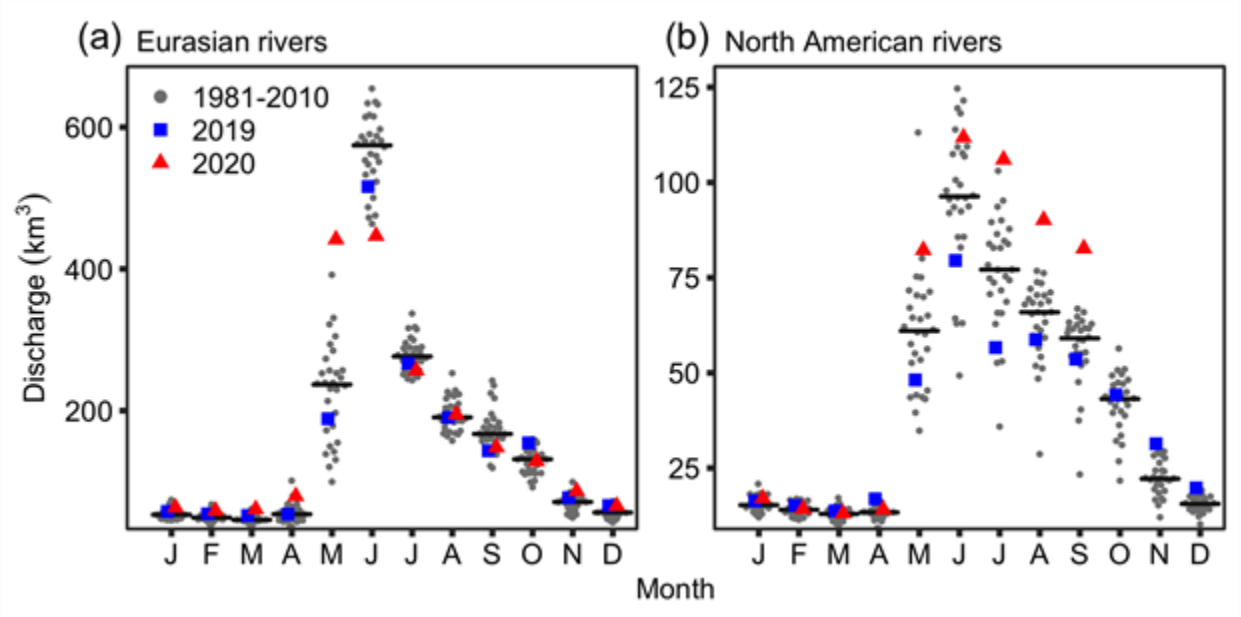

Fig. 3. Monthly discharge (km^3) in (a) Eurasian and (b) North American rivers for 2020 and 2019 compared to monthly discharge throughout the 1981-2010 reference period. The black bars indicate the average monthly discharge during the reference period. Note the different scales for the (a) Eurasian and (b) North American river discharge.

For the Eurasian rivers in 2020, extraordinarily high May discharge (+3.1 std. dev. above average) was followed by extraordinarily low June discharge (-2.3 std. dev. below average; Fig. 3). This pattern observed across the Eurasian rivers is consistent with the observed high terrestrial snow cover and snow water equivalent during winter 2019/20, followed by a remarkably warm spring in 2020 (Ballinger et al. 2020; Mudryk et al. 2020). This led to an early melt of a large snowpack, shifting more of the freshet runoff period from June to May. Discharge for May and June combined was 13% higher in 2020 compared to the baseline period.

In contrast to 2020, 2019 was a relatively low-discharge year. The combined discharge of the eight largest Arctic rivers was 2233 km^3, 118 km^3 or 5% less than the 1981-2010 average (Fig. 4). Discharge from the two North American rivers and the six Eurasian rivers was ~9% and ~4% less than average, respectively.

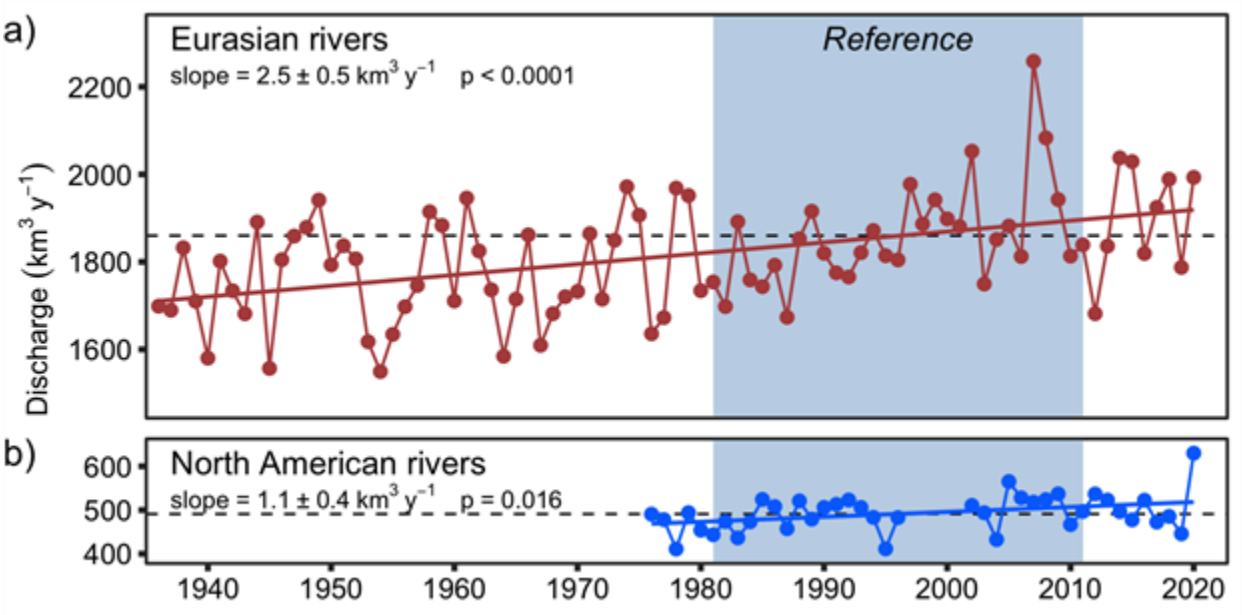

Fig. 4. Long-term trends in annual discharge ($km^3\ yr^{-1}$) for (a) Eurasian and (b) North American Arctic rivers through 2020. Gaps in the North American rivers time series span from 1996 through 2001 due to missing Yukon data (1996 to 2001) and missing Mackenzie data (1997 and 1998). Dashed lines show the mean annual discharge throughout the 1981-2010 reference period for the Eurasian (1860 $km^3\ yr^{-1}$) and North American (491 $km^3\ yr^{-1}$) rivers.

Low annual discharge in 2019 from the North American rivers was driven by low May, June, and July discharge (-0.8, -0.9, -1.4 std. dev. below average, respectively; Fig. 3). Similarly, Eurasian rivers had lower than average discharge in May and June (-0.5, -0.9 std. dev. below average, respectively; Fig. 3). These low summer discharge observations are consistent with the below-average snow water equivalent in April 2019 in both the Eurasian and North American Arctic (Mudryk et al. 2019).

The 85-year time series available for the Eurasian Arctic rivers demonstrates a positive linear trend. Their combined annual discharge is increasing by 2.5 km^3 per year. For the North American Arctic rivers, the increase over the period of record (1976-2020) was 1.1 km^3 per year (Fig. 4). These long-term observations indicate that Arctic river discharge continues to trend upward, providing powerful evidence for the intensification of the Arctic hydrologic cycle (Shiklomanov et al. 2021).

Methods and data

Discharge values are based on observational discharge data from the downstream-most stations listed in Table 2. Discharge measurements for the six Eurasian rivers began in 1936, whereas discharge measurements did not begin until 1973 for the Mackenzie River and 1976 for the Yukon River. Discharge data for the Kolyma at Srednekolymsk are not available for 2019 and 2020; they were calculated based on monthly correlations with the next downstream station, the Kolyma at Kolymskoe. Average monthly values for 1978-2001 were used to calculate the correction factor. The Yukon is missing discharge values from October-December 2020. We therefore used long-term average values for those three months, which account for less than 17% of the mean annual discharge. All discharge data reported here are available through the Arctic Great Rivers Observatory at arcticgreatrivers.org/discharge/.

Table 2. Discharge station information. Discharge data are collected by national hydrological institutions in Russia (Roshydromet), the United States (U.S. Geological Survey; USGS) and Canada (Water Survey of Canada; WSC)

River	Station Location	Station Code	Latitude (°)	Longitude (°)	Catchment Area (km^2)
Kolyma	Srednekolymsk	1801	67.47	153.69	361000
Lena	Kusur	3821	70.68	127.39	2430000
Yenisey	Igarka	9803	67.43	86.48	2440000
Ob'	Salehard	11808	66.63	66.60	2950000
Pechora	Ust' Tsilma	70850	65.42	52.28	248000
Severnaya Dvina	Ust' Pinega	70801	64.13	41.92	348000
Mackenzie	Arctic Red River	10LC014	67.45	-133.74	1750600
Yukon	Pilot Station	15565447	61.93	-162.88	831391

Acknowledgments

We thank the United States Geological Survey (Yukon), Water Survey of Canada (Mackenzie) and Roshydromet (Severnaya Dvina, Pechora, Ob', Yenisey, Lena, and Kolyma) for the discharge data used here. This work was supported by grants from the National Science Foundation in support of the Arctic Great Rivers Observatory (NSF 1602615, 1603149, 1602680, 1602879). The processing and analysis of near-real time data for Russian Arctic rivers were supported in part by the Russian Foundation for Basic Research (grant 18-05-60192).

References

Aagaard, K., and E. C. Carmack, 1989: The role of sea ice and other fresh water in the Arctic circulation. *J. Geophys. Res.*, **94**(C10), 14485-14498, https://doi.org/10.1029/jc094ic10p14485.

Ballinger, T. J., and Coauthors, 2020: Surface air temperature. *Arctic Report Card 2020*, R. L. Thoman, J. Richter-Menge, and M. L. Druckenmiller, Eds., https://doi.org/10.25923/gcw8-2z06.

Hersbach, H., and Coauthors, 2020: The ERA5 global reanalysis. *Q. J. Roy. Meteor. Soc.*, **146**, 1999-2049, https://doi.org/10.1002/qj.3803.

Holmes, R. M., A. I. Shiklomanov, A. Suslova, M. Tretiakov, J. W. McClelland, R. G. Spencer, and S.E. Tank, 2018: River discharge. *Arctic Report Card 2018*, E. Osborne, J. Richter-Menge, and M. Jeffries, Eds., https://doi.org/10.25923/krcx-z320.

McClelland, J. W., S. J. Déry, B. J. Peterson, R. M. Holmes, and E. F. Wood, 2006: A pan-arctic evaluation of changes in river discharge during the latter half of the 20th century. *Geophys. Res. Lett.*, **33**(6), L06715, https://doi.org/10.1029/2006gl025753.

McClelland, J. W., R. M. Holmes, K. H. Dunton, and R. W. Macdonald, 2011: The Arctic Ocean estuary. *Estuaries Coasts*, **35**(2), 353-368, https://doi.org/10.1007/s12237-010-9357-3.

Mudryk, L., R. Brown, C. Derksen, K. Luojus, B. Decharme, and S. Helfrich, 2019: Terrestrial snow cover. *Arctic Report Card 2019*, J. Richter-Menge, M. L. Druckenmiller, and M. Jeffries, Eds., https://doi.org/10.25923/bw4d-my28.

Mudryk, L., A. Elias Chereque, R. Brown, C. Derksen, K. Luojus, and B. Decharme, 2020: Terrestrial snow cover. *Arctic Report Card 2020*, R. L. Thoman, J. Richter-Menge, and M. L. Druckenmiller, Eds., https://doi.org/10.25923/p6ca-v923.

Peterson, B. J., R. M. Holmes, J. W. McClelland, C. J. Vörösmarty, R. B. Lammers, A. I. Shiklomanov, I. G. Shiklomanov, and S. Rahmstorf, 2002: Increasing river discharge to the Arctic Ocean. *Science*, **298**(5601), 2171-2173, https://doi.org/10.1126/science.1077445.

Shiklomanov, A. I., T. I. Yakovleva, R. B. Lammers, I. Ph. Karasev, C. J. Vörösmarty, and E. Linder, 2006: Cold region river discharge uncertainty-estimates from large Russian rivers. *J. Hydrol.*, **326**(1-4), 231-256, https://doi.org/10.1016/j.jhydrol.2005.10.037.

Shiklomanov, A. I., S. Déry, M. Tretiakov, D. Yang, D. Magritsky, A. Georgiadi, and W. Tang, 2021: River freshwater flux to the Arctic Ocean. Arctic Hydrology, Permafrost and Ecosystems, D. Yang, D. L. Kane, Springer, Cham, 703-738, https://doi.org/10.1007/978-3-030-50930-9_24.

November 17, 2021

2020 Foreign Marine Debris Event—Bering Strait

DOI: 10.25923/jwag-eg41

G. Sheffield[1], A. Ahmasuk[2], F. Ivanoff[3], A. Noongwook[4], and J. Koonooka[5]

[1]Alaska Sea Grant, Marine Advisory Program, University of Alaska Fairbanks, Nome, AK, USA
[2]Marine Advocate, Kawerak Inc., Nome, AK, USA
[3]Norton Sound Economic Development Corporation, Unalakleet, AK, USA
[4]Tribal Council, Native Village of Savoonga, Savoonga, AK, USA
[5]Tribal Council, Native Village of Gambell, Gambell, AK, USA

Highlights

- During 2020, the Bering Strait region of Alaska experienced a marine debris event that brought garbage ashore that was different from the types and amount typically observed.
- Notification of, and response to, this event was undertaken by the regional public out of concern for their food security, marine wildlife health, human health, and conservation.
- Without significant collaborative transboundary communication and/or enforcement of existing international marine pollution rules, the Bering Strait region should expect similar or higher levels of marine garbage in the future as industrial maritime ship traffic increases.

Introduction

The Bering Strait region of Eastern Chukotka (Russia) and western Alaska (USA) encompasses a narrow international waterway providing the sole transit corridor for a diverse assortment of federally-managed marine resources (e.g., marine mammals, seabirds, fish, and invertebrates), as well as all vessel traffic between the Pacific and Arctic Oceans. Two prominent northward flowing currents, the Anadyr and Alaska Coastal currents, produce a strong, typically one-way flow from the Bering Sea to the Chukchi Sea (Overland and Roach 1987) and are considered responsible for carrying anthropogenic debris northward (Mua et al. 2019; Kylin 2020).

The Alaskan Bering Strait region is extremely remote with an expansive coastline and little to no presence from the authorized federal agencies tasked with research, management, or response to the marine environment. Those personnel are typically located in the urban centers of Alaska and/or Washington state, far from western Alaska's coast.

The communities of the Alaskan Bering Strait region are diverse and include Iñupiaq, St. Lawrence Island/Siberian Yupik, Yup'ik, as well as non-Native peoples. All reside along the coast, reflecting the importance of the marine ecosystem (see Fig. 1.). Reliance on marine resources for subsistence purposes is essential to each community's nutritional, cultural, and economic well-being. Though there is often a lack of science data from western Alaska, there is no lack of regional knowledge regarding the marine environment. Coastal communities with active and comprehensive maritime subsistence activities typically are the first to discover anomalous events, alert regional partner institutions, and subsequently conduct the event response. The regional impetus to respond is out of food security, wildlife health, human health, and/or conservation concerns.

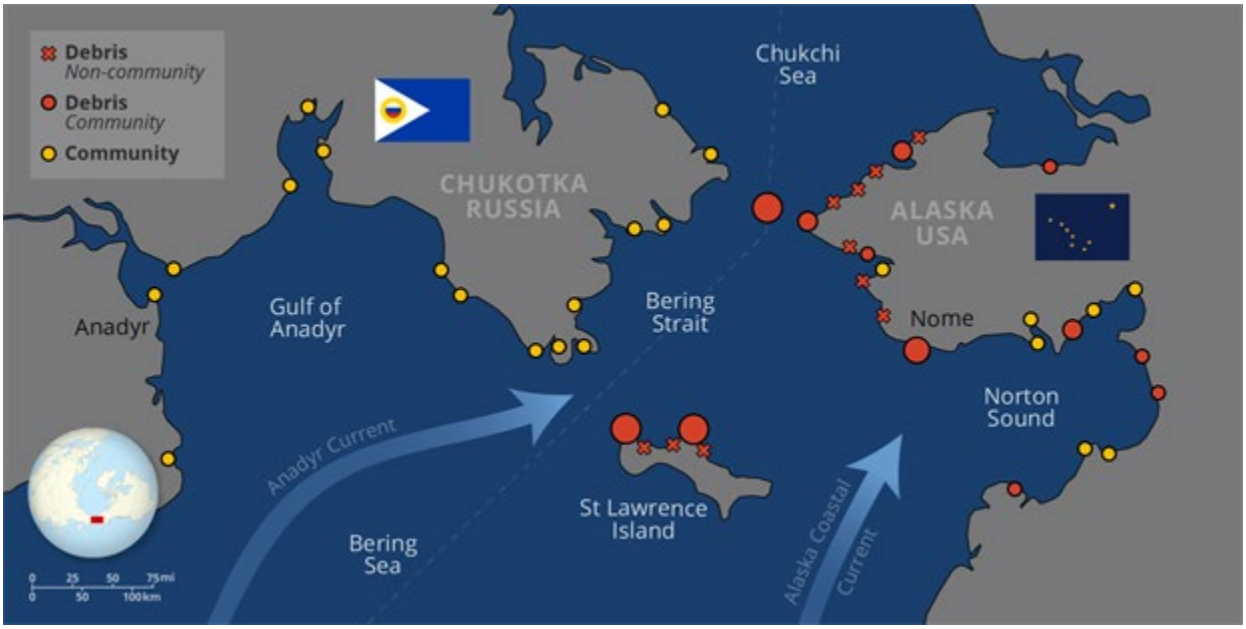

Fig. 1. A map of the Bering Strait region. Coastal communities are indicated by yellow circles. Alaskan communities reporting foreign debris are indicated by red dots with the circle size corresponding to the numbers of reports. Areas with debris reported with assistance from the US Coast Guard and/or traveling community members are indicated by red "X"s. The reporting Chukchi Sea communities of Kivalina and Wainwright are not shown. The primary northbound ocean currents, Anadyr Current (Chukotka) and the Alaska Coastal Current (Alaska), are indicated by the two arrows.

In the last decade, the peoples of the region have responded to anomalous events affecting marine species, including petroleum oil-fouling (Stimmelmayr et al. 2018), biogenic oil-fouling (Smith 2020), and novel disease and/or mortality events (Stimmelmayr et al. 2013; Bodenstein et al. 2015; Van Hemert et al. 2021). Additionally, the Bering Strait region experiences industrial fisheries debris washing ashore. Since 2006, the Norton Sound Economic Development Corporation (NSEDC) has conducted community environmental clean-up efforts (e.g., historic industrial, military materials, etc.). Over 1.1 million pounds (approximately 500 metric tons) have been collected from 15 member communities, with much of that as commercial fisheries equipment typically in the form of nets, floats, and other equipment (Fred Jay Ivanoff, Senior Crew Leader, NSEDC, 2021, personal communication). With large international commercial fisheries in the southern Bering Sea and strong northward flowing ocean currents, St. Lawrence Island consistently receives fisheries equipment ashore. Overall, the rest of the Bering Strait region receives a much lesser amount of fisheries-related materials ashore.

As a result of less and thinner seasonal sea ice, more open water, and rapidly reorganizing marine ecosystems (Stevenson and Lauth 2019; Eisner et al. 2020; Thoman et al. 2020), industrial maritime vessel traffic (e.g., Pollock and Pacific cod commercial fishing, Northern Sea Route large vessel traffic, etc.), which mostly originates far from the Bering Strait region, has significantly increased in frequency and duration in the northern Bering Sea (USCMTS 2019). These intensified activities increase the likelihood of future anomalous marine events that will require community vigilance and response throughout the Bering Strait region.

Marine debris event in 2020

Starting during late July 2020, tribal leadership at St. Lawrence Island voiced serious concerns regarding the amounts and types of debris washing ashore and provided qualitative reports (Table 1) to Kawerak, Inc. and the University of Alaska-Alaska Sea Grant (UAF-ASG) office in Nome. Kawerak and UAF-ASG responded initially by contacting the federal authorities. They used the existing regional communication network to gather and provide information as the event unfolded. Additionally, Kawerak and UAF-ASG created a regionally relevant public awareness poster with contact information for regional distribution, coordinated with regional media to provide information, and worked with the urban-based federal response agencies to provide the opportunity to speak (remotely) to the public about the emerging event. Through mid-November, individuals from 14 coastal communities (Fig. 1) discovered and documented over 350 individual items ashore, most with Russian, Korean, and/or other Asian lettering or branding (Table 2, Fig. 2). This number should be considered a minimum, with qualitative reports of mostly uncounted debris extending for miles. Reporting communities included locations in Norton Sound (Elim, Kotlik, Shaktoolik, Unalakleet), Bering Strait (Gambell, Savoonga, Diomede, Brevig Mission, Wales, Nome), and the Chukchi Sea region (Shishmaref, Deering, Kivalina, Wainwright). Additional reports of debris ashore (e.g., deck boots) were also received from the US Coast Guard during their aerial missions in the Bering Strait region, and these were incorporated with all reports received.

Table 1. Examples of the qualitative reporting of items from the 2020 marine debris event.

Month	Location	Report
July	Gambell	"5-10 miles of litter"
July	Savoonga	"There is trash and debris for miles along the shoreline"
July	Nome	"From Sinuk River to Nome (~25 miles) there were 174 items noted"
August	Gambell	"In 3 miles of shoreline we picked up trash that filled 19 (40 gal.) trash bags that each weighed ~50 lbs/apiece"
August	Savoonga	"Lots of trash washed in with lots of dead seabirds (murres, fulmars)" and "seen quite a bit of [deck boots] to the East and to the West"
August	Unalakleet	"Lots of Russian plastic [water] jugs"
September	Gambell	"Seeing lots of debris and even vegetables [washed in] of late"
September	Brevig Mission	"Quite a bit of debris of different varieties"
September	Wales	"In 4 miles there were a handful of milk bottles, > dozen beer/alcohol bottles, several aerosol cans, and one can of aerosol foam"
September	Shishmaref	"During the flight from Wales to Shishmaref (~50 miles), recently washed in trash (plastic bags, pallets, plastic bottles, small plastic containers, deck boots, and even a large black ship's fender) was consistently observed on the beach."

Table 2. Examples of the quantitative reporting of items from the 2020 marine debris event.

Type	# of Items	Examples
Water	117 bottles	Russian brands (6), Korean brands (3), Chinese brand (1), and 43 undetermined bottles with no label but similar in shape and size to labelled water/beverage containers.
Beverages	46 bottles	Juice: aloe vera, pineapple, peach, tomato, and "cocktail"; Dairy/yogurt beverages; soda; milk; kvass; and one undetermined beverage
Deck Boots	47 boots	Several styles and colors, primarily orange.
Equipment	~46 items	Russian "pike" bamboo pole with welded hooks for retrieving longline buoys, 55 gallon oil drums (empty), long line buoy with a fishing company's (Vladivostok, Russia) Pacific Cod permit tag number, a case of packing bands in a cardboard(!) box from Busan, S. Korea, two trawl net floats, packet of crystalline polypropylene, life jackets, chemical bottle, lighter, various plastic containers, and plastic bags, etc.
Food packaging	32 items	Cheese, chips, jam, candy, chocolate/peanut butter paste, cookies, pickles, dessert topping, garlic, ginger, peppers, instant pasta/soup, mayonnaise, ketchup, sour cream, tomatoes, soy sauce, yogurt, soybean oil, and undetermined condiment bottles
Aerosol cans	26 cans	Roach insecticide, lubricating oil, spray paint, butane, polyurethane foam, air freshener, and muscular pain relief spray
Bathroom cleaner	14 bottles	Toilet bowl cleaners, drain clog remover, dishwashing liquid
Hygienic products	8 items	Shampoo, stick deodorant, body wash (Men's)
Alcohol	5 bottles	Beer, vodka
Foods	9 items	Biscuits (in a repurposed Russian food container), apple, lemon, green pepper, pumpkins, orange
Clothing (adult)	4 items	Russian Navy sailor cap, patent leather shoe, plastic slipper with liner, slip-on shoe
Water bottle	(1) six liter bottle containing 78 items	Plastic food packaging wrappers: meat, vegetables, pasta, rice, candy/gum, spice packets, baking powder, yogurt; disposable gloves, sponge, etc.

Fig. 2. Items from 2020 foreign marine debris event: (a) plastics scattered along the shoreline; photo by L. Apatiki, (b) shampoo bottle; photo by T. Pelowook, (c) miscellaneous aerosol cans of butane, paint, and lubricating oil, foods, and bottles of bathroom cleaners, water bottles, etc; photo by G. Sheffield, (d) 1L carton of milk; photo by A. Ahmasuk, (e) deck boot; photo by G. Sheffield, (f) longline anchor buoy from a Vladivostok-based fishing company with the Pacific cod permit attached; photo by R. Tokeinna.

The equipment washed ashore was commercial fisheries related, including a case of packing bands still in a cardboard box from Busan, South Korea, several life jackets, two 55-gallon drums with Russian branding, dozens of deck boots, countless blue plastic "bucket liner" or packaging bags, and even a longline buoy with permit tag (for Pacific cod) belonging to a Vladivostok-based commercial fishing company. The predominant debris washed ashore were empty single serving beverages, bottled water, and/or packaging associated with foods and snacks. Most plastic items were un-weathered, in pristine condition, indicating they had entered the water recently. The most recent date of manufacturing noted on any item was April 2020. Hazardous materials included cans and other containers that had and/or still contained roach insecticides, toilet cleaners, drain clog remover, lubricating oils, butane gas, and spray paints. Of note, one large plastic water bottle recovered near the community of Shishmaref contained 78 plastic and/or foil items associated with cooking meats, vegetables, starches, as well as cooking for a large number of people (e.g., disposable gloves, etc.). This one bottle containing multiple items was a reminder that the items documented were an absolute minimum, and highlighted the potential for more plastics to be released in the future. There was no clothing or hygienic debris typically associated with women or children, which supports attributing this mass debris event to commercial fisheries, which mostly employ male crew members.

Community members remained vigilant and voluntarily reported, documented, and even shipped debris to Nome in hopes of identifying the responsible party for these violations of the existing international pollution convention, and to get them to stop polluting regional waters. The largest number of villages' simultaneously reporting trash ashore occurred during September 2020, with the last foreign debris reported from Little Diomede in mid-November at the start of seasonal sea ice formation. Regional residents continued to note that the 2020 event was more widespread, of longer duration, and included

more internationally manufactured or branded everyday garbage (e.g., water/beverage bottles, snack packaging, aerosol cans, and foods) ashore than previous years. Of note, there were two items of clothing (a Russian Navy cap and a patent leather shoe, both in pristine condition) that washed ashore on St. Lawrence Island during September that were potentially associated with a large Russian military exercise near St. Lawrence Island during late August (Isachenkov 2020; Sutton 2020).

During 2020 it was not just commercial fishing equipment coming ashore; debris also included everyday garbage such as plastics, food items, and hazardous materials. Each item documented ashore is in violation of international regulations to prevent garbage pollution from ships as outlined in Annex V of the International Convention for the Prevention of Pollution from Ships (MARPOL) (International Maritime Organization 2021). The documented plastic debris, fishing equipment, and hazardous materials not only negatively impact regional marine resources, but also the peoples and communities that directly rely on them for nutritional, cultural, and economic well-being.

Possible reasons for the increase of marine debris in the Bering Strait region during 2020 include:

- An increase in marine traffic to the region: Unfortunately, however, we have not found accessible quantitative information on the change in ship traffic in the northern Bering Sea during 2020.
- Different people are now using the Bering Strait region: During 2020, industrial fishing vessels and/or commerce vessels, originating far from the Bering Strait region, arrived to exploit novel volumes of commercially-viable marine resources (e.g., Pacific cod and pollock) (Spies et al. 2020; Stevenson and Lauth 2019) and/or unprecedented maritime northern transit conditions (Humpbert 2021; Smith 2021).
- A foreign vessel sunk: Based on authors' consultation with the US Coast Guard, such information may not be currently available at the international level for the Bering and Chukchi Seas.

Conclusions

The 2020 debris event and response demonstrated that, during a maritime environmental or food security-related event in the Bering Strait region, the federally-authorized responding agencies located far from the coast of western Alaska are reliant on regional peoples—not only for awareness of the event but also for detailed information and response. Regional residents, tribal leadership, and communities documented, reported, conducted clean-up activities, and investigated the source of debris on a voluntary basis using personal resources, little to no training, and limited response capacity.

Without regular and relevant collaborative transboundary communications and/or enforcement of existing international marine pollution rules, the Bering Strait region should expect similar or higher levels of marine garbage in the future as industrial ship traffic increases. The Arctic Council's working group Protection of the Arctic Marine Environment (PAME) seems an appropriate forum for collaboration on addressing this issue. Identifying a primary point of contact within the Russian Federation would be ideal for collaborative time-sensitive communications to address the immediate and shared environmental, ecological, and industrial concerns regarding marine debris that face both Alaska and Chukotka in the unique Bering Strait region.

Acknowledgments

The authors would like to acknowledge the community members and tribal leadership throughout the Bering Strait region that acted on their food security and wildlife/public health concerns by responding to this anomalous marine debris event. Without their voluntary efforts to communicate, document, and in many cases, package and send in what they were seeing, we would not have the information presented here. We also thank the US Coast Guard (District 17), NOAA Marine Debris Program (Genwest Systems), Alaska Dept. of Environmental Conservation, NOAA Office of Response and Restoration, NOAA Office of Emergency Response (Genwest Systems), NOAA National Ocean Service, Alaska Division of Community and Regional Affairs, US Fish and Wildlife Service, US Environmental Protection Agency, and the Inuit Circumpolar Council for their interest in the debris event and attempts to identify a point of contact with the Russian Federation to discuss this emerging issue.

References

Bodenstein, B., K. Beckmen, G. Sheffield, K. Kuletz, C. Van Hemert, B. Berlowski, and V. Shearn-Boschler, 2015: Avian cholera causes marine bird mortality in the Bering Sea of Alaska. *J. Wildl. Dis.*, **51**(4), 934-937, https://doi.org/10.7589/2014-12-273.

Eisner, L. B., Y. I. Zuenko, E. O. Basyuk, L. L. Britt, J. T. Duffy-Anderson, S. Kotwicki, C. Ladd, and W. Cheng, 2020: Environmental impacts on walleye pollock (*Gadus chalcogrammus*) distribution across the Bering Sea shelf. *Deep-Sea Res. Pt. II*, 181-182, 104881, https://doi.org/10.1016/j.dsr2.2020.104881.

Humpert, M., 2021: "Winter transits along the Northern Sea Route open up a new frontier in Arctic shipping". Arctic Today, 25 Jan. 2021, https://www.arctictoday.com/winter-transits-along-the-northern-sea-route-open-up-a-new-frontier-in-arctic-shipping/.

International Maritime Organization, 2021: Prevention of pollution by garbage from ships. https://www.imo.org/en/OurWork/Environment/Pages/Garbage-Default.aspx.

Isachenkov, V., 2020: "Russian Navy conducts major maneuvers near Alaska." Associated Press, 28 Aug. 2020, US News & World Report, https://www.usnews.com/news/world/articles/2020-08- 28/russian-navy-conducts-major-maneuvers-near-alaska.

Kylin, H., 2020: Marine debris on two Arctic beaches in the Russian Far East. *Polar Res.*, **39**, https://doi.org/10.33265/polar.v39.3381.

Mua, J., S. Zhang, L. Qu, F. Jin, C. Fang, X. Ma, W. Zhang, and J. Wang, 2019: Microplastics abundance and characteristics in surface waters from the Northwest Pacific, the Bering Sea, and the Chukchi Sea. *Mar. Pollut. Bull.*, **143**, 58-65, https://doi.org/10.1016/j.marpolbul.2019.04.023.

Overland, J. E., and A. T. Roach, 1987: Northward flow in the Bering and Chukchi seas. *J. Geophys. Res.-Oceans*, **92**, 7097-7105, https://doi.org/10.1029/JC092iC07p07097.

Smith, R. B., 2020: "Oily substance found near Savoonga remains a mystery". The Nome Nugget, 24 Jul. 2020, http://www.nomenugget.com/news/oily-substance-found-near-savoonga-remains-mystery.

Smith, R. B., 2021: "Russian tanker passes through Bering Strait in the midst of winter". The Nome Nugget, 15 Jan. 2021, http://www.nomenugget.com/news/russian-tanker-passes-through-bering-strait-midst-winter.

Spies, I., K. M. Gruenthal, D. P. Drinan, A. B. Hollowed, D. E. Stevenson, C. M. Tarpey, and L. Hauser, 2020: Genetic evidence of a northward range expansion in the eastern Bering Sea stock of Pacific cod. *Evol. Appl.*, **13**(2), 362-375, https://doi.org/10.1111/eva.12874.

Stevenson, D. E., and R. R. Lauth, 2019: Bottom trawl surveys in the northern Bering Sea indicate recent shifts in the distribution of marine species. *Polar Biol.*, **42**, 407-421, https://doi.org/10.1007/s00300-018-2431-1.

Stimmelmayr, R., G. M. Ylitalo, G. Sheffield, K. B. Beckmen, K. A. Burek-Huntington, V. Metcalf, and T. Rowles, 2018: Oil fouling in three subsistence-harvested ringed (*Phoca hispida*) and spotted (*Phoca largha*) seals from the Bering Strait region, Alaska: Polycyclic aromatic hydrocarbon bile and tissue levels and pathological findings. *Mar. Pollut. Bull.*, **130**, 2018, 311-323, https://doi.org/10.1016/j.marpolbul.2018.02.040.

Stimmelmayr, R., J. Garlich-Miller, and W. Neakok, 2013: Ulcerative dermatitis disease syndrome—a new disease in walrus and ice seals? *Workshop on Assessing Pacific Walrus Population Attributes from Coastal Haul-Outs*. USFWS Administrative Report, R7/MMM 13-1, Anchorage, AK, Marine Mammals Management, US Fish and Wildlife Service, 69-70, https://www.fws.gov/r7/fisheries/mmm/walrus/pdf/Bilateral%20workshop%20Report_v3.pdf.

Sutton, H. I., 2020: "Russian Navy submarine surfaces off Alaska; likely same one that fired cruise missile earlier in exercise". Forbes Magazine, 28 Aug. 2020, https://www.forbes.com/sites/hisutton/2020/08/28/russian-navy-submarine-seen-off- alaska-likely-fired-a-cruise-missile/?sh=169ead2a6f39.

Thoman, R., and Coauthors, 2020: The record low Bering Sea ice extent in 2018: Content, impacts, and an assessment of the role of anthropogenic climate change. *Bull. Amer. Meteor. Soc.*, **101**(1), S53-S58, https://doi.org/10.1175/BAMS-D-19-0175.1.

U.S. Committee on the Marine Transportation System (USCMTS), 2019: A ten-year projection of maritime activity in the U.S. Arctic region, 2020-2030. Washington, D.C., https://www.cmts.gov/downloads/CMTS_2019_Arctic_Vessel_Projection_Report.pdf.

Van Hemert, C., and Coauthors, 2021: Investigation of algal toxins in a multispecies seabird die-off in the Bering and Chukchi Seas. Short communications. *J. Wildl. Dis.*, **57**(2), 399-407, https://doi.org/10.7589/JWD-D-20-00057.

November 24, 2021

Glacier and Permafrost Hazards

DOI: 10.25923/v40r-0956

G. J. Wolken[1,2], A. K. Liljedahl[3], M. Brubaker[4], J. A. Coe[5], G. Fiske[3], H. Hvidtfeldt Christiansen[6], M. Jacquemart[7,8], B. M. Jones[9], A. Kääb[10], F. Løvholt[11], S. Natali[3], A. C. A. Rudy[12], and D. Streletskiy[13]

[1]International Arctic Research Center, University of Alaska Fairbanks, Fairbanks, AK, USA
[2]Alaska Division of Geological & Geophysical Surveys, Department of Natural Resources, Fairbanks, AK, USA
[3]Woodwell Climate Research Center, Falmouth, MA, USA
[4]Alaska Native Tribal Health Consortium, Anchorage, AK, USA
[5]Geologic Hazards Science Center, USGS, Golden, CO, USA
[6]The University Centre in Svalbard, UNIS, Svalbard, Norway
[7]Laboratory of Hydraulics, Hydrology, and Glaciology (VAW), Department of Civil, Environmental and Geomatic Engineering, ETH Zurich, Zurich, Switzerland
[8]Swiss Federal Institute of Forest, Snow, and Landscape Research (WSL), Birmensdorf, Switzerland
[9]Water and Environmental Research Center, Institute of Northern Engineering, University of Alaska Fairbanks, Fairbanks, AK, USA
[10]Department of Geosciences, University of Oslo, Oslo, Norway
[11]Geohazards and Dynamics, NGI, Oslo, Norway
[12]Northwest Territories Geological Survey, Government of the Northwest Territories, Yellowknife, NT, Canada
[13]Department of Geography, The George Washington University, Washington, DC, USA

Highlights

- Retreating glaciers and thawing permafrost are causing local- to regional-scale hazards that threaten lives and livelihoods, infrastructure, sustainable resource development, and national security.
- Permafrost hazards are gradually impacting people across the Arctic, while glacier/permafrost hazard cascades are abrupt, more localized, and most life threatening.
- Broad-scale hazard identification and assessment across the Arctic are needed to better inform stakeholder decision making.

Introduction

Air temperature increases in the Arctic over the last two decades have been more than twice the global average, prompting an acceleration in glacier mass loss and permafrost degradation (IPCC 2019; Hugonnet et al. 2021; Smith et al. 2021). Beyond the global implications of these rapid changes (e.g., carbon release and sea level rise), the emergence and increase in cryosphere hazards threaten national security (e.g., military infrastructure and population displacement) and the lives of Arctic residents across local to regional scales. Here, we focus on hazards related to glaciers and permafrost and define hazard as the potential occurrence of a natural physical process that may adversely impact human or ecological systems (IPCC 2019).

Observations of glacier and permafrost hazards

About five million people live in the Northern Hemisphere permafrost region, which includes glaciers, and within this region, glacier and permafrost hazards are affecting lives, infrastructure, and ecosystem services (Ramage et al. 2021; Fig. 1). Recent degradation of glaciers and permafrost in the Arctic are leading to emerging biogeochemical threats that have the potential to disrupt ecosystem function and endanger human health (Miner et al. 2021). Thawing of ice-rich permafrost can cause ground subsidence with negative implications for infrastructure, ecosystems, and human lives and livelihoods (Suter et al. 2019; Gibson et al. 2021), while even a warming of permafrost can cause a reduction in its bearing capacity, impacting its ability to support structures (Streletskiy et al. 2012). This is especially apparent in the Russian Arctic where there are centers of high population and industrial economic activity in permafrost zones that act as foci of human-induced permafrost degradation, exacerbating climatically driven changes in the permafrost system (Vasiliev et al. 2020). For example, the recent oil tank collapse in Norilsk, Russia that resulted in the release of 21,000 cubic meters of diesel oil was at least partially attributed to the extremely warm conditions of 2020 in addition to a long-term warming trend in the region (Rajendran et al. 2021). Thawing of cold continuous permafrost in Point Lay and Wainwright, Alaska, caused a complete water system failure for multiple homes and buildings, including the health clinic (Cameron and Romanovsky 2021). As recently as 2009, the borough assumed the risk of thawing as "low" because the permafrost was classified as "continuous" and thought to be cold and stable (Cameron and Romanovsky 2021), yet permafrost degradation through the process of thermal erosion of ground ice also drained the community's drinking water source lake (Fig. 2; Dobbin 2016). Mountain permafrost degradation can also increase the likelihood of landslides (Hock et al. 2019). For example, a rock avalanche endangered two farms and destroyed a considerable amount of livestock pastures in Signaldalen, northern Norway (Frauenfelder et al. 2018). Field observations showed that the upper limit of the failure corresponded to the lower altitudinal limit of permafrost. The combination of gradual long-term warming and record-high mean near-surface temperatures caused the rock avalanche.

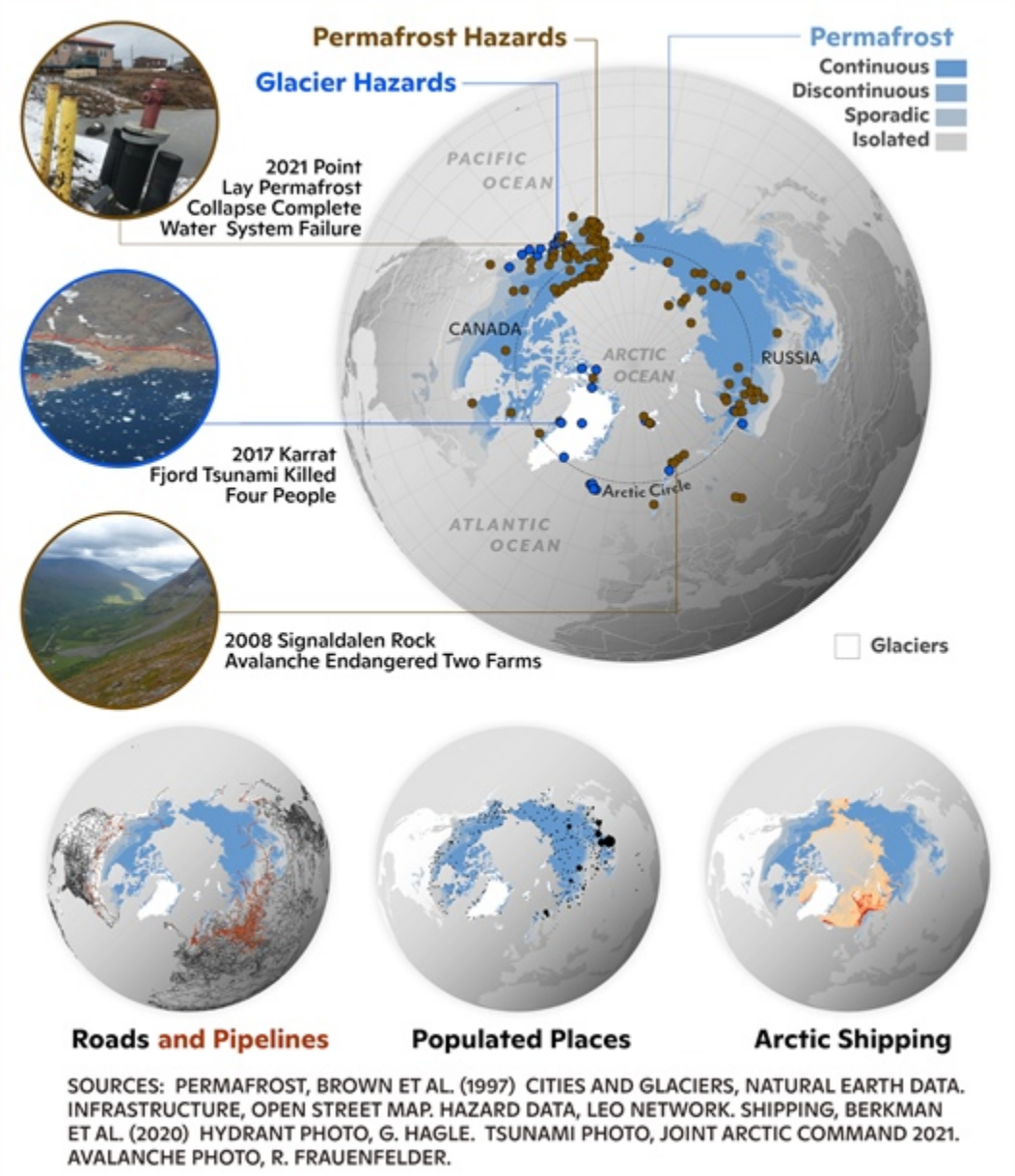

Fig. 1. Examples of observed glacier and permafrost hazards in recent years. Locations of hazard events are presented along with current glacier/ice sheet and permafrost extent, roads and pipelines, populated places (graduated circles scaling with population), and shipping routes. The three highlighted events are described in the main text.

Permafrost, Brown et al. (1997); Cities and glaciers, Natural Earth data; Infrastructure, OpenStreetMap; Hazard data, LEO Network; Shipping, Berkman et al. (2020); Hydrant photo, G. Hagle; Tsunami photo, Joint Arctic Command 2021; Avalanche photo, R. Frauenfelder

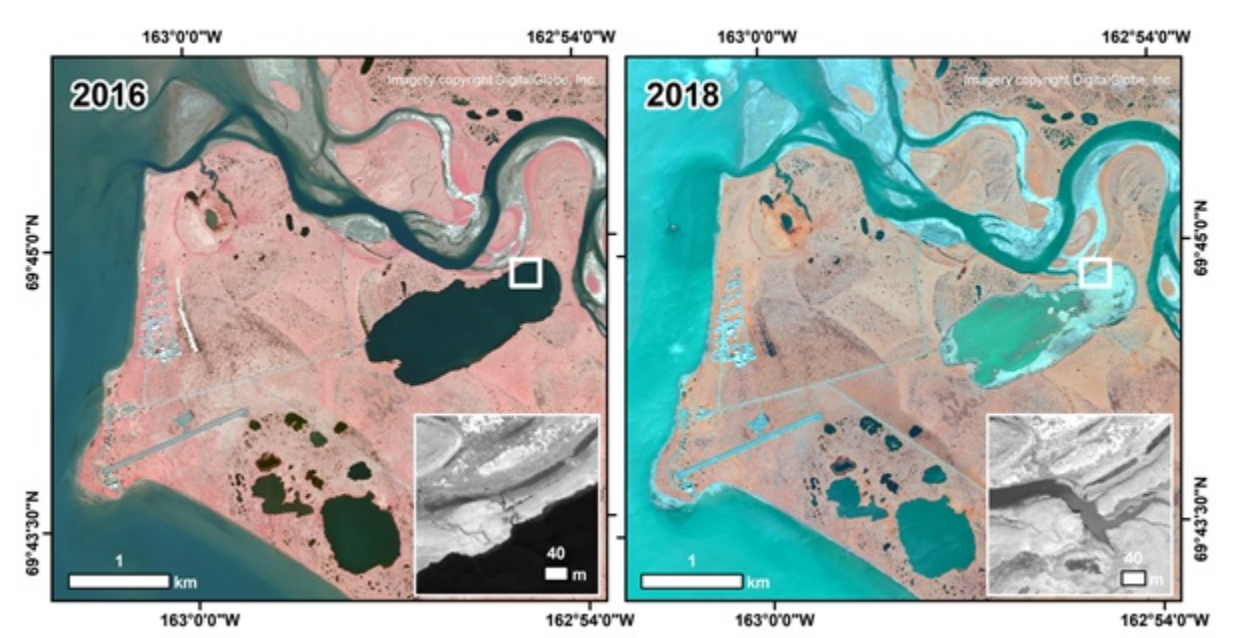

Fig. 2. The drinking water source lake in Point Lay, Alaska, catastrophically drained in fall 2016 because of permafrost degradation. The drainage was a result of bank overtopping and thermal erosion of an ice wedge (surface flow as opposed to subterranean drainage). The small inset shows the thermo-erosional gully that developed during the lateral drainage event. Drainage of thermokarst lakes in the Arctic is a natural process that is increasing in frequency because of climate change (Nitze et al. 2020), which is enhancing hazards in lowland permafrost regions (Arp et al. 2020).

Glacier retreat exposes over-steepened slopes that are prone to destabilization and, if in the presence of deep water, can cause landslide-generated tsunamis (Dai et al. 2020). The Karrat Fjord rock avalanche in 2017 generated a tsunami that killed four people in the village of Nuugaatsiaq, Greenland (Gauthier et al. 2018). Persistent unstable slope hazards keep residents of Nuugaatsiaq from returning home, while similar hazards (Barry Arm fjord) in northwest Prince William Sound, Alaska, have prompted advisories of unsafe travel and possible tsunami inundation. Unstable glacierized mountain regions in southeast Alaska have produced landslides that have generated the tallest tsunamis in the world (Higman et al. 2018), and despite the remote location, these hazards threaten communities, marine traffic, and infrastructure including major communication cables of importance to national security. Glacial lake outburst floods (GLOFs or Jökulhlaups) are abrupt releases of water from glacierized catchments that can significantly endanger downstream communities and infrastructure as well (Kienholz et al. 2020). In response to regular GLOFs from the Vatnajökull ice cap, the government of Iceland has developed a warning system to give local residents time to evacuate and, considering the regularity of GLOF occurrences, knowledge of where to expect flooding. Surging glaciers, where the glacier moves 10-100 times faster than typical, can also be hazardous and have made travel routes impassable in Svalbard, Norway.

A cascade of glacier and permafrost hazards

Glacier and permafrost hazards occur along a spectrum of spatial, temporal, and intensity scales. The largest disasters in terms of reach, damage, and lives lost that involve glaciers and permafrost occur typically through a combination or chain of processes, each potentially representing a hazard by itself. For instance, slope failures and glacier detachments can trigger cascading hazards, especially when slope

failures enter water bodies and cause outburst floods, debris flows, and tsunamis (Haeberli et al. 2017; Higman et al. 2018; Jacquemart et al. 2020). These cascading hazards can present a risk to people and infrastructure at great distances (10^2 km) from the initiating slope failure, and changes in climate can shift hazard zones and scales. For instance, as calving glaciers retreat, larger water bodies are often exposed, increasing the potential for rock avalanches to enter the water and generate devastating displacement waves, which increase the reach and intensity of the hazard.

Drivers of glacier and permafrost hazards

Thawing of permafrost and melting of land ice that formed and was retained over millennia are altering the Arctic landscape baseline condition, with extreme weather events further amplifying the potential for glacier and permafrost hazards. Permafrost temperatures have increased across the circumpolar region since the 1980s (Smith et al. 2021), and permafrost degradation has been documented across much of the Arctic (Liljedahl et al. 2016; Vasiliev et al. 2020). The onset of ice-rich permafrost degradation has been linked to long-term gradual warming combined with extreme events such as unusually warm summers and deep snow cover (Farquharson et al. 2019). A period of unusually warm air temperatures between 2012 and 2016 in southeast Alaska coincided with an increase in rock-avalanche activity and size (Bessette-Kirton and Coe 2020). The influence of degrading permafrost on landslide occurrence is increasingly recognized throughout the Arctic, including Norway (Hilger et al. 2021), Iceland (Sæmundsson et al. 2018), Russia (Leibman et al. 2015), and Canada (Lewkowicz and Way 2019).

Observations of extreme precipitation, such as more intense and prolonged rainfall (e.g., atmospheric rivers), appear to be increasing (Francis et al. 2021). While extreme precipitation events alone can trigger deadly debris flows, such as in Sitka (August 2015) and Haines, Alaska (December 2020), increased rainfall, combined with warming air temperatures, is also documented to drive landslide development in ice-rich permafrost terrain (Kokelj et al. 2015). Similarly, the combination of increased rainfall, unusual warmth that increases glacial ice melt, more crevasses, and retreat and steepening of a glacier appears to encourage glacier surges (Sevestre et al. 2018).

Mountain permafrost is the least monitored permafrost type in the Arctic, and processes linking glaciers and permafrost are poorly understood. Paleorecords and newly discovered processes, however, point to conditions that elevate hazard potential in glacier and permafrost areas. In Norway, the frequency of postglacial landslide activity was dominated by events in the beginning of the Holocene when and where ice sheet retreat was most rapid (Bellwald et al. 2016). Newly discovered processes, e.g., the release of entire glacier tongues from their beds, have been documented in the Arctic, but more data are needed to understand the conditions that favor devastating mass flows of water, ice, and debris (Jacquemart et al. 2020).

Outlook and needs

As the Arctic landscape continues to respond to warming conditions, attention to glacier and permafrost hazards will become increasingly important. The clustering of landslide and glacier detachment events in the immediate aftermath of warming episodes, such as following the last deglaciation, clearly flags the likelihood of increased hazard due to global warming. The recent major landslide tsunami events in Paatuut, Greenland 2000 (Dahl-Jensen et al. 2004), Karrat Fjord, Greenland 2017 (Svennevig et al. 2020), and Taan Fjord, Alaska 2017 (Higman et al. 2018) serve as recent stand-out examples of glacier and

permafrost hazards in the Arctic. These events highlight the need for broad-scale hazard identification and assessment to improve our knowledge of glacier and permafrost hazards and better inform stakeholder decision making.

The following are challenges and needs regarding Arctic glacier and permafrost hazards:

- A core need is more extensive baseline data (e.g., ground ice content), via remote sensing, field observations, and community science, to identify hazards and evaluate potential landscape change for adaptation and mitigation planning;
- Existing permafrost and glacier monitoring networks could assist in identifying areas of concern, while also guiding the formation of new monitoring networks;
- Long-term observation of mountain permafrost in the Arctic and refined understanding of how permafrost degradation and glacier retreat processes impact slope stability are needed; and
- Future efforts to address glacier and permafrost hazards in the Arctic will require implementation of a co-production approach (e.g., community members, scientists, and engineers) to find effective adaptation and preparedness options (i.e., early warning systems) to enhance resilience.

Acknowledgments

We thank Matt Thomas, Twila Moon, Rick Thoman, Rex Baum, Brian Shiro, Janet Slate, and three anonymous reviewers for their constructive reviews of this article. G. J. Wolken received partial support from the Alaska Climate Adaptation Science Center. B. M. Jones was supported by the US National Science Foundation under grants OISE-1927553 and OPP-1806213. Any use of trade, firm, or product names is for descriptive purposes only and does not imply endorsement by the U.S. Government.

References

Arp, C. D., B. M. Jones, K. M. Hinkel, D. L. Kane, M. S. Whitman, and R. Kemnitz, 2020: Recurring outburst floods from drained lakes: An emerging Arctic hazard. *Front. Ecol. Environ.*, **18**(7), 384-390, https://doi.org/10.1002/fee.2175.

Bellwald, B., B. O. Hjelstuen, H. P. Sejrup, and H. Haflidason, 2016: Postglacial mass movements and depositional environments in a high-latitude fjord system—Hardangerfjorden, Western Norway. *Mar. Geol.*, **379**, 157-175, https://doi.org/10.1016/j.margeo.2016.06.002.

Berkman, P. A, G. Fiske, and D. Lorenzini, 2020: Baseline of next-generation Arctic marine shipping assessments - Oldest continuous pan-Arctic satellite Automatic Identification System (AIS) data record of maritime ship traffic, 2009-2016. Arctic Data Center, https://doi.org/10.18739/A2TD9N89Z.

Bessette-Kirton, E. K., and J. A. Coe, 2020: A 36-year record of rock avalanches in the St. Elias Mountains of southeast Alaska, with implications for future hazards. *Front. Earth Sci.*, **8**, 293, https://doi.org/10.3389/feart.2020.00293.

Brown, J., O. J. Ferrians Jr., J. A. Heginbottom, and E. S. Melnikov, 1997: Circum-Arctic Map of Permafrost and Ground-Ice Conditions. Circum-Pacific Map CP-45, 1:10,000,000-Scale. Washington, DC, U.S. Geological Survey in Cooperation with the Circum-Pacific Council for Energy and Mineral Resources. 1 sheet, https://doi.org/10.3133/cp45.

Cameron, R., and V. Romanovsky, 2021: Thawing permafrost and subsidence causing on-going water system challenges. LEO Network (leonetwork.org). Accessed 13 September 2021.

Dahl-Jensen, T., and Coauthors, 2004: Landslide and tsunami 21 November 2000 in Paatuut, West Greenland. *Nat. Hazards*, **31**, 277-287, https://doi.org/10.1023/B:NHAZ.0000020264.70048.95.

Dai, C., and Coauthors, 2020: Detection and assessment of a large and potentially tsunamigenic periglacial landslide in Barry Arm, Alaska. *Geophys. Res. Lett.*, **47**(22), e2020GL089800, https://doi.org/10.1029/2020GL089800.

Dobbin, P., 2016: DEC looks into whether drums in village's drinking water lake pose any hazards. Alaska's News Source (9 Aug 2016), https://www.alaskasnewssource.com/content/news/Officials-try-to-determine-if-Point-Lays-drinking-water-is-safe-or-contaminated-389669191.html, Accessed 13 Sep 2021.

Farquharson, L. M., V. E. Romanovsky, W. L. Cable, D. A. Walker, S. V. Kokelj, and D. Nicolsky, 2019: Climate change drives widespread and rapid thermokarst development in very cold permafrost in the Canadian High Arctic. *Geophys. Res. Lett.*, **46**(12), 6681-6689, https://doi.org/10.1029/2019GL082187.

Francis, J. A., N. Skific, S. J. Vavrus, and J. Cohen, 2021: Measuring "weather whiplash" events in North America: A new large-scale regime approach. Preprint *ESSOAr*, https://doi.org/10.1002/essoar.10507297.1.

Frauenfelder, R., K. Isaksen, M. J. Lato, and J. Noetzli, 2018: Ground thermal and geomechanical conditions in a permafrost-affected high-latitude rock avalanche site (Polvartinden, northern Norway). *Cryosphere*, **12**(4), 1531-1550, https://doi.org/10.5194/tc-12-1531-2018.

Gauthier, D., S. A. Anderson, H. M. Fritz, and T. Giachetti, 2018: Karrat Fjord (Greenland) tsunamigenic landslide of 17 June 2017: Initial 3D observations. *Landslides*, **15**(2), 327-332, https://doi.org/10.1007/s10346-017-0926-4.

Gibson, C. M., T. Brinkman, H. Cold, D. Brown, and M. Turetsky, 2021: Identifying increasing risks of hazards for northern land-users caused by permafrost thaw: Integrating scientific and community-based research approaches. *Environ. Res. Lett.*, **16**(6), 064047, https://doi.org/10.1088/1748-9326/abfc79.

Haeberli, W., Y. Schaub, and C. Huggel 2017: Increasing risks related to landslides from degrading permafrost into new lakes in de-glaciating mountain ranges. *Geomorphology*, **293**, 405-417, https://doi.org/10.1016/j.geomorph.2016.02.009.

Higman, B., and Coauthors, 2018: The 2015 landslide and tsunami in Taan Fiord, Alaska. *Sci. Rep.*, **8**, 12993, https://doi.org/10.1038/s41598-018-30475-w.

Hilger, P., R. L. Hermanns, J. Czekirda, K. S. Myhra, J. S. Gosse, and B. Etzelmüller, 2021: Permafrost as a first order control on long-term rock-slope deformation in (Sub-) Arctic Norway. *Quat. Sci. Rev.*, **251**, 106718, https://doi.org/10.1016/j.quascirev.2020.106718.

Hock, R., and Coauthors, 2019: High Mountain Areas, in: IPCC Special Report on the Ocean and Cryosphere in a Changing Climate (SROCC) [H. -O. Pörtner, and Coauthors (eds.)], IPCC, Geneva. In press.

Hugonnet, R., and Coauthors, 2021: Accelerated global glacier mass loss in the early twenty-first century. *Nature*, **592**, 726-731, https://doi.org/10.1038/s41586-021-03436-z.

IPCC, 2019: IPCC Special Report on the Ocean and Cryosphere in a Changing Climate [H. -O. Pörtner, and Coauthors (eds.)]. In press.

Jacquemart, M., M. Loso, M. Leopold, E. Welty, E. Berthier, J. S. Hansen, J. Sykes, and K. Tiampo, 2020: What drives large-scale glacier detachments? Insights from Flat Creek glacier, St. Elias Mountains, Alaska. *Geology*, **48**(7), 703-707, https://doi.org/10.1130/G47211.1.

Kienholz, C., and Coauthors, 2020: Deglacierization of a marginal basin and implications for outburst floods, Mendenhall Glacier, Alaska. *Front. Earth Sci.*, **8**, 137, https://doi.org/10.3389/feart.2020.00137.

Kokelj, S. V., J. Tunnicliffe, D. Lacelle, T. C. Lantz, K. S. Chin, and R. Fraser, 2015: Increased precipitation drives mega slump development and destabilization of ice-rich permafrost terrain, northwestern Canada. *Global Planet Change*, **129**, 56-68, https://doi.org/10.1016/j.gloplacha.2015.02.008.

Leibman, M. O., A. V. Khomutov, A. A. Gubarkov, Y. A. Dvornikov, and D. R. Mullanurov, 2015: The research station "Vaskiny Dachi", central Yamal, West Siberia, Russia—A review of 25 years of permafrost studies. *Fennia*, **193**(1), 3-30, https://doi.org/10.11143/45201.

Lewkowicz, A. G., and R. G. Way, 2019: Extremes of summer climate trigger thousands of thermokarst landslides in a High Arctic environment. *Nat. Commun.*, **10**, 1329, https://doi.org/10.1038/s41467-019-09314-7.

Liljedahl, A. K., and Coauthors, 2016: Pan-Arctic ice-wedge degradation in warming permafrost and its influence on tundra hydrology. *Nat. Geosci.*, **9**, 312-318, https://doi.org/10.1038/ngeo2674.

Miner, K. R., J. D'Andrilli, R. Mackelprang, A. Edwards, M. J. Malaska, M. P. Waldrop, and C. E. Miller, 2021: Emergent biogeochemical risks from Arctic permafrost degradation. *Nat. Climate Change*, **11**, 809-819, https://doi.org/10.1038/s41558-021-01162-y.

Nitze, I., S. W. Cooley, C. R. Duguay, B. M. Jones, and G. Grosse, 2020: The catastrophic thermokarst lake drainage events of 2018 in northwestern Alaska: Fast-forward into the future. *Cryosphere*, **14**, 4279-4297, https://doi.org/10.5194/tc-14-4279-2020.

Rajendran, S., F. N. Sadooni, H. A. -S. Al-Kuwari, A. Oleg, H. Govil, S. Nasir, and P. Vethamony, 2021: Monitoring oil spill in Norilsk, Russia using satellite data. *Sci. Rep.*, **11**, 3817, https://doi.org/10.1038/s41598-021-83260-7.

Ramage, J., L. Jungsberg, S. Wang, S. Westermann, H. Lantuit, and T. Heleniak, 2021: Population living on permafrost in the Arctic. *Popul. Environ.*, **43**, 22-38, https://doi.org/10.1007/s11111-020-00370-6.

Sæmundsson, Þ., C. Morino, J. K. Helgason, S. J. Conway, and H. G. Pétursson, 2018: The triggering factors of the Móafellshyrna debris slide in northern Iceland: Intense precipitation, earthquake activity and thawing of mountain permafrost. *Sci. Total. Environ.*, **621**, 1163-1175, https://doi.org/10.1016/j.scitotenv.2017.10.111.

Sevestre, H., D. I. Benn, A. Luckman, C. Nuth, J. Kohler, K. Lindbäck, and R. Pettersson, 2018: Tidewater glacier surges initiated at the terminus. *J. Geophys. Res.-Earth Surf.*, **123**(5), 1035-1051, https://doi.org/10.1029/2017JF004358.

Smith, S. L., and Coauthors, 2021: [Arctic] Permafrost [in "State of the Climate in 2020"]. *Bull. Amer. Meteor.*, **102**(8), S293-S297, https://doi.org/10.1175/BAMS-D-21-0086.1.

Streletskiy, D. A., N. I. Shiklomanov, and F. E. Nelson, 2012: Permafrost, infrastructure and climate change: A GIS-based landscape approach to geotechnical modeling. *Arct. Antarct. Alp. Res.*, **44**(3), 368-380, https://doi.org/10.1657/1938-4246-44.3.368.

Suter, L., D. Streletskiy, and N. Shiklomanov. 2019: Assessment of the costs of climate change impacts on critical infrastructure in the circumpolar Arctic. *Polar Geogr.*, **42**(4), 267-286, https://doi.org/10.1080/1088937X.2019.1686082.

Svennevig, K., T. Dahl-Jensen, M. Keiding, J. P. Merryman Boncori, T. B. Larsen, S. Salehi, A. Munck Solgaard, and P. H. Voss, 2020: Evolution of events before and after the 17 June 2017 rock avalanche at Karrat Fjord, West Greenland—A multidisciplinary approach to detecting and locating unstable rock slopes in a remote Arctic area. *Earth Surf. Dyn.*, **8**(4), 1021-1038, https://doi.org/10.5194/esurf-8-1021-2020.

Vasiliev, A. A., D. S. Drozdov, A. G. Gravis, G. V. Malkova, K. E. Nyland, and D. A. Streletskiy, 2020: Permafrost degradation in the Western Russian Arctic. *Environ. Res. Lett.*, **15**(4), 045001, https://doi.org/10.1088/1748-9326/ab6f12.

December 7, 2021

The Changing Arctic Marine Soundscape

DOI: 10.25923/jagc-4a84

K. M. Stafford[1]

[1]Applied Physics Laboratory, University of Washington, Seattle, WA, USA

Highlights

- Less sea ice and increasing storminess are making Arctic waters louder during the open water season due to increased wind and wave noise.
- Arctic marine mammals are changing their migratory patterns and subarctic visitors are heard for more of the year and further north as sea ice loss opens habitat for them.
- Arctic shipping traffic between the Pacific and Atlantic Oceans continues to increase and with it, ambient noise levels are increasing in the frequency bands used by marine mammals.

Introduction

In the global ocean, the combination of naturally occurring sounds, including those from wind, waves, underwater earthquakes, and marine animals, make up the underwater 'soundscape.' Unique to polar regions is the role sea ice plays in the soundscape, both by generating noise and by dampening noise from the atmosphere. The ice-covered Arctic can experience some of the lowest ambient sound levels in the ocean due to the lack of wind-driven waves in ice-covered regions. Changes in sea ice—reduced thickness, age, extent and changing seasonality—are, however, altering the Arctic underwater acoustic environment in numerous ways. Over the past ~15 years, advances in both long-term deployable acoustic instrumentation and the ability to analyze the resulting terabytes of data, have resulted in sound recordings that provide up to multi-year soundscapes from the Pacific and Atlantic Arctic, north of the Arctic Circle. These data now allow us to understand how loud the oceans are and provide evidence of changes in the geophony (natural sounds of the earth and atmosphere), biophony (sounds produced by living organisms), and anthrophony (human-made sounds). In the Arctic, the main sources of naturally occurring sounds include waves, winds, sea ice, and marine mammals. Sources of human noise include oil and gas exploration and extraction, commercial shipping, research vessels, tugs and barges to supply villages, and local skiffs. However, as seasonal sea ice decreases and the 'open water season' lengthens, both natural and anthropogenic influences are changing the underwater soundscape of the Arctic.

Geophony

Wind and breaking waves create sound underwater. In ice-free water there is a direct correlation between increasing wind speeds and increasing ambient sound levels (PAME 2019). And in shallow waters, such as those found in much of the nearshore Arctic, sound levels tend to be higher for the same wind speed than they are in deep waters (PAME 2019). In contrast, the ice-covered Arctic can have some of the lowest ambient sound levels globally due to the lack of wind-driven waves (Han et al. 2021). However, the dynamics of sea ice (Fig. 1a), including ice formation and deformation, pressure ridging, and cracking, can greatly increase ambient sound levels over a broad range of frequencies (PAME 2019).

Comparison of wind speed and sea ice cover data in both the Pacific and Atlantic Arctic has shown a clear relationship between wind speed over different sea ice extents with sound levels many times higher under open water than they are under heavy ice (PAME 2019, Fig. 2). Increases in the duration of open water in the Arctic, combined with increased extreme wind events (Zhang et al. 2021) suggest that overall ambient sound levels will continue to increase throughout the Arctic and will remain high as climate change continues to expand open water periods and regions into the future.

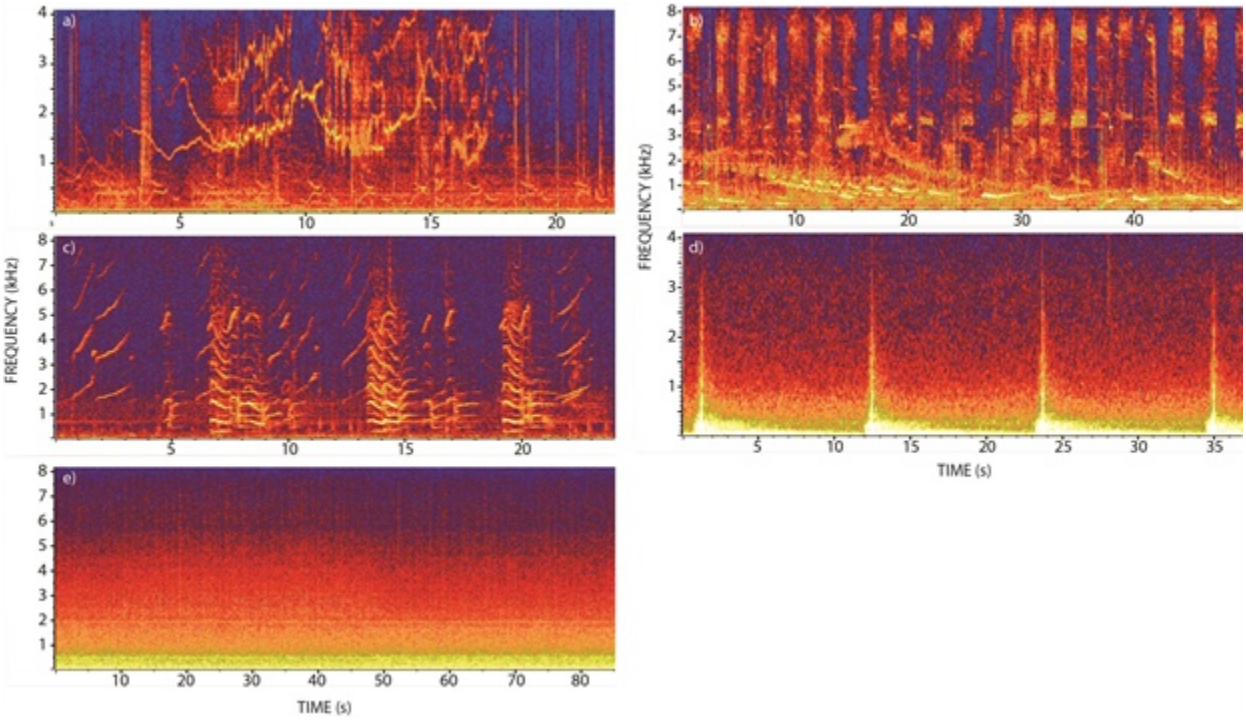

Fig. 1. Spectrograms and associated sound files of (a) sea ice noise recorded December 2012 in Bering Strait, (b) chorus of bowhead and beluga whales, bearded seals, and walrus recorded near St. Lawrence Island, winter 2018, (c) killer whales recorded near St. Lawrence Island, summer 2017, (d) airgun pulses from September 2013 recorded in Fram Strait, (e) ship noise recorded in the NE Chukchi Sea, September 2017.

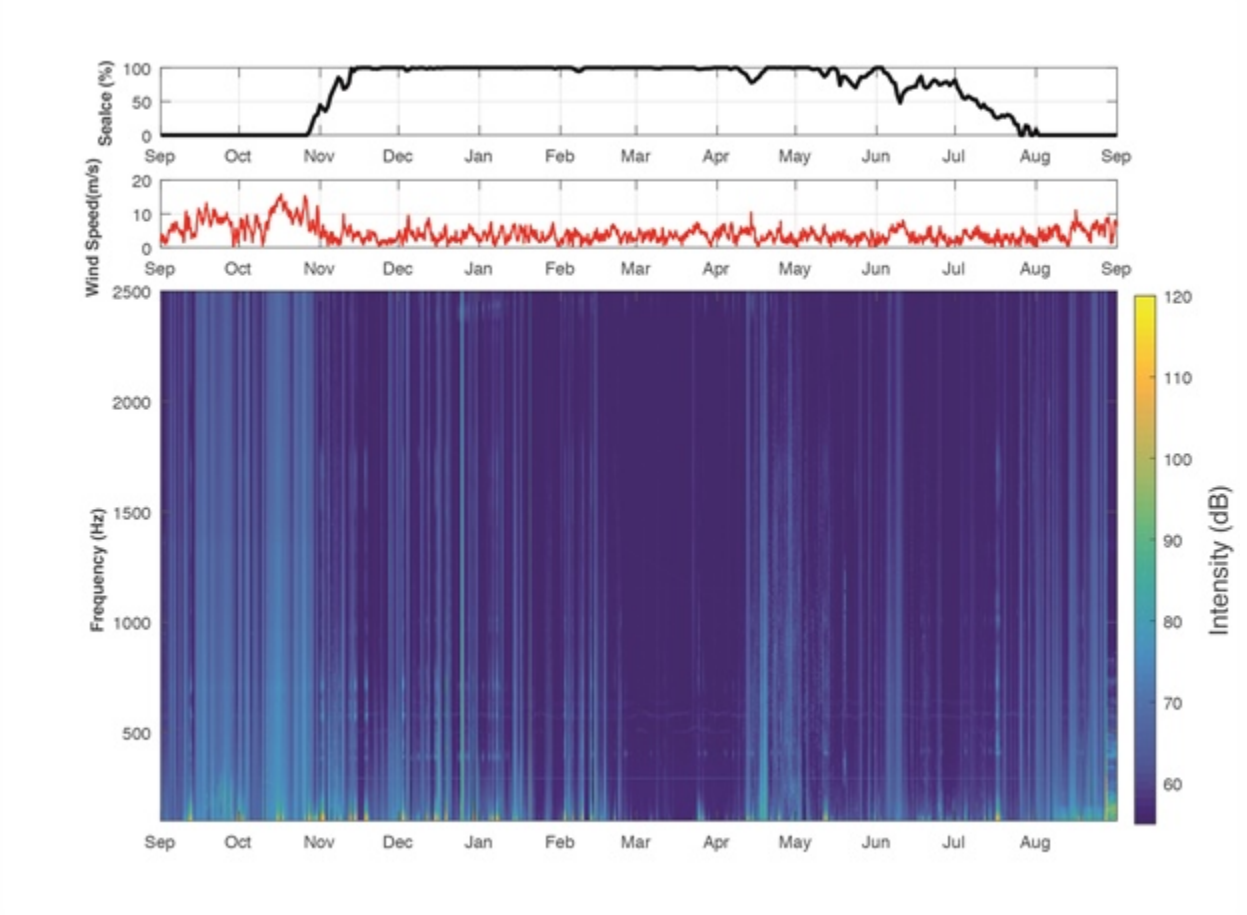

Fig. 2. Beaufort Sea shelf data over a year showing sea ice concentration (top panel), wind speed (middle panel), and ambient noise from 100 to 2500 Hz (bottom panel) showing the impact sea ice and wind have on the overall soundscape. Noise levels (shown as Intensity) are louder when sea ice concentrations are 0 and wind speeds are high.

Biophony

Throughout the Arctic, marine mammals' acoustic displays are the dominant contributor to the soundscape. Marine animals, including marine mammals, rely on sound more than other senses to navigate, to find food, for reproductive displays, and to communicate over relatively long distances, and the sounds they produce can be reflective of their behavioral state. For instance, many marine mammals use different signals at different times of the year; in the winter and spring, most Arctic species make reproductive displays that are more elaborate and cover a greater range of frequencies than signals they produce when migrating or feeding (Stafford et al. 2021). In areas that are overwintering hotspots, such as the region to the northwest of St. Lawrence Island, Alaska, the chorus of sounds from multiple species can make it difficult for human listeners to distinguish individual animals or even species (Fig. 1b).

Underwater/under ice monitoring in the Arctic has provided novel information on the seasonal occurrence of Arctic marine mammals over year-long periods (e.g., PAME 2019, and references therein; Ahonen et al. 2019). Much of this information corroborates observations from Indigenous Knowledge holders. In the past few years, acoustic data have been documenting changes in the seasonal distribution of Arctic marine mammals, including during times that humans are not present. In the

Pacific Arctic, bowhead whales have been recorded in mid-winter in the Beaufort Sea (Insley et al. 2021; Stafford et al. 2021), far from their wintering grounds in the northern Bering Sea (Huntington et al. 2020). Likewise, acoustic data indicate both bowhead and beluga whales in the Pacific Arctic have delayed migrating out of the Beaufort and Chukchi Seas in the fall (Stafford et al. 2021).

Other biologically driven changes in the soundscape of the Arctic include the detection of subarctic species further north and for longer time periods. This includes decadal-scale changes in the presence of blue and fin whales in Fram Strait (Ahonen et al. 2021); fin whales overwintering in Davis Strait (Simon et al. 2010); and fin, minke, humpback and killer whales (Fig. 1c) moving further north and spending more time in the Chukchi Sea (Hannay et al. 2013; Stafford 2019). While in many instances, these subarctic species provide only short-lived contributions to the overall soundscape, their acoustic detections are clear evidence of a changing Arctic (Moore et al. 2019).

Anthrophony–when 'sound' becomes 'noise'

Globally there has been increasing concern about the impacts of underwater noise on marine animals. In the Arctic, this concern has generally focused on marine mammals. In large part, this is because many species are critical to food security and culture in the Arctic and there are concerns about sound displacing or changing the distribution and accessibility of animals (Huntington et al. 2020). In response to these concerns, numerous national and international organizations have recognized the potential for industrialization of the Arctic to increase underwater noise, and potentially harm endemic species (PAME 2019; Halliday et al. 2020). There is a growing body of literature on how increases in noise affect marine mammals but, especially in a region as relatively inaccessible as the Arctic, understanding the extent of such impacts is difficult. In the Arctic, many anthropogenic sources overlap in frequency with the sounds produced and received by marine mammals. Such signals are more likely to interfere with the animals' ability to hear and respond to sounds important to them. Low-frequency sounds are more likely to be problematic for bowhead whales, mid-frequencies for ice seals and walrus, and high frequencies for narwhal and belugas (PAME 2019; Halliday et al. 2020).

Sources of man-made sounds in the Arctic include seismic exploration using air guns (which produce loud, low-frequency pulses by releasing pressurized air) for oil and gas and seafloor mapping (Fig. 1d, resource extraction (drilling)) and ships (Fig. 1e), including small boats and larger tourism, research, and commercial vessels. Most of these man-made sources of noise are relatively low frequency. Low frequency sounds, such as those produced by ships and airguns, can carry for hundreds to thousands of kilometers (PAME 2019; Halliday et al. 2020).

The most persistent, and a growing source of anthrophony in the Arctic is cargo and fishing vessels, most of which sail the Northern Sea Route (NSR) across the top of the Russian Federation from the Pacific to the Atlantic (Fig. 3). Fewer vessels use the Northwest Passage, through the Canadian Arctic Archipelago, but that route, too, has seen increased ship traffic with 44% more vessels from 2013 to 2019 (PAME 2021). Most large ships travel through the Arctic during the open water season, but in January 2021, at least four liquid natural gas tankers sailed the NSR without icebreaker support (Northern Sea Route Information Office 2021). Because extensive commercial shipping in the Arctic is a relatively new phenomenon, Arctic species may have a lower tolerance of, and react more strongly to, such noise (PAME 2019). Studies of marine mammals in other oceans have shown that the ranges over which animals communicate is greatly reduced and stress levels increase when large ships pass by (Würsig and Koski 2021). And, as with wind noise discussed above, increases in overall noise levels

decrease the range over which Arctic marine mammals can communicate and may have long-term impacts on their ability to navigate, communicate, and reproduce (Halliday et al. 2020, Fig. 4).

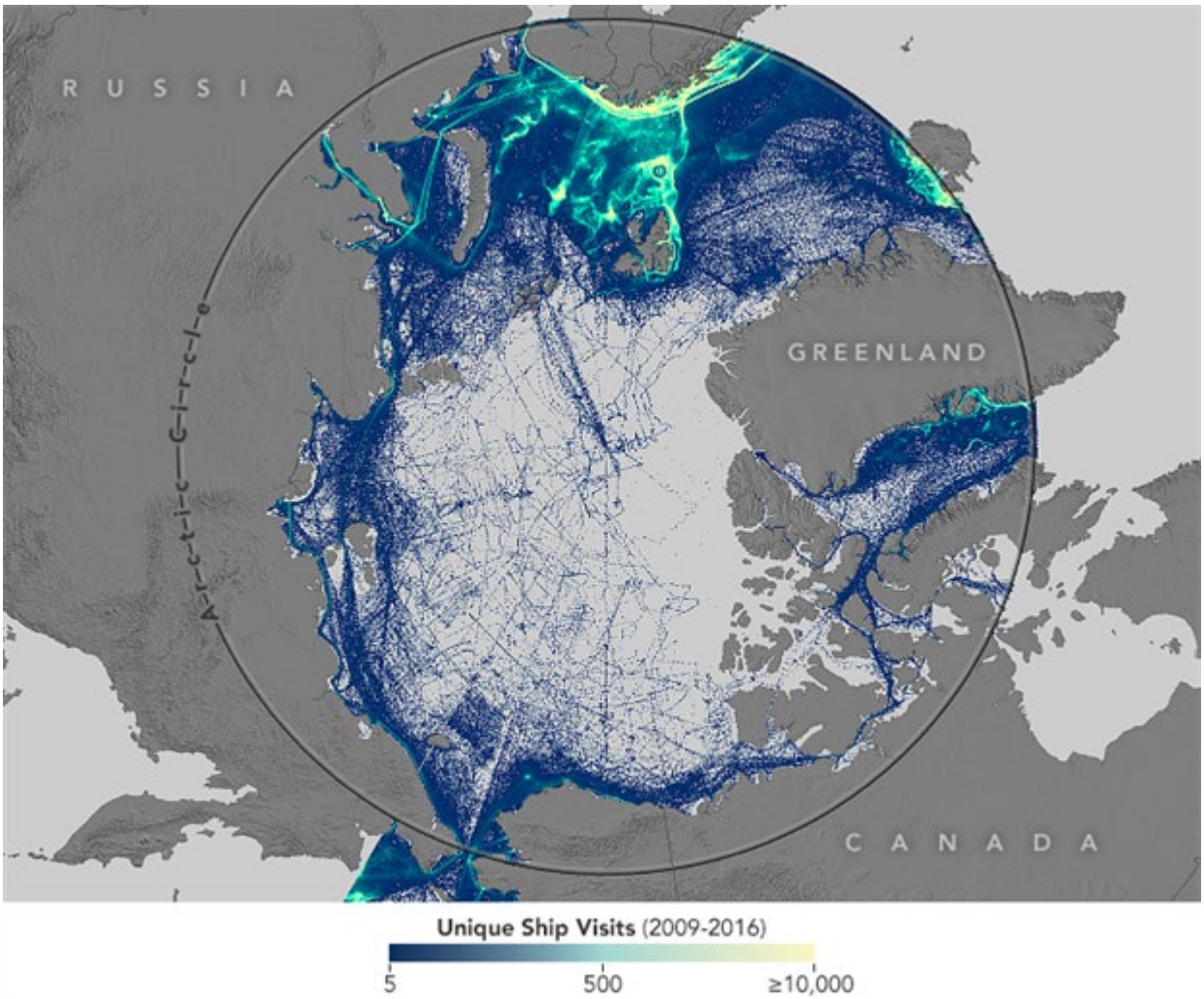

Fig. 3. Unique ship passages in the Arctic from 2009 to 2016 (Figure from NASA Earth Observatory with Automatic Identification Signals from ships provided by Woodwell Climate Research Center).

Fig. 4. Bowhead whales feeding as tug and barge pass by in the Beaufort Sea, September 2021 (photo K. Stafford).

Acknowledgments

Funding was provided to K. M. Stafford from the Office of Naval Research Marine Mammals and Biology Program N000142012413.

References

Ahonen, H., K. M. Stafford, C. Lydersen, C. L. Berchok, S. E. Moore, and K. M. Kovacs, 2021: Interannual variability in acoustic detection of blue and fin whale calls in the Northeast Atlantic High Arctic between 2008 and 2018. *Endanger. Species Res.*, **45**, 209-224, https://doi.org/10.3354/esr01132.

Ahonen, H., K. M. Stafford, C. Lydersen, L. de Steur, and K. M. Kovacs, 2019: A multi-year study of narwhal occurrence in the western Fram Strait—detected via passive acoustic monitoring. *Polar Res.*, **38**, 181, https://doi.org/10.33265/polar.v38.3468.

Halliday, W. D., M. K. Pine, and S. J. Insley, 2020: Underwater noise and Arctic marine mammals: review and policy recommendations. *Environ. Rev.*, **28**, 438-448, https://doi.org/10.1139/er-2019-0033.

Han, D. -G., and Coauthors, 2021: Effects of geophony and anthrophony on the underwater acoustic environment in the East Siberian Sea, Arctic Ocean. *Geophys. Res. Lett.*, **48**, e2021GL093097, https://doi.org/10.1029/2021GL093097.

Hannay, D. E., J. Delarue, X. Mouy, B. S. Martin, D. Leary, J. N. Oswald, and J. Vallarta, 2013: Marine mammal acoustic detections in the northeastern Chukchi Sea, September 2007-July 2011. *Cont. Shelf Res.*, **67**, 127–146, https://doi.org/10.1016/j.csr.2013.07.009.

Huntington, H. P., and Coauthors, 2020: Evidence suggests potential transformation of the Pacific Arctic ecosystem is underway. *Nat. Climate Change*, **10**, 342–348, https://doi.org/10.1038/s41558-020-0695-2.

Insley, S. J., W. D. Halliday, X. Mouy, and N. Diogou, 2021: Bowhead whales overwinter in the Amundsen Gulf and Eastern Beaufort Sea. *Roy. Soc. Open Sci.*, **8**, 202268, https://doi.org/10.1098/rsos.202268.

Moore, S. E., T. Haug, G. A. Vikingsson, and G. B. Stenson, 2019: Baleen whale ecology in arctic and subarctic seas in an era of rapid habitat alteration. *Prog. Oceanogr.*, **176**, 102118, https://doi.org/10.1016/j.pocean.2019.05.010.

Northern Sea Route Information Office, 2021. NSR shipping traffic. Accessed 15 September 2021, https://arctic-lio.com/nsr-shipping-traffic-activities-in-january-april-2021/.

PAME, 2019: Underwater Noise in the Arctic: A State of Knowledge Report, Roveniemi, May 2019.

PAME, 2021: Shipping in the Northwest Passage: comparing 2013 with 2019, Roveniemi, May 2019.

Simon, M., K. M. Stafford, K. Beedholm, C. M. Lee, and P. T. Madsen, 2010: Singing behavior of fin whales in the Davis Strait with implications for mating, migration and foraging. *J. Acoust. Soc. Amer.*, **128**, 3200-3210, https://doi.org/10.1121/1.3495946.

Stafford, K. M., 2019: Increasing detections of killer whales (*Orcinus orca*), in the Pacific Arctic. *Mar. Mammal Sci.*, **35**(2), 696-706, https://doi.org/10.1111/mms.12551.

Stafford, K. M., J. J. Citta, S. Okkonen, and J. Zhang, 2021: Bowhead and beluga whale acoustic detections in the western Beaufort Sea 2008-2018. *PLoS ONE*, **16**, e0253929, https://doi.org/10.1371/journal.pone.0253929.

Würsig, B., and W. R. Koski, 2021: Naturally and potentially disturbed behavior of bowhead whales. The Bowhead Whale, J. G. M. Thewissen JGM and J. C. George, Eds. Elsevier Publishing; ISBN: 978-0-12-818969-6.

Zhang, F., X. Pang, R. Lei, M. Zhai, X. Zhao, and C. Q, 2021: Arctic sea ice motion change and response to atmospheric forcing between 1979 and 2019. *Int. J. Climatol.*, 1-23, https://doi.org/10.1002/joc.7340.

November 9, 2021

The Impact of COVID-19 on Food Access for Alaska Natives in 2020

DOI: 10.25923/5cb7-6h06

N. Johnson[1,2], K. S. Erickson (Inupiaq)[3], D. B. Ferguson[4], M. B. Jäger (Citizen Potawatomi Nation)[5], L. L. Jennings (Wixárika & Pascua Yaqui)[6], A. R. Juan (Tohono O'odham Nation)[7], S. Larson (Ahtna and Supiaq)[8], W. K. S. Smythe (Haida)[9], C. Strawhacker[10], A. Walker (Akimel O'otham)[11], and S. R. Carroll (Ahtna)[6]

[1]National Snow and Ice Data Center, Boulder, CO, USA
[2]Cooperative Institute for Research in Environmental Sciences, University of Colorado Boulder, Boulder, CO, USA
[3]Ikaaġun Engagement, Anchorage, AK, USA
[4]Department of Environmental Science, University of Arizona, Tucson, AZ, USA
[5]Native Nations Institute, University of Arizona, Tucson, AZ, USA
[6]Mel & Enid Zuckerman College of Public Health and Native Nations Institute, University of Arizona, Tucson, AZ, USA
[7]International Indian Treaty Council, Tucson, AZ, USA
[8]Chickaloon Village Traditional Council, Chickaloon, AK, USA
[9]American Indian Studies and Earth and Environmental Science, University of Minnesota Duluth, Duluth, MN, USA
[10]Office of Polar Programs, National Science Foundation, Alexandria, VA, USA
[11]Climate Science Alliance, San Diego, CA, USA

Highlights

- The COVID-19 pandemic has exacerbated existing challenges for Alaska Natives in accessing traditional and store-bought foods.
- The strength of Indigenous cultural and economic practices such as food sharing networks helped mitigate these challenges.
- Policies and programs that support access to traditional foods and Indigenous sovereignty strengthen the ability of individuals and communities to respond to significant events that break down supply chains and restrict mobility.

The COVID-19 pandemic led to the cancellation of the 2020 Nay'dini'aa Na'Kayax' (Chickaloon Native Village) culture camp, which had been held annually for the previous 20 summers—or since time immemorial, as the formal camp continued a tradition of gathering to share food, stories, and knowledge. The previous summer, Nay'dini'aa Na'Kayax' welcomed Indigenous Foods Knowledges Network (IFKN) members to join the camp. IFKN convenes Indigenous community members and researchers from the Arctic and US Southwest for place-based knowledge exchange about Indigenous foods. At the camp, network members learned how to fillet and preserve salmon alongside village youth, sharing meals and stories around the campfire. The cancellation of the 2020 camp, along with

similar celebrations and gatherings across Alaska, disrupted intergenerational knowledge sharing about Indigenous food systems.

In light of these disruptions, IFKN leadership saw an opportunity to engage in a research project that asked: How has the COVID-19 pandemic impacted food access for Indigenous individuals in Alaska and the US Southwest? In this essay, we share what we have learned from interviews conducted with Alaska Native experts as part of this project. Experts were individuals who had knowledge of traditional foods and who maintained a close connection with their home community and land in 2020.

Challenges to food access in Alaska during the COVID-19 pandemic

For the experts we spoke with, the pandemic created direct and indirect challenges related to food access in Alaska, including restricted access to traditional harvesting areas and harvesting infrastructure (Jenkins 2020; Sullivan 2021) (Table 1). Several experts noted that quarantine restrictions prevented them from traveling to seasonal harvesting areas used by family members for generations. This also limited access to infrastructure such as cabins, fish nets, and smoke houses (Fig. 1). Additionally, some extended families chose not to stay at harvesting camps together due to the emphasis on social distancing. Conversely, some experts reported that more people were at fish camp in summer 2020 due to closures of schools and workplaces, which created an opportunity for uninterrupted time on the land for those able to take advantage. Harvesters modified trips to limit social interaction by carrying extra gas and therefore avoided refueling stops where they would normally exchange information with others. Shared infrastructure, such as hunting cabins that are often used by separate hunting parties at the same time, saw similar limits to access. The cancellation of formal camps and land-based programs, such as the 2020 Nay'dini'aa Na'Kayax' culture camp, also limited access to traditional foods for families without an active harvester or their own harvesting infrastructure. In some cases, formal teaching of traditional food harvesting skills, such as classes offered through Ilisaġvik College in Utqiaġvik, shifted to an online format.

Table 1. Challenges to food access for Alaska Natives during the COVID-19 pandemic, their causes, solutions, and the scales of action related to each solution.

Challenge	Cause(s)	Solutions	Scales of Response
Unable to access harvesting territory	Quarantine restrictions	Shift location of harvest (e.g., by driving from a larger town rather than flying back to a small village); Use food sharing networks to ship food by freight; Use frozen or previously preserved harvested food	- Individual - Family
Unable to access harvesting infrastructure	Quarantine restrictions; Social distancing requirements	Rent, purchase, or build new infrastructure (e.g., boat rental, car purchase, indoor fish drying rack); Carry additional fuel when hunting (in lieu of refueling en route)	- Individual - Family

Challenge	Cause(s)	Solutions	Scales of Response
Harvesting with others outside of household	Social distancing requirements	Use of masks; limiting numbers at fish camp; Avoid mixing groups on the land	- Individual - Family
Cancellation of community feasts, celebrations, potlatches	Social distancing requirements	Reorganize distribution (e.g., socially distanced pick up or drop off); Increase funding for harvester support programs with distribution to elders and other community members in need; Use CARES funding for freezer purchase	- Family - Community - Native Village
Store-bought food access	Supply chain issues; Ravn Airlines bankruptcy and flight cancellations; Quarantine restrictions; Other issues (e.g., state reduction of ferry service)	Sharing store-bought food with family, neighbors; Shipping food by freight; Use of soup kitchens and food pantries; Distribution of food boxes; Authorization of Emergency Hunt	- Individual - Family - Native Village/ Non-governmental organization - Federal Subsistence Board
Declining Mental Health; Feeling stressed/depressed	Social isolation due to quarantine/social distancing requirements	Participation in harvesting activities; Participation in organized activities for children/youth (reduced in 2020); Provision of mental health services (reduced in 2020)	- Individual - Family - Regional corporation
Low salmon numbers in 2020 and 2021	Exact cause unknown, but probable causes include climate and other environmental stressors, commercial fishing practices	Harvest different foods; Experiment with agriculture; Fish donations	- Individual - Family - Community - Corporations and non-governmental organizations

Fig. 1. Donna Erickson cuts fish at camp near Unalakleet, Alaska. The boat and smoke house are part of her family's harvesting infrastructure. Photo: Jeff Erickson.

COVID-19 precautions also resulted in the loss of social aspects of food sharing, with the cancellation of extended family gatherings, community celebrations, and ceremonies. Experiencing cultural gatherings is an integral component of Indigenous food systems, as sharing food and stories connects people, land, animals, and waters (Inuit Circumpolar Council-Alaska 2015, 2019). By summer 2020, most large gatherings were restricted, contributing to feelings of loneliness, boredom, and social isolation. Some experts described feeling less motivated to participate in harvesting activities due to pandemic-related stress and depression; others shared concerns about loss of physical activity and companionship for community Elders who were unable to harvest. Experts also mentioned the disruption of extended food sharing networks that rely on opportunistic exchange when someone travels from one community to another (e.g., for a sports tournament). These networks are used to access foods that are not harvested locally.

Although unrelated to COVID-19, a number of experts referenced the low numbers of salmon in major Alaska rivers during the 2020 salmon runs that created an additional stress on food systems. Salmon fishing was closed in some locations, while in others, reduced quotas significantly restricted access. In the Interior, families prepared nets and repaired fish wheels only to learn that fishing was not permitted. One expert from southeast Alaska reported that their family caught few salmon due to a combination of social distancing and the smallest sockeye run in memory. Other environmental issues

mentioned included climate change impacts on sea ice and seasonality of harvesting, a declining caribou population, algal contamination of shellfish, and garbage in the Bering Sea (see essay *Marine Debris*).

Experts also reported governance challenges related to the ability to change harvesting practices during COVID-19. For example, the Organized Village of Kake (OVK) used an emergency hunt authorization to increase their supply of fresh meat during summer 2020. The island community was experiencing shortages due to pandemic-related supply chain issues and state cuts to the ferry service that resupplied food from the mainland. The State of Alaska sued the federal government over the authorization of the hunt, arguing that the state should maintain jurisdiction over natural resources (Douglas 2020; Resneck 2020). Native organizations, like the First Alaskans Institute, supported the OVK and the importance of prioritizing subsistence use of resources above commercial and sport fishing and hunting. The US District Court for Alaska sided with the federal government, allowing emergency hunt authorizations to continue (Estus 2020).

Beyond barriers to traditional food access, COVID-19 related restrictions, supply chain disruptions, and business closures created challenges for access to store-bought foods. One prominent example is the sudden closure in April 2020 of Ravn Airlines, which filed for bankruptcy largely due to pandemic-related disruptions to service (Anderson 2020). This left a number of communities, such as Atqasuk on the North Slope, without scheduled air service and with disruptions to freight supply for local grocery stores (Sullivan 2020). In other small communities connected to the road network, quarantine requirements made it difficult to drive to larger towns where groceries could be purchased more affordably. One expert estimated a 30 percent increase in his family's grocery bills due to freight charges when he was unable to drive to Fairbanks to shop. Many individuals reported shortages of store-bought goods, particularly early in the pandemic, including staple foods as well as ammunition and jars used for canning harvested foods.

Actions that supported access to food during the COVID-19 pandemic

Despite substantial challenges, individuals reported being able to access the food they needed thanks to both existing practices and programs as well as innovative responses (Table 1). The food sharing networks that are an essential part of Alaska Native food systems were robust and helped individuals, households, and families weather the stresses posed by COVID-19 impacts. Food sharing with neighbors, Elders, and those without a harvester in their family were common responses. Those who were unable to return home for harvesting received shipments of food from relatives. Alternative distribution methods for sharing—food drop-offs or pickups arranged to support social distancing—were utilized as social events were cancelled.

Institutional adaptations to support access to traditional foods were also implemented. Existing harvester support programs that pay hunters to provide food to Elders and others who lack access continued to fill this essential function; some Native villages used COVID-19 CARES Act funds to provide additional resources for these programs. Some villages received donations or purchased fish to distribute. Regional ANCSA (Alaska Native Claims Settlement Act) corporations and tribes provided additional sources of food resources, both traditional (e.g., salmon, fish eggs, and shrimp) and nontraditional foods. Other institutions, including schools and church groups, provided access to prepared meals. Where they existed, such as in Utqiaġvik, food pantries also increased access to food for individuals experiencing food shortages. One expert described the establishment of a soup kitchen in her community; while it had been in the works before the pandemic, COVID-19 provided additional incentive to launch the new institution.

Individuals unable to access traditional harvesting territories and infrastructure adapted in various ways. Some rented boats, purchased cars, and improvised outdoor and indoor drying methods so that they could harvest while being located in larger towns (Fig. 2). One expert harvested new species, including porcupine and beaver, based on hearing from Elders that these animals were historically harvested. The practice of storing food in times of plenty to eat in times of need also proved invaluable, with frozen, dried, and jarred fish taking on particular importance during a season of salmon shortages. The use of freezers was mentioned as particularly important; some Native villages, such as Rampart and Arctic Village, used CARES Act funding to support freezer purchases. Other Native villages used funds to purchase and distribute boxes of store-bought food or provide gift cards for the local store. Finally, several experts described agricultural pursuits during the pandemic such as planting home gardens, distributing seeds in the community, and organizing to build community greenhouses (Fig. 3).

Fig. 2. (a) A makeshift fish rack constructed during the COVID-19 pandemic. Photo: Sikuaq Erickson. (b) Drying meat during quarantine. Photo: Darlene Katchatag.

Fig. 3. First gathering for the Alaska Native Farmer Training at Calypso Farm and Ecology Center in Ester, Alaska, August 2021. Photo: Eva Dawn Burk.

Learning from the challenges presented by a pandemic

This study was designed to provide an overview of impacts from COVID-19 relatively early in the pandemic. Interviews were conducted at a time when many were hopeful that the pandemic was receding. The experts we interviewed identified the interruption of the cultural dimension of food sharing as the largest impact of COVID-19 on Indigenous food systems in Alaska in 2020. As the pandemic continued, some social gatherings were reinstated. In the summer of 2021, for example, Nay'dini'aa Na'Kayax' was again able to hold its culture camp, albeit with fewer participants to support social distancing. A subsequent surge of cases driven by the COVID-19 Delta variant prompted further

precautions and cancellations of large gatherings in the fall of 2021 (Slontik et al 2021). What we report therefore reflects a particular period of the pandemic.

Our study points to programmatic and policy priorities to support food sovereignty during significant events such as the COVID-19 pandemic. First, existing practices and initiatives that support access to traditional foods, such as food sharing networks and harvester support programs, continued to function well during the pandemic. This finding runs contrary to media messages that emphasize the challenges faced by Indigenous communities rather than highlighting solutions and innovations. That these networks and programs worked well under the additional stress created by COVID-19 underscores their significance and the importance of continuing to support them.

Second, the ability to harvest traditional foods depends on mobility and access to infrastructure. When these are restricted, one solution is to support flexibility in harvesting and resource management. For example, proxy hunting could allow friends and relatives to use the quota of an individual who is unable to access harvesting territory or infrastructure. This flexibility relies on full tribal sovereignty and ensuring Indigenous representation on boards and decision-making bodies responsible for setting resource policy.

Methods and approach: Building upon trust and relationships to gather information

This project draws on the concept of relational accountability to people, animals, and places (Jäger et al. 2019). An Indigenous Research Advisory Committee (RAC) worked closely with the project team (PT) of university-based researchers to develop the proposal and carry out each stage of the project. In fall 2020, we co-developed an interview guide and completed Institutional Review Board approvals at the University of Arizona and the University of Colorado Boulder. From January-May 2021, PT members conducted 31 semi-structured interviews of experts (16 in Alaska, 15 in the US Southwest) who were either members of the IFKN network or recruited by members of the RAC. Alaska Native experts were from four out of five cultural regions of Alaska (Inupiaq, Yup'ik & Cup'ik, Athabascan/Dene, and Eyak, Haida Tsimshian, Tlingit), with half from the Inupiaq region (Fig. 4); they were female (9), male (6), and two-spirit (1) and ranged in age from Elders (70+ years old) to young adults in their 20s. The recruitment of experts was successful because of strong, pre-existing relationships, including those established through IFKN meetings as well as those held by RAC members.

Fig. 4. Map showing five cultural regions of Alaska and the number of interviews with Alaska Native experts conducted in each region. Cultural centers are indicated on the map but do not reflect specific locations where interviews were conducted. Map credit: NOAA Climate Program Office, adapted from the Alaska Native Heritage Center.

After conducting interviews, the PT conducted a thematic qualitative analysis of interview transcripts using a grounded theory approach to identify important themes (Thornberg and Charmaz 2014). The PT and RAC then reviewed the themes and analyzed the data. Experts and IFKN steering committee members were sent a copy of the analysis and input was solicited at an online meeting. All project activities were conducted remotely on Zoom or by phone.

Acknowledgments

The authors are grateful for funding from the Office of Polar Programs and Navigating the New Arctic at the National Science Foundation (award numbers 1745499, 2035161, and 2035233). The project also received support from the Morris K. Udall and Stewart L. Udall Foundation. Thank you to all the cultural practitioners and experts for sharing your knowledge and stories. Finally, we thank all Knowledge Keepers: human, land, and non-human kin.

References

Anderson, T., 2020: Wheels up: Ravn will return to the skies under new ownership. Alaska Business, https://www.akbizmag.com/monitor/wheels-up-ravn-will-return-to-the-skies-under-new-ownership/ (27 August 2020).

Douglas, J., 2020: The Alaska Native village of Kake defends their right to hunt. High Country News, https://www.hcn.org/articles/indigenous-affairs-justice-the-alaska-native-village-of-kake-defends-their-right-to-hunt (12 October 2020).

Estus, J., 2020: Emergency hunts in Alaska can continue. Indian Country Today, https://indiancountrytoday.com/news/emergency-hunts-in-alaska-can-continue (27 November 2020).

Inuit Circumpolar Council-Alaska, 2015: Alaskan Inuit Food Security Conceptual Framework: How to Assess the Arctic From an Inuit Perspective: Summary Report and Recommendations Report. Anchorage, AK. https://iccalaska.org/wp-icc/wp-content/uploads/2016/03/Food-Security-Summary-and-Recommendations-Report.pdf.

Inuit Circumpolar Council Alaska, 2019: Alaskan Inuit Food Sovereignty Summit Report. Anchorage, Alaska.

Jäger, M. B., and Coauthors, 2019: Building an Indigenous foods knowledges network through relational accountability. *JAFSCD*, **9**(B), 45-51, https://doi.org/10.5304/jafscd.2019.09B.005.

Jenkins, E., 2020: Amid food supply chain concerns, tribal governments request emergency hunts. KTOO Public Media, https://www.ktoo.org/2020/04/14/amid-food-supply-chain-concerns-tribal-governments-request-emergency-hunts/ (14 April 2020).

Resneck, J., 2020: Native rights group backs Kake in lawsuit over emergency subsistence hunt. Alaska Public Radio, https://www.alaskapublic.org/2020/09/04/native-rights-group-backs-kake-in-lawsuit-over-emergency-subsistence-hunt/ (4 September 2020).

Slontik, D. E., E. Medina, and M. Baker, 2021: Hospitals in Alaska struggle to handle a worsening outbreak. The New York Times, https://www.nytimes.com/2021/09/22/us/covid-alaska-hospital.html (22 September 2021).

Sullivan, M., 2020: Alaska airline shutdown: 'How are we gonna get our food, our mail, our medical needs?' Indian Country Today, https://indiancountrytoday.com/news/alaska-airline-shutdown-how-are-we-gonna-get-our-food-our-mail-our-medical-needs (30 May 2020).

Sullivan, M., 2021: 'We don't exist out here' without subsistence. Indian Country Today, https://indiancountrytoday.com/news/we-dont-exist-out-here-without-subsistence (19 October 2021).

Thornberg, R., and K. Charmaz, 2014: Grounded theory and theoretical coding. The SAGE handbook of qualitative data analysis, 153-169.

December 6, 2021

Authors and Affiliations

A. Ahmasuk, Marine Advocate, Kawerak Inc., Nome, AK, USA

T. J. Ballinger, International Arctic Research Center, University of Alaska Fairbanks, Fairbanks, AK, USA

L. T. Berner, Geophysical Institute, University of Alaska Fairbanks, Fairbanks, AK, USA

U. S. Bhatt, Geophysical Institute, University of Alaska Fairbanks, Fairbanks, AK, USA

J. W. Bjerke, Norwegian Institute for Nature Research, FRAM - High North Research Centre for Climate and the Environment, Tromsø, Norway

J. E. Box, Geological Survey of Denmark and Greenland, Copenhagen, Denmark

B. Brettschneider, National Weather Service Alaska Region, NOAA, Anchorage, AK, USA

M. Brubaker, Alaska Native Tribal Health Consortiuhvidm, Anchorage, AK, USA

J. Cappelen, Danish Meteorological Institute, Copenhagen, Denmark

S. R. Carroll (Ahtna), Mel & Enid Zuckerman College of Public Health and Native Nations Institute, University of Arizona, Tucson, AZ, USA

J. A. Clark, Geophysical Institute, University of Alaska Fairbanks, Fairbanks, AK, USA

J. A. Coe, Geologic Hazards Science Center, USGS, Golden, CO, USA

J. C. Comiso, Cryospheric Sciences Laboratory, Goddard Space Flight Center, NASA, Greenbelt, MD, USA

L. W. Cooper, Chesapeake Biological Laboratory, University of Maryland Center for Environmental Science, Solomons, MD, USA

J. N. Cross, Pacific Marine Environmental Laboratory, NOAA, Seattle, WA, USA

B. Decharme, Météo-France/CNRS, Centre National de Recherches Météorologiques, Toulouse, France

C. Derksen, Climate Research Division, Environment and Climate Change Canada, Toronto, ON, Canada

D. Divine, Norwegian Polar Institute, Fram Centre, Tromsø, Norway

M. L. Druckenmiller, Cooperative Institute for Research in Environmental Sciences, University of Colorado Boulder, Boulder, CO, USA; National Snow and Ice Data Center, Boulder, CO, USA

A. Elias Chereque, Department of Physics, University of Toronto, Toronto, ON, Canada

H. E. Epstein, Department of Environmental Sciences, University of Virginia, Charlottesville, VA, USA

K. S. Erickson (Inupiaq), Ikaaġun Engagement, Anchorage, AK, USA

S. Farrell, Department of Geographical Sciences, University of Maryland, College Park, MD, USA

R. S. Fausto, Geological Survey of Denmark and Greenland, Copenhagen, Denmark

D. B. Ferguson, Department of Environmental Science, University of Arizona, Tucson, AZ, USA

X. Fettweis, SPHERES Research Unit, University of Liège, Liège, Belgium

G. Fiske, Woodwell Climate Research Center, Falmouth, MA, USA

B. C. Forbes, Arctic Centre, University of Lapland, Rovaniemi, Finland

K. E. Frey, Graduate School of Geography, Clark University, Worcester, MA, USA

G. V. Frost, Alaska Biological Research, Inc., Fairbanks, AK, USA

S. Gerland, Norwegian Polar Institute, Fram Centre, Tromsø, Norway

S. J. Goetz, School of Informatics, Computing and Cyber Systems, Northern Arizona University, Flagstaff, AZ, USA

J. M. Grebmeier, Chesapeake Biological Laboratory, University of Maryland Center for Environmental Science, Solomons, MD, USA

C. Haas, Alfred Wegener Institute, Helmholtz Centre for Polar and Marine Research, Bremerhaven, Germany

E. Hanna, School of Geography and Lincoln Centre for Water and Planetary Health, University of Lincoln, Lincoln, UK

I. Hanssen-Bauer, Norwegian Meteorological Institute, Blindern, Oslo, Norway

S. Hendricks, Alfred Wegener Institute, Helmholtz Centre for Polar and Marine Research, Bremerhaven, Germany

R. M. Holmes, Woodwell Climate Research Center, Falmouth, MA, USA

H. Hvidtfeldt Christiansen, The University Centre in Svalbard, UNIS, Svalbard, Norway

F. Ivanoff, Norton Sound Economic Development Corporation, Unalakleet, AK, USA

M. Jacquemart, Laboratory of Hydraulics, Hydrology, and Glaciology (VAW), Department of Civil, Environmental and Geomatic Engineering, ETH Zurich, Zurich, Switzerland; Swiss Federal Institute of Forest, Snow, and Landscape Research (WSL), Birmensdorf, Switzerland

M. B. Jäger (Citizen Potawatomi Nation), Native Nations Institute, University of Arizona, Tucson, AZ, USA

L. L. Jennings (Wixárika & Pascua Yaqui), Mel & Enid Zuckerman College of Public Health and Native Nations Institute, University of Arizona, Tucson, AZ, USA

N. Johnson, National Snow and Ice Data Center, Boulder, CO, USA; Cooperative Institute for Research in Environmental Sciences, University of Colorado Boulder, Boulder, CO, USA

B. M. Jones, Water and Environmental Research Center, Institute of Northern Engineering, University of Alaska Fairbanks, Fairbanks, AK, USA

A. R. Juan (Tohono O'odham Nation), International Indian Treaty Council, Tucson, AZ, USA

A. Kääb, Department of Geosciences, University of Oslo, Oslo, Norway

L. Kaleschke, Alfred Wegener Institute, Helmholtz Centre for Polar and Marine Research, Bremerhaven, Germany

S. -J. Kim, Korea Polar Research Institute, Incheon, Republic of Korea

J. Koonooka, Tribal Council, Native Village of Gambell, Gambell, AK, USA

N. J. Korsgaard, Geological Survey of Denmark and Greenland, Copenhagen, Denmark

Z. Labe, Colorado State University, Fort Collins, CO, USA

M. J. Lara, Department of Plant Biology, University of Illinois, Urbana, IL, USA; Department of Geography, University of Illinois, Urbana, IL, USA

S. Larson (Ahtna and Supiaq), Chickaloon Village Traditional Council, Chickaloon, AK, USA

A. K. Liljedahl, Woodwell Climate Research Center, Falmouth, MA, USA

B. D. Loomis, Goddard Space Flight Center, NASA, Greenbelt, MD, USA

F. Løvholt, Geohazards and Dynamics, NGI, Oslo, Norway

K. Luojus, Arctic Research Centre, Finnish Meteorological Institute, Helsinki, Finland

M. J. Macander, Alaska Biological Research, Inc., Fairbanks, AK, USA

K. D. Mankoff, Geological Survey of Denmark and Greenland, Copenhagen, Denmark

P. Marsh, Department of Geography, Wilfrid Laurier University, Waterloo, ON, Canada

J. W. McClelland, Marine Science Institute, University of Texas at Austin, Port Aransas, TX, USA

W. N. Meier, National Snow and Ice Data Center, Boulder, CO, USA; Cooperative Institute for Research in Environmental Sciences, University of Colorado Boulder, Boulder, CO, USA

T. A. Moon, Cooperative Institute for Research in Environmental Sciences, University of Colorado Boulder, Boulder, CO, USA; National Snow and Ice Data Center, Boulder, CO, USA

T. L. Mote, Department of Geography, University of Georgia, Athens, GA, USA

L. Mudryk, Climate Research Division, Environment and Climate Change Canada, Toronto, ON, Canada

S. Natali, Woodwell Climate Research Center, Falmouth, MA, USA

A. Niemi, Freshwater Institute, Fisheries and Oceans Canada, Winnipeg, MB, Canada

A. Noongwook, Tribal Council, Native Village of Savoonga, Savoonga, AK, USA

J. E. Overland, Pacific Marine Environmental Laboratory, NOAA, Seattle, WA, USA

T. Park, Ames Research Center, NASA, Mountain View, CA, USA; Bay Area Environmental Research Institute, Moffett Field, CA, USA

D. Perovich, Thayer School of Engineering, Dartmouth College, Hanover, NH, USA

A. A. Petty, Goddard Space Flight Center, NASA, Greenbelt, MD, USA

G. K. Phoenix, School of Biosciences, University of Sheffield, Sheffield, UK

D. J. Pilcher, Pacific Marine Environmental Laboratory, NOAA, Seattle, WA, USA; Cooperative Institute for Climate, Ocean, and Ecosystem Studies, University of Washington, Seattle, WA, USA

R. Ricker, Norwegian Research Centre, Tromsø, Norway

F. Rosell, Department of Natural Sciences and Environmental Health, University of South-Eastern Norway, Bø, Norway

A. C. A. Rudy, Northwest Territories Geological Survey, Government of the Northwest Territories, Yellowknife, NT, Canada

L. Scott, Woodwell Climate Research Center, Falmouth, MA, USA

S. P. Serbin, Environmental and Climate Sciences Department, Brookhaven National Laboratory, Upton, NY, USA

G. Sheffield, Alaska Sea Grant, Marine Advisory Program, University of Alaska Fairbanks, Nome, AK, USA

A. I. Shiklomanov, University of New Hampshire, Durham, NH, USA; Arctic and Antarctic Research Institute, St. Petersburg, Russia

W. K. S. Smythe (Haida), American Indian Studies and Earth and Environmental Science, University of Minnesota Duluth, Duluth, MN, USA

R. G. M. Spencer, Florida State University, Tallahassee, FL, USA

K. M. Stafford, Applied Physics Laboratory, University of Washington, Seattle, WA, USA

A. Steer, Norwegian Polar Institute, Fram Centre, Tromsø, Norway

N. Steiner, Institute of Ocean Sciences, Fisheries and Oceans Canada, Sidney, BC, Canada

L. V. Stock, Cryospheric Sciences Laboratory, Goddard Space Flight Center, NASA, Greenbelt, MD, USA

C. Strawhacker, Office of Polar Programs, National Science Foundation, Alexandria, VA, USA

D. Streletskiy, Department of Geography, The George Washington University, Washington, DC, USA

A. Suslova, Woodwell Climate Research Center, Falmouth, MA, USA

S. E. Tank, University of Alberta, Edmonton, AB, Canada

K. D. Tape, Geophysical Institute, University of Alaska Fairbanks, Fairbanks, AK, USA

M. Tedesco, Lamont-Doherty Earth Observatory, Columbia University, Palisades, NY, USA; Goddard Institute of Space Studies, NASA, New York, NY, USA

R. L. Thoman, Alaska Center for Climate Assessment and Policy, University of Alaska Fairbanks, Fairbanks, AK, USA; International Arctic Research Center, University of Alaska Fairbanks, Fairbanks, AK, USA

X. Tian-Kunze, Alfred Wegener Institute, Helmholtz Centre for Polar and Marine Research, Bremerhaven, Germany

M. -L. Timmermans, Yale University, New Haven, CT, USA

H. Tømmervik, Norwegian Institute for Nature Research, FRAM - High North Research Centre for Climate and the Environment, Tromsø, Norway

M. Tretiakov, Arctic and Antarctic Research Institute, St. Petersburg, Russia

M. Tschudi, Aerospace Engineering Sciences, University of Colorado, Boulder, CO, USA

A. Walker (Akimel O'otham), Climate Science Alliance, San Diego, CA, USA

D. A. Walker, Institute of Arctic Biology, University of Alaska Fairbanks, Fairbanks, AK, USA

J. E. Walsh, International Arctic Research Center, University of Alaska Fairbanks, Fairbanks, AK, USA

M. Wang, Cooperative Institute for Climate, Ocean, and Ecosystem Studies, University of Washington, Seattle, WA, USA; Pacific Marine Environmental Laboratory, NOAA, Seattle, WA, USA

M. Webster, Geophysical Institute, University of Alaska Fairbanks, Fairbanks, AK, USA

A. Wehrlé, Institute of Geography, University of Zurich, Zurich, Switzerland

H. C. Wheeler, School of Life Sciences, Anglia Ruskin University, Cambridge, UK

Ø. A. Winton, Geological Survey of Denmark and Greenland, Copenhagen, Denmark

G. J. Wolken, International Arctic Research Center, University of Alaska Fairbanks, Fairbanks, AK, USA; Alaska Division of Geological & Geophysical Surveys, Department of Natural Resources, Fairbanks, AK, USA

K. Wood, Cooperative Institute for Climate, Ocean, and Ecosystem Studies, University of Washington, Seattle, WA, USA; Pacific Marine Environmental Laboratory, NOAA, Seattle, WA, USA

D. Yang, Environmental and Climate Sciences Department, Brookhaven National Laboratory, Upton, NY, USA; Department of Ecology and Evolution, Stony Brook University, Stony Brook, NY, USA